Course of Geothermics

Prof. Magdala Tesauro

Course Outline:

1. Thermal conditions of the early Earth and present-day Earth's structure
2. Thermal parameters of the rocks
3. Thermal structure of the lithospheric continental areas (steady state)
4. Thermal structure of the lithospheric oceanic areas
5. Thermal structure of the lithosphere for transient conditions in various tectonic settings
6. Heat balance of the Earth
7. Thermal structure of the sedimentary basins
8. Thermal maturity of sediments
9. Mantle convection and hot spots
10. **Magmatic processes and volcanoes**
11. Heat transfer in hydrogeological settings
12. Geothermal Systems

UNIVERSITÀ DEGLI STUDI DI TRIESTE

Temperature and magmatic processes

Melting generation is a consequence of:

- Decompression occurring during upper mantle rising (at midoceanic ridges).
- Water enrichment of the upper mantle due to dehydration of the subducting plate.
- Chemical elements (trace elements) enrichment/depletion of the upper mantle during metasomatic processes.

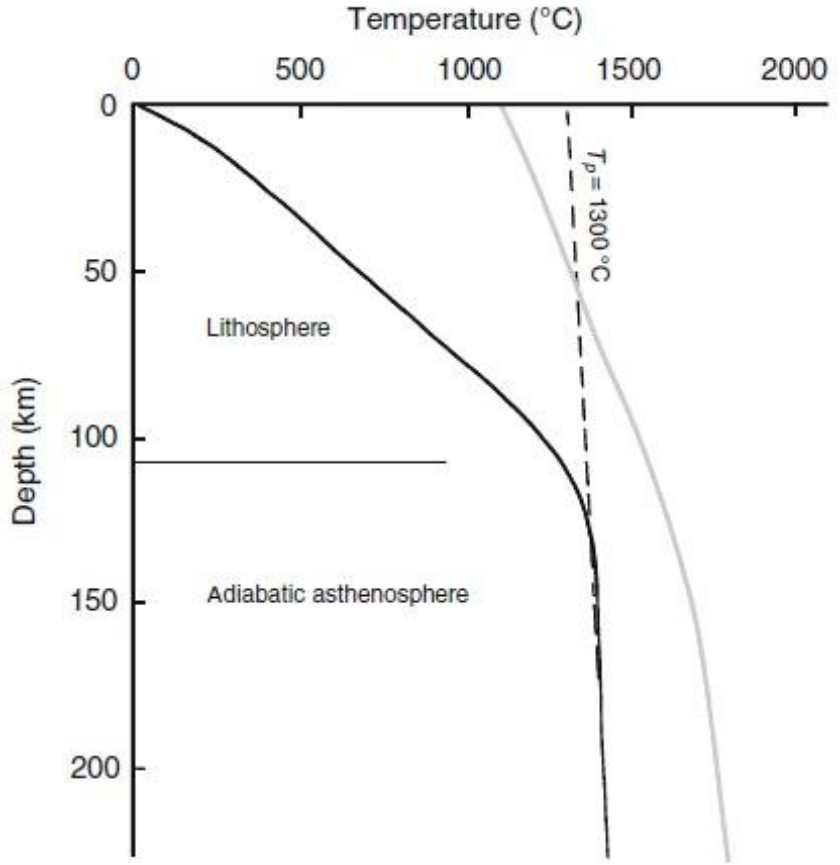

Garnet Peridotite Solidus

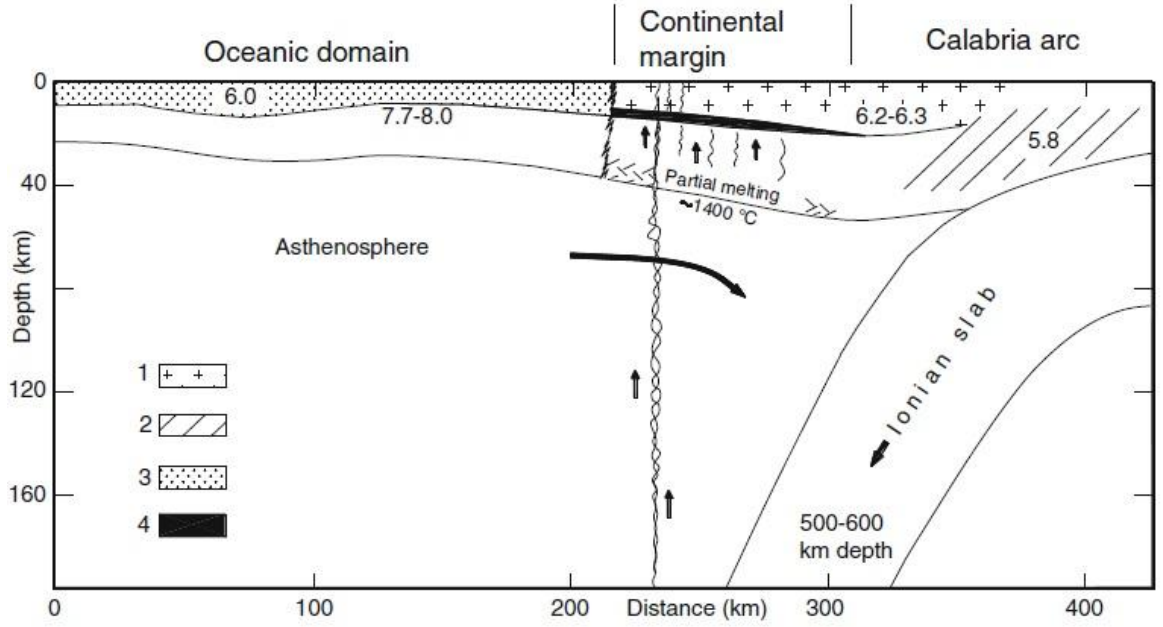

1–continental crust, 2–low velocity layers, 3–oceanic crust, 4-crustal underplating

Temperature, melting, and density

T of main volcanic rocks during eruptions are: 700–900°C for rhyolite, 800–1100°C for dacite, 950–1200°C for andesite, and 1000–1200°C for basalt.

According to lab experiments, for an anhydrous garnet peridotite (in absence of a fluid phase H_2O and CO_2) T_S and T_L depend on *P* (increasing with the increase of the depth, *z*):

$$T_S(z) = 3.0\,z + 1100 \quad \text{solidus} \qquad\qquad T_S(z) < T(z) < T_L(z)$$

$$T_L(z) = 1.5\,z + 1850 \quad \text{liquidus}$$

$$x_f = [T(z) - T_S(z)]/[(T_L(z) - T_S(z)]$$

x_f = percentage of melt at a given depth *z* (in km) and temperature *T(z)* in °C

Density of a magma varies from 2.2 g/cm³ (rhyolitic composition) to 2.8 g/cm³ (basaltic composition)

$$\rho = \sum x_i M_i / \sum x_i V_i$$

xi, Mi, and Vi = molar fraction, molecular weight, and molar volume of the various chemical species.

Dependence of the partial melt fraction on *P* and *T*

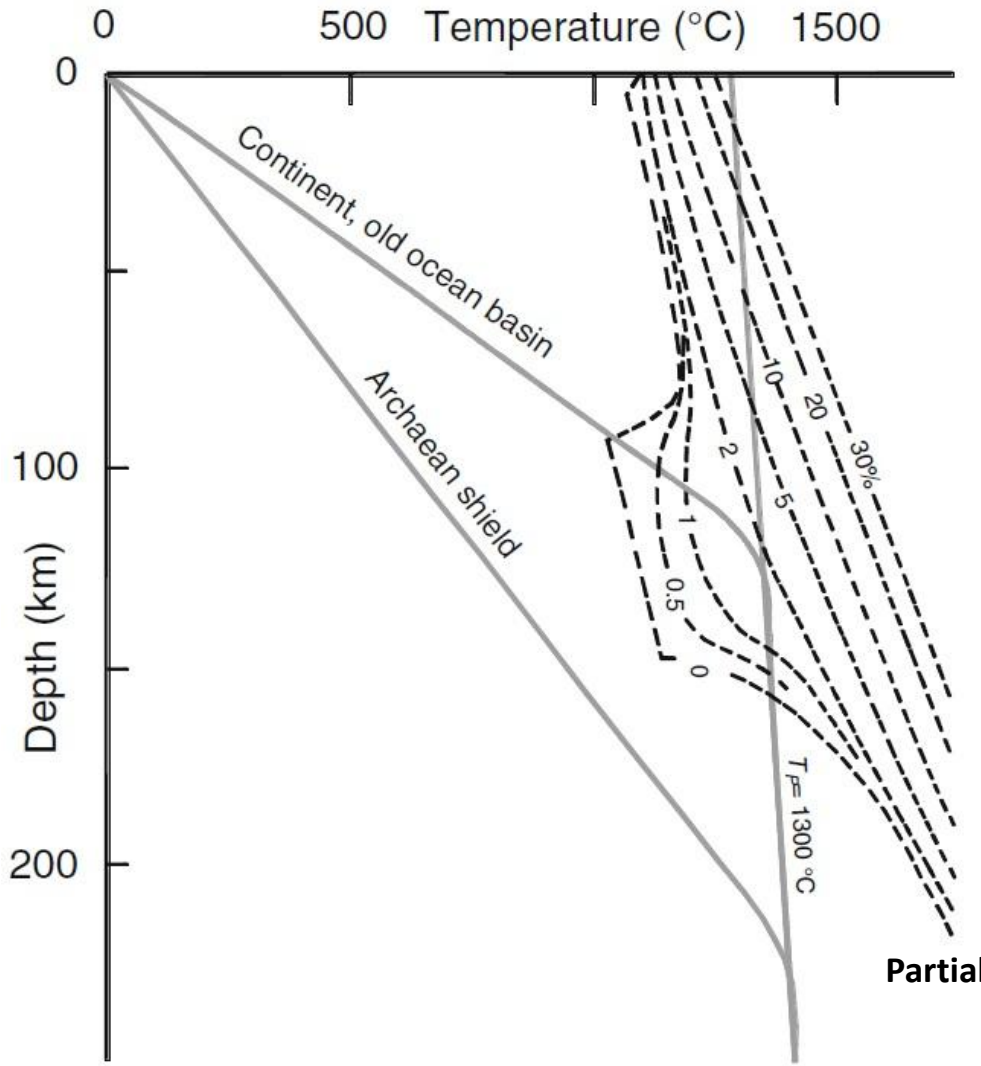

H_2O=0.01%

The solidus curve shows a negative slope between 70 and 100 km, where the amphibole changes into pyroxene, olivine and garnet and releases water.

Melt volume and temperature

Relationship between melt volume and temperature in the melting interval:

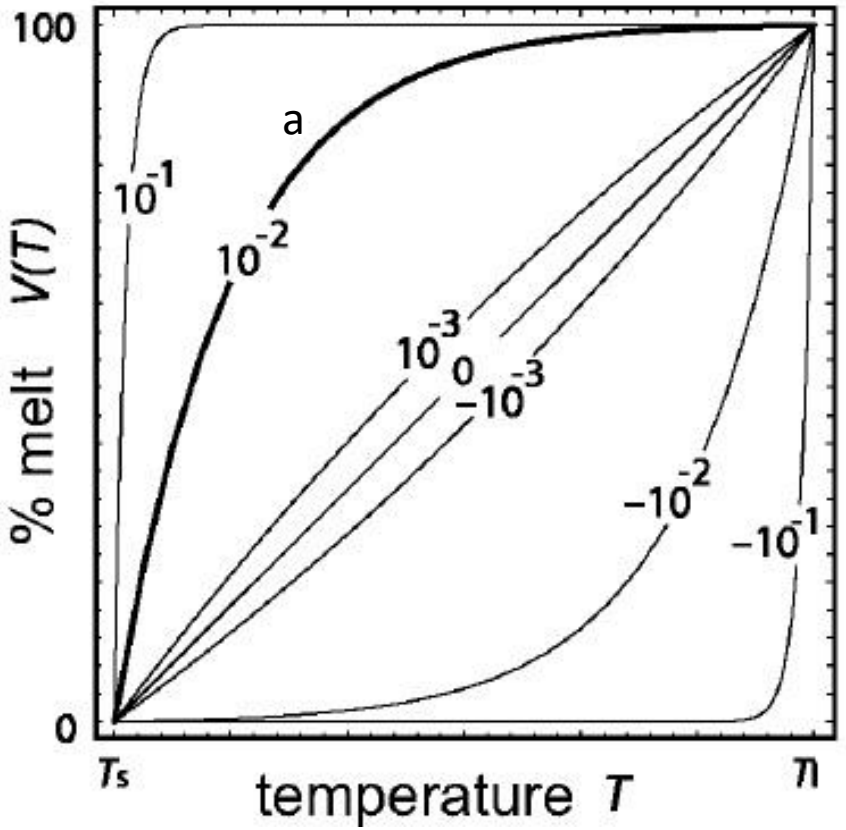

Stuwe, 2002

$$V(T) = \frac{e^{aT} - e^{aT_s}}{e^{aT_l} - e^{aT_s}} \qquad \frac{dV}{dT} = \left(\frac{a}{e^{aT_l} - e^{aT_s}}\right) e^{aT}$$

- If *a* has a large positive value, then most of the rock melts near the solidus.
- If *a* has large negative values, then most of the melting occurs near the liquidus.
- For values of *a* —> zero, melting becomes linear in temperature:

$$V(T) = T/(T_l - T_s)$$

Realistic values for *a* are positive and possibly around 0.01
(rocks usually contain hydrated phases)

T_s=Solidus temperature T_l=Liquidus temperature

Magma Viscosity

Viscosity of a magma depends on its chemical composition (ionic or molecular cohesion):

- **Basic melts have lower viscosity (10-10^4 Pa s) than acid melts (10^{11}-10^{12} Pa s), since they have higher ratio between oxygen atoms (not forming structural bridges) and silicon.**
- **Peralkaline magma have low viscosity, since metal cations (Na^+,K^+,Ca^+,Mg^+) decrease the degree of melt polymerization (interrupt Si-O-Si-O chain).**

Newton's relation

$$\sigma = \sigma_0 + \eta \left(\frac{d\varepsilon}{dt}\right)^n$$

σ_0 = shear stress required for the flow onset.
In Newtonian fluids σ_0=0 and n = 1.
For a pseudoplastic magma (Non-Newtonian fluids) σ_0 = 0 and n<1.
For a Bingham fluid σ_0 has a finite value and n = 1
η=effective viscosity

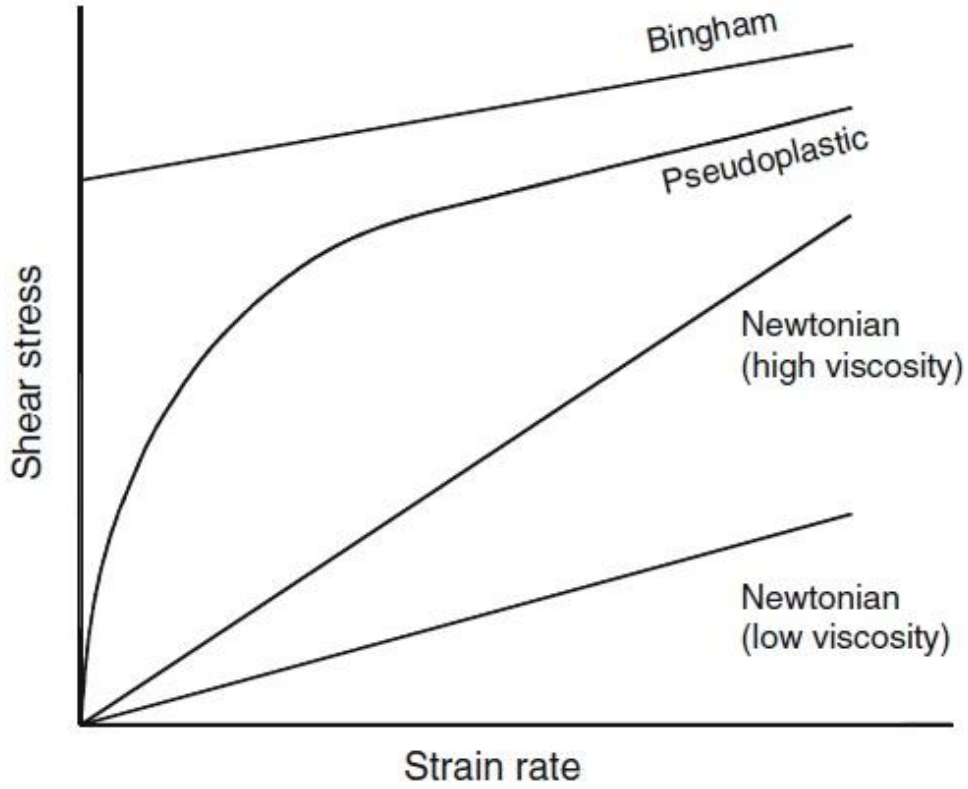

Many rocks deform roughly 8 times as rapid if the applied stress is doubled

Magma Viscosity

Dynamic viscosity variations with temperature and pressure *p*:

$$\eta = A_\eta \exp\left(\frac{E* + p\ V*}{RT}\right)$$

V* = activation volume, R = gas constant and A_η constant material.
The activation energy E* is mainly dependent on the ratio (Si + Al)/O of the melt.

At high pressure structural variations in silicate melts decrease the viscosity, due to the role of Al^{3+} (octahedral coordination is strongly favored at high pressure). For example, giadeitic melts ($NaAlSi_2O_6$) undergo a decrease in viscosity from about 3.5 x10^3 Pa s at 0.5 GPa up to 0.5x10^3 Pa s at 2.5 GPa.

- **Non-Arrhenian Newtonian viscosity of silicate melts as a function of *T* and melt composition, including the influence of volatile (*H_2O* and *F*):**

$$\mu = \mu_\infty \exp\left(\frac{B}{T - C}\right)$$

coefficients *B* and *C* depend on composition

$$\mu_\infty = 10^{-4.55}\ \text{Pa s}$$

Giordano et al., 2008, EPSL, 271

(All melts converge to a single, common value of viscosity at high-*T*)

Viscosities of common volatile-free magma types at their liquidus temperatures.

Magma	Liquidus temperature (K)	Viscosity (Pa s)
Komatiite	1600	1
Basalt	1500	10^2
Andesite	1300	10^4
Dacite	1100	10^8
Rhyolite	1000	10^{11}

Magma Viscosity (Composition)

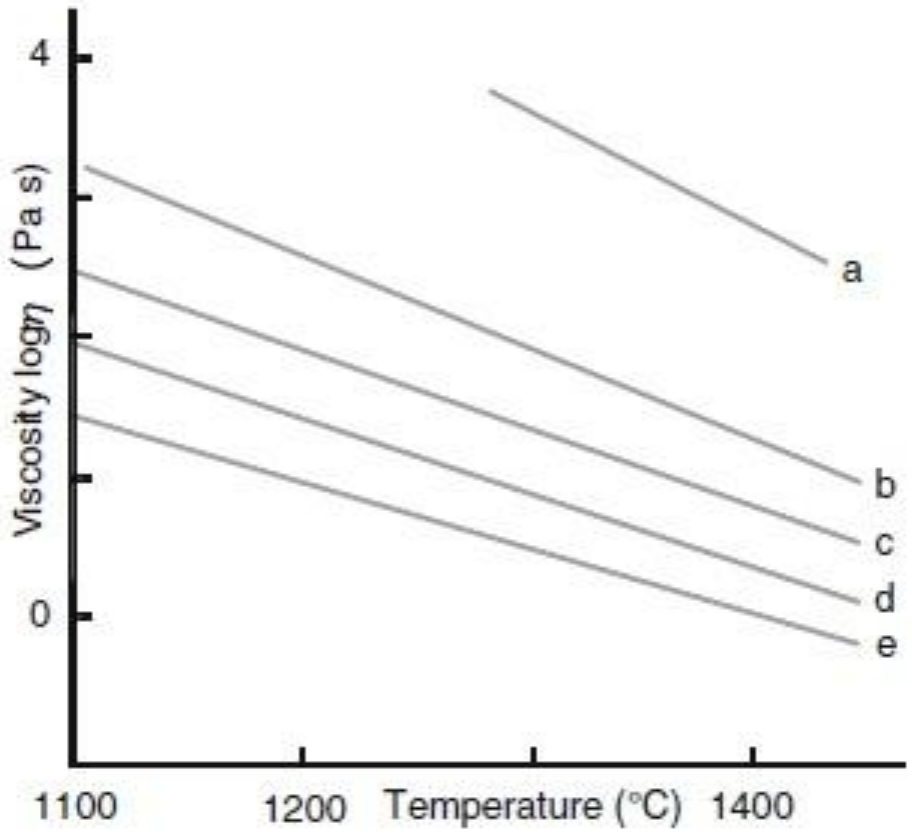

a-pantellerite; b-basic andesite; c-oceanic island tholeiite; d-olivine basalt; e-olivine melanephelinite.

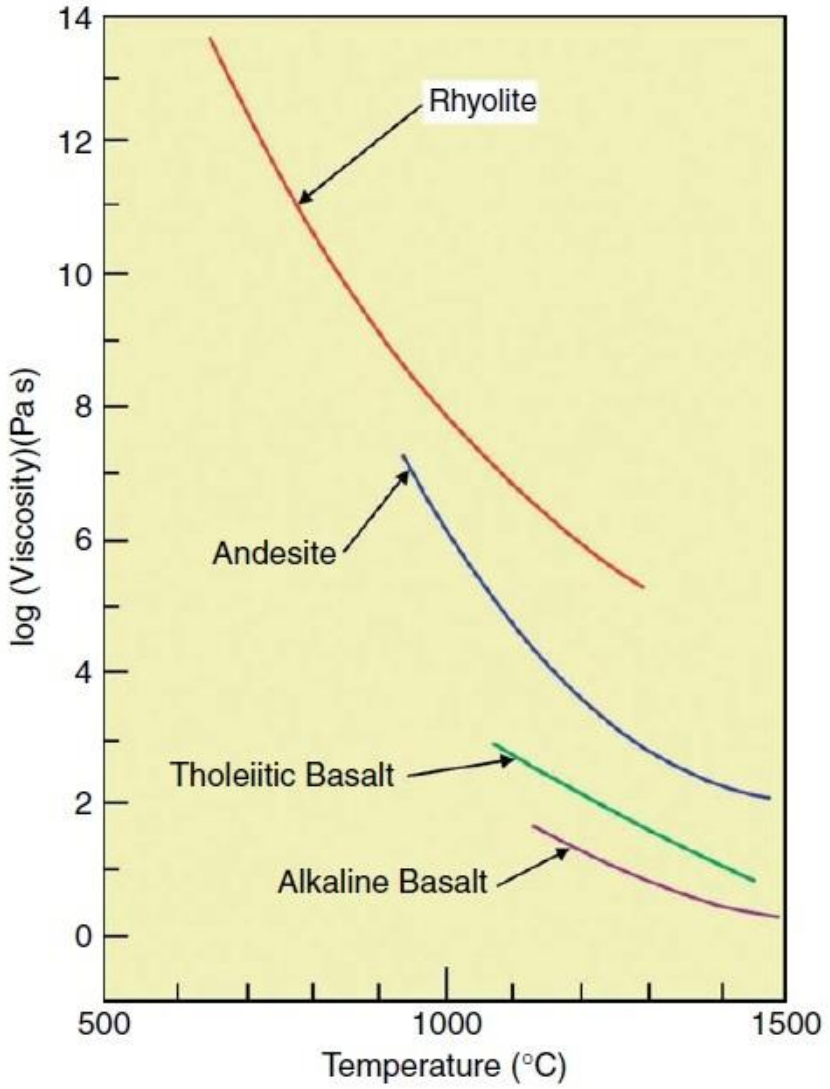

Newhall, 2007, Treatise of Geophysics, vol. 4

Magma Viscosity (Water)

- There is a non-linear effect of H_2O in decreasing viscosity: over the range from 0-3% H_2O, water has a very strong effect in reducing the viscosity, since the water is present as OH^- groups, which cause weakening or breaking of aluminosilicate bonds.
- A higher concentration of water has smaller effect on the viscosity, since it is present as H_2O molecules.

Mafic melts

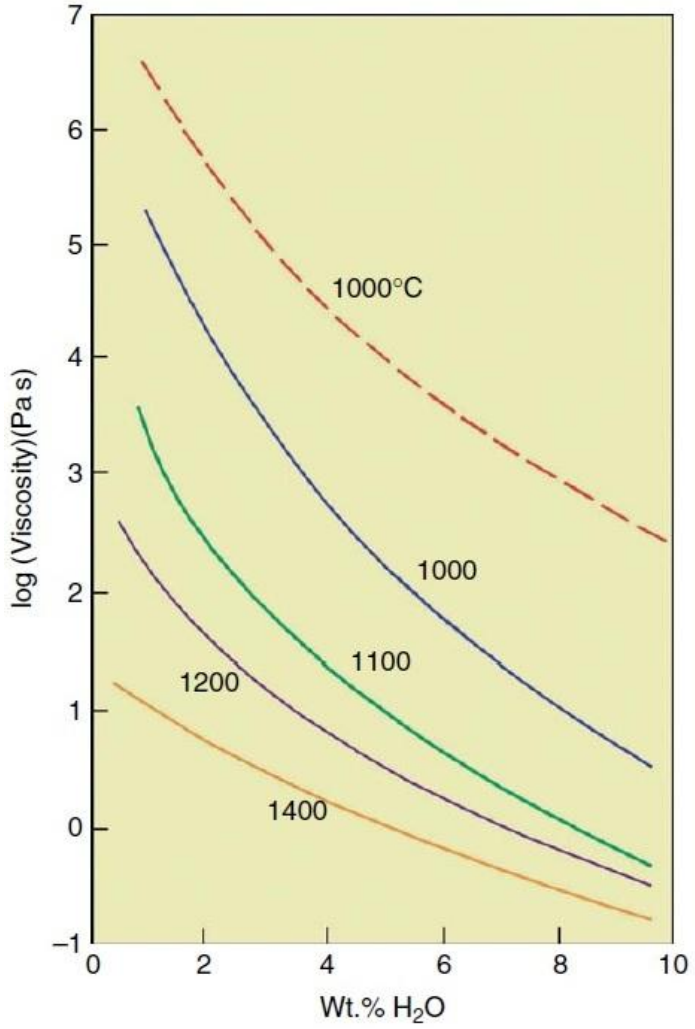

Rhyolitic melts

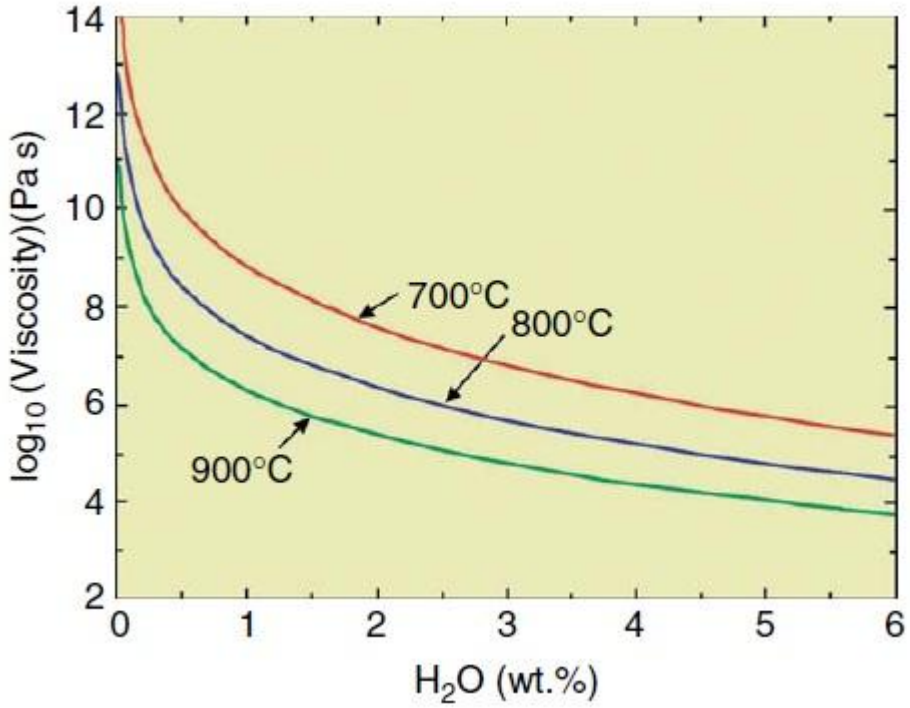

Newhall, 2007, Treatise of Geophysics, vol. 4

Magma Viscosity (crystals content)

- **Suspended crystals in magma increases the viscosity, the critical threshold is ~55 %: below effective potential of diffusion in the form of lava, above potential to become intrusive bodies.**

From lab experiments: $\eta = \eta_L(1 - 1.67\,x_s)^{-2.5}$

x_s = volume fraction of suspended solid
η_L = viscosity of the liquid

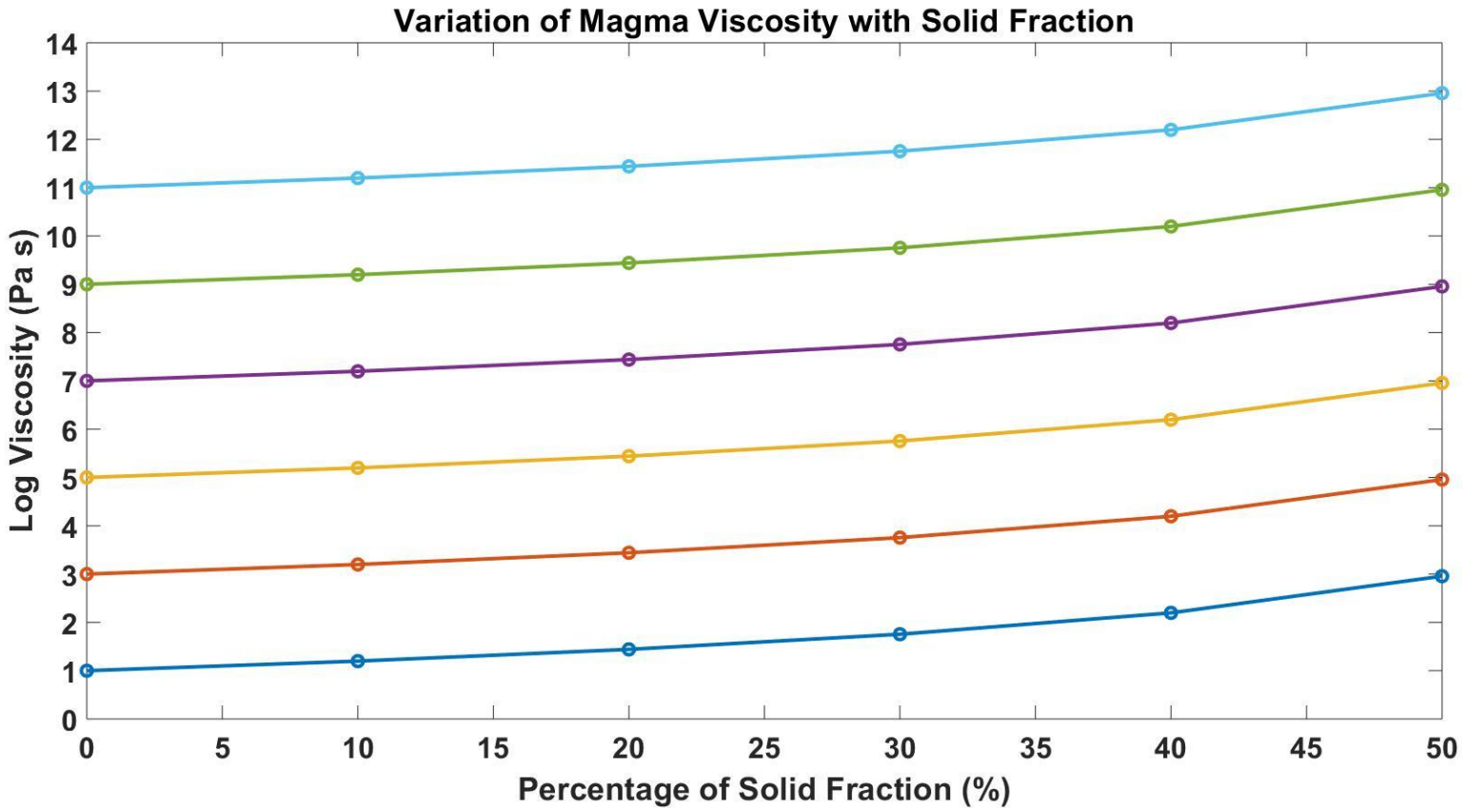

Magma Viscosity (crystals content)

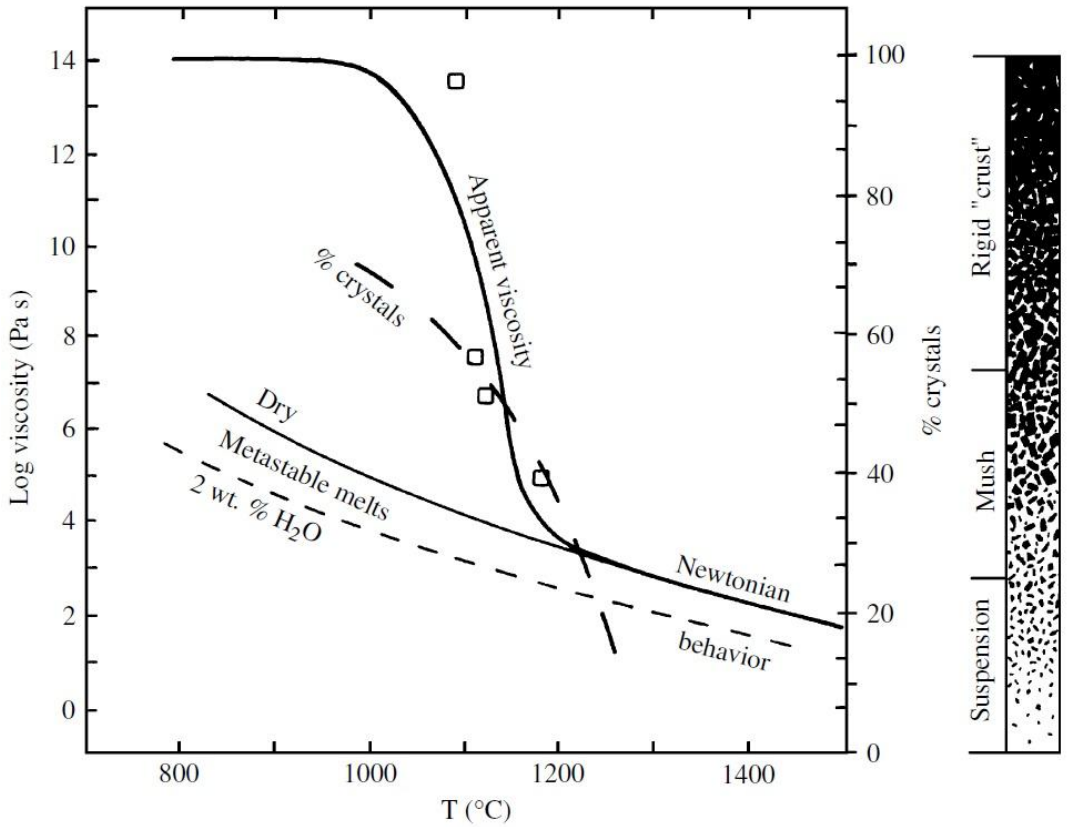

Myron, 2003, Igneous and metamorphic petrology 2° Ed

- As magma cools below the liquidus, the viscosity increases, according to the decrease of temperature, increase concentration of crystals, and increase of silica concentration of the residual melt.
- The magma viscosity increases of about nine orders as soon as the percentage of the crystals increase from 30% to 70%.
- If anhydrous minerals are crystallizing, water concentration increases in the residual melt, causing a decrease of viscosity, but as soon as melt becomes satured in water, so that it exolves forming bubbles, the viscosity of the melt increases, due to the decreased water concentration and the increase of crystallinity due to the raise of the liquidus temperature

Magma Flow

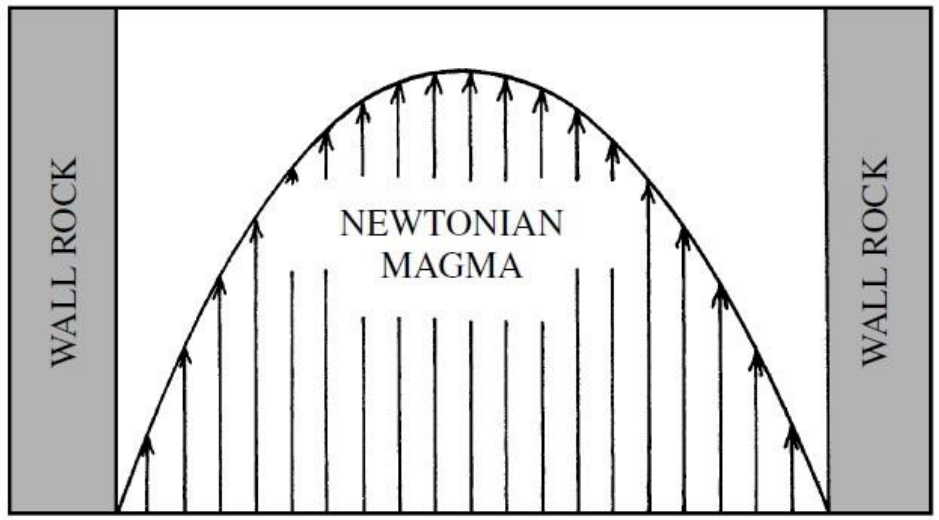

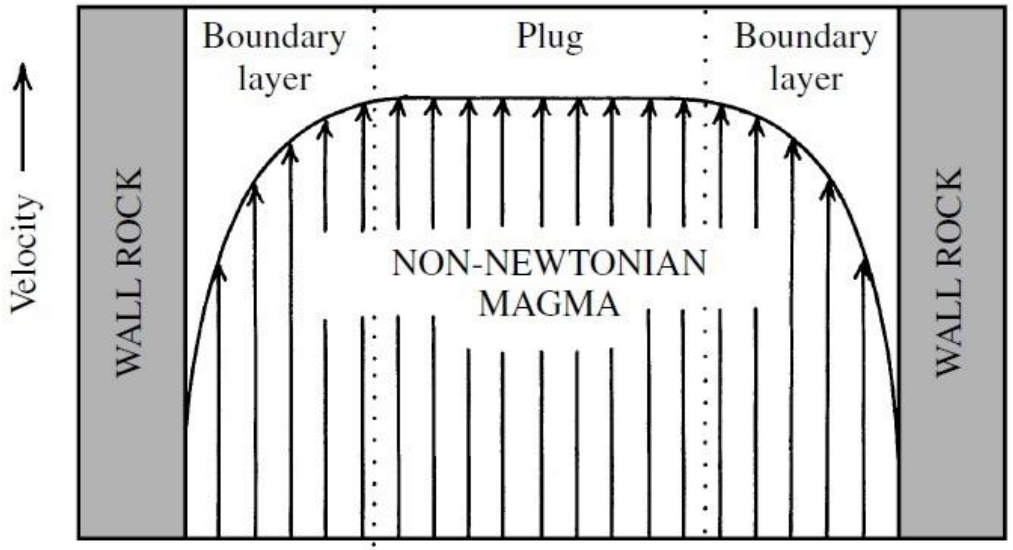

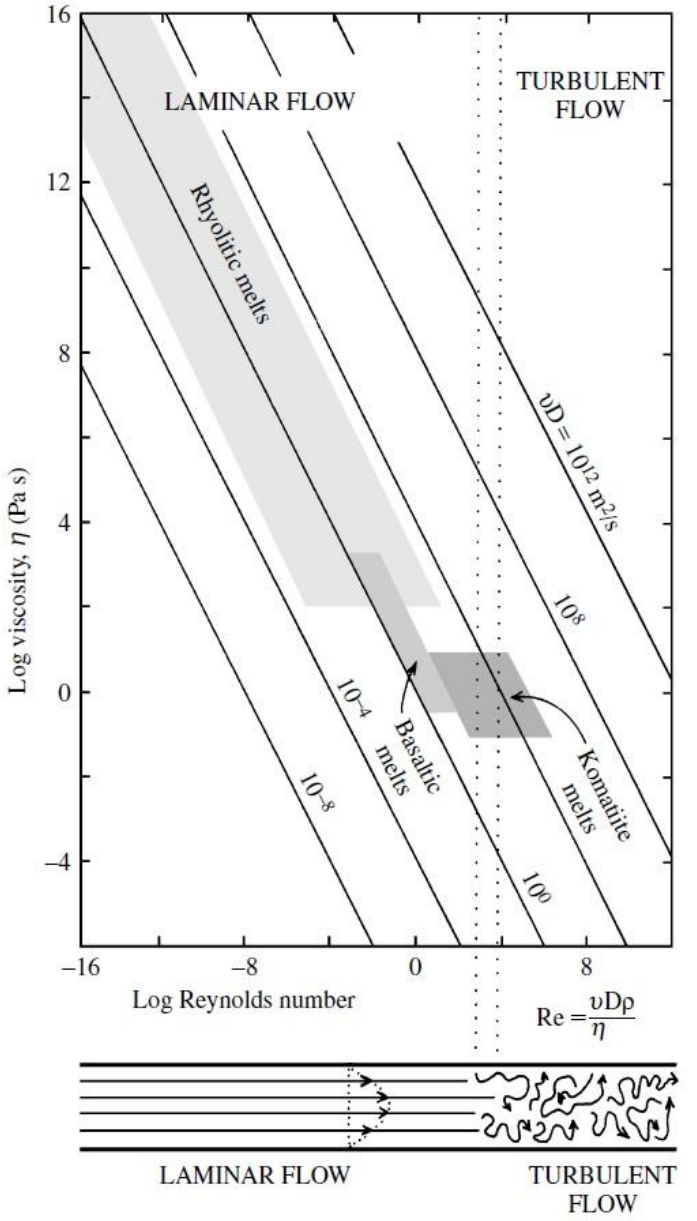

Myron, 2003, Igneous and metamorphic petrology 2° Ed

Magma Volatiles

- The solubility of the volcanic gases in a magma increases with *P* and decreases with *T*, while their concentration depends mostly on the rock composition through which the magma rises.
- The solubility of water in magmas can reach 9–12 wt%, while that of CO_2 reaches values of 0.5–4.0 wt%, but drops to zero at 0.1 MPa. Solubility of CO_2 increases in presence of H_2O and causes an increase of polymerization.
- Among gases, H_2O and CO_2 can be present in a significant concentration in a magma (magmas are less rich in *HCl*, *HF*, SO_2, SO_3, *S*, N_2).
- The most easily and widely measured indicator of magma degassing is (SO_2), since it is much more abundant in magmatic gas than in the atmosphere.
- Because the solubility of SO_2 in silicate melt is greater than that of CO_2 and less than that of *HCl* or *HF*, rising magma might produce CO_2 at first, then increasing SO_2/CO_2 ratios, and eventually increasing HCl/SO_2 or HF/SO_2 ratios.
- SO_2 within the crust is a product of the oxidation of elemental sulfur released during the decomposition of sulfides at high temperatures (when they come in contact with basaltic magmas).
- In rhyolites containing between 69 and 78 wt% Si, water is the most abundant (3-7 wt%) and follows CO_2 up to 1,000 ppm, chlorine 600 to 2,700 ppm, fluorine 400 to 1,500 ppm, and sulfur ~200 ppm.

- Effects of bubbles on magma viscosity depends on the degree of vesiculation, the size and distribution of bubbles, and the melt viscosity (influence viscosity of acidic magma).
- During the decompression of magma with an initial dissolved gas content of 5–7 wt%, the bubbles could occupy up to 99 % of its volume.

Magma Volatiles Solubility

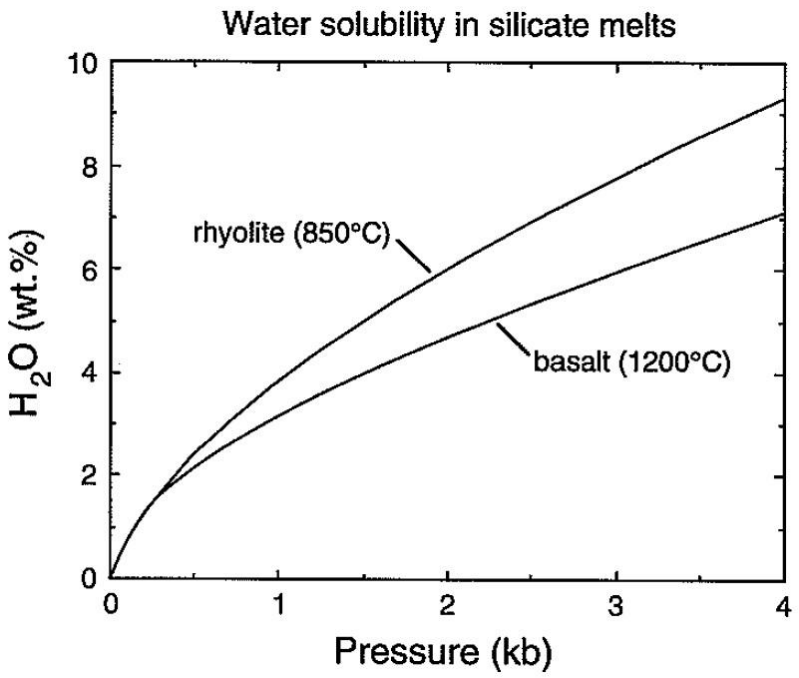

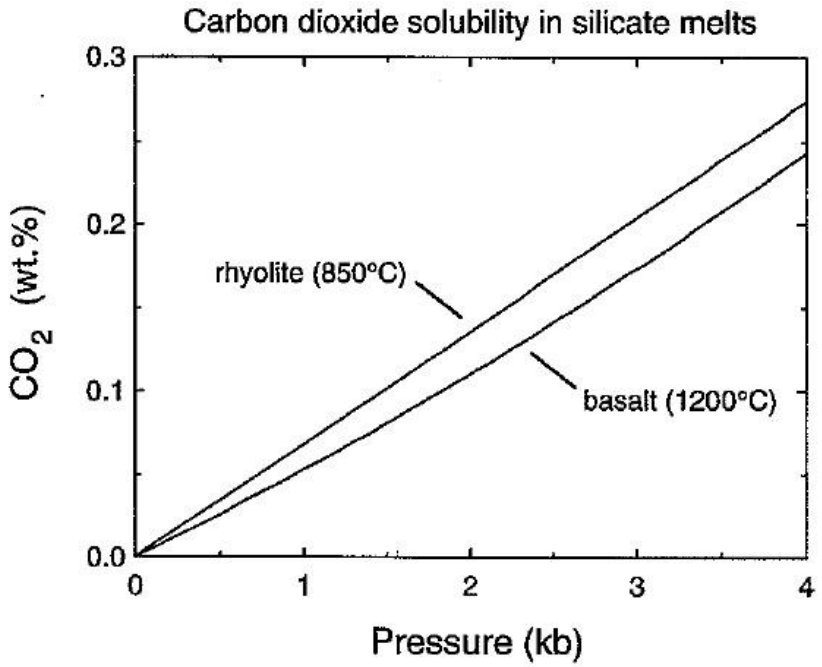

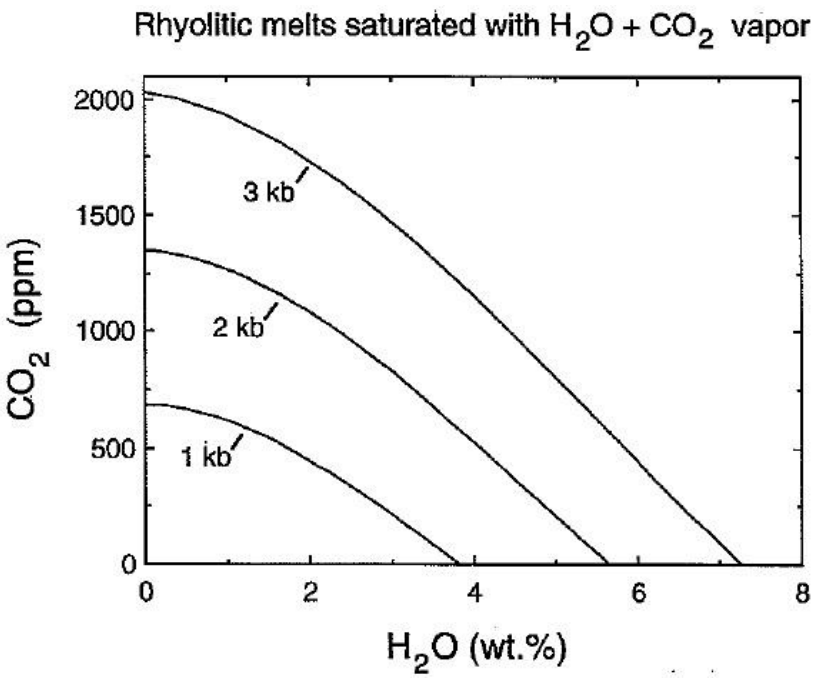

Wallace and Anderson, 1999

- Dissolved water in silicate melts occurs as OH^- groups and H_2O molecules, depending on total water concentration. As soon as total dissolved water concentrations increase over 3-3.5 % of total water the proportion of H_2O molecules increases.
- The amount of CO_2 in silicate melts is 50-100 times less than the solubility of H_2O at comparable *P* and *T*.
- CO_2 dissolves in silica-poor melts as CO_3^{2-}, while in high-silica melts as CO_2 molecules and thus is more soluble in rhyolitic melt than basaltic melt.
- For vapor-satured silicate melts, the solubility of individual volatile components are dependent in part on the abundance of other volatiles that are present in the system, since the amount of a given component dissolved in the melt is proportional to the partial pressure of the volatile component in the coexisting equilibrium vapor.
- In a silicate melt saturated with vapor consistent only of H_2O and CO_2 the sum of the partial pressures of these components (P_{H2O} *and* P_{CO2}) in the vapor phase must equal the total *P* in a vapor-satured melt.

Phase equilibria for a wet and dry magma

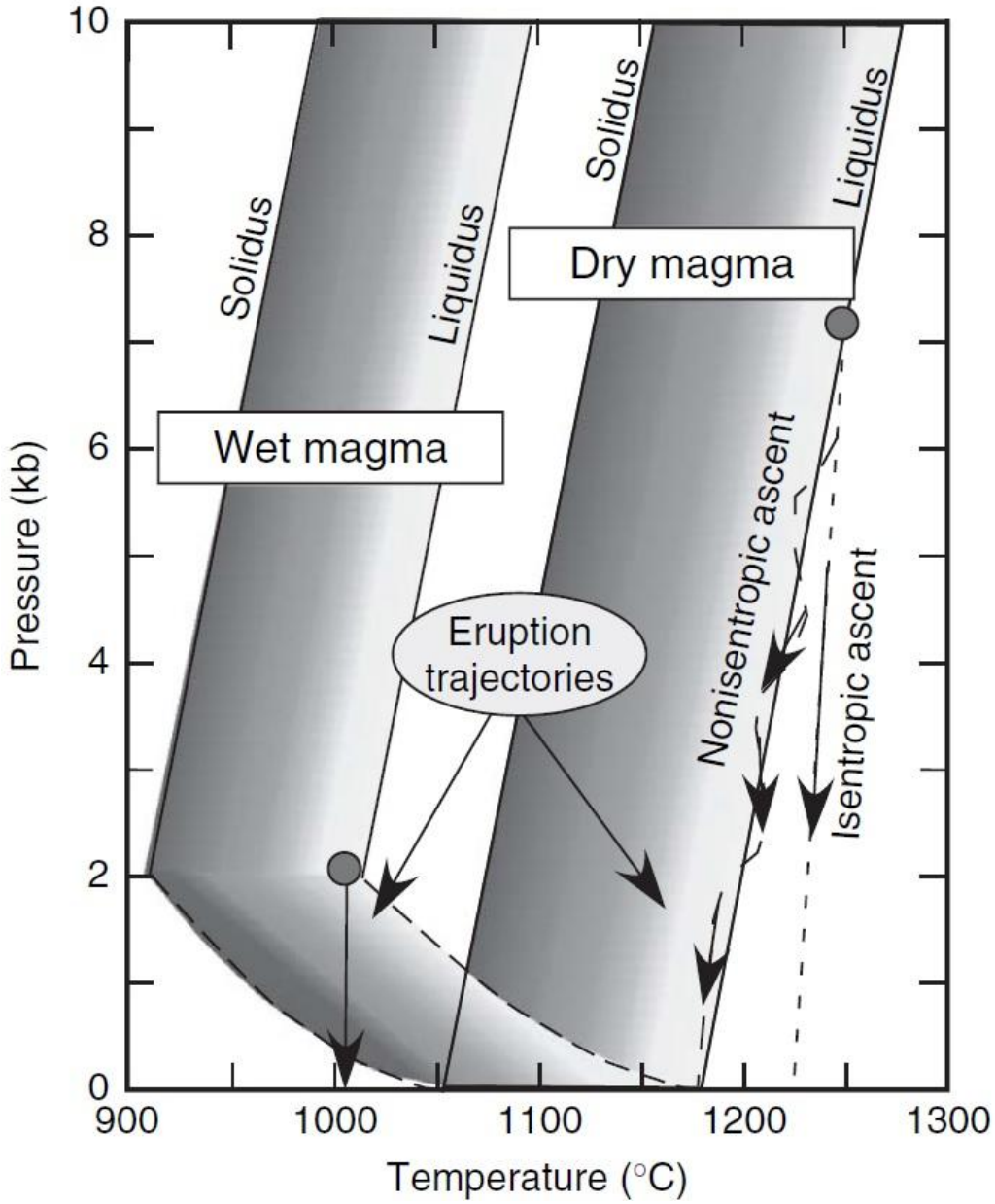

- The solubility of volatiles is directly proportional to the confining pressure and there is also a point at which no more water can be dissolved in the magma.
- At *P*= 2 kb (200 MPa), corresponding to the saturation point, the wet magma is undersaturated with water and the phase diagram is similar to that of the dry magma (just at lower *T*).

Marsh, 2007, Treatise of Geophysics, vol. 6

Magmatic Systems

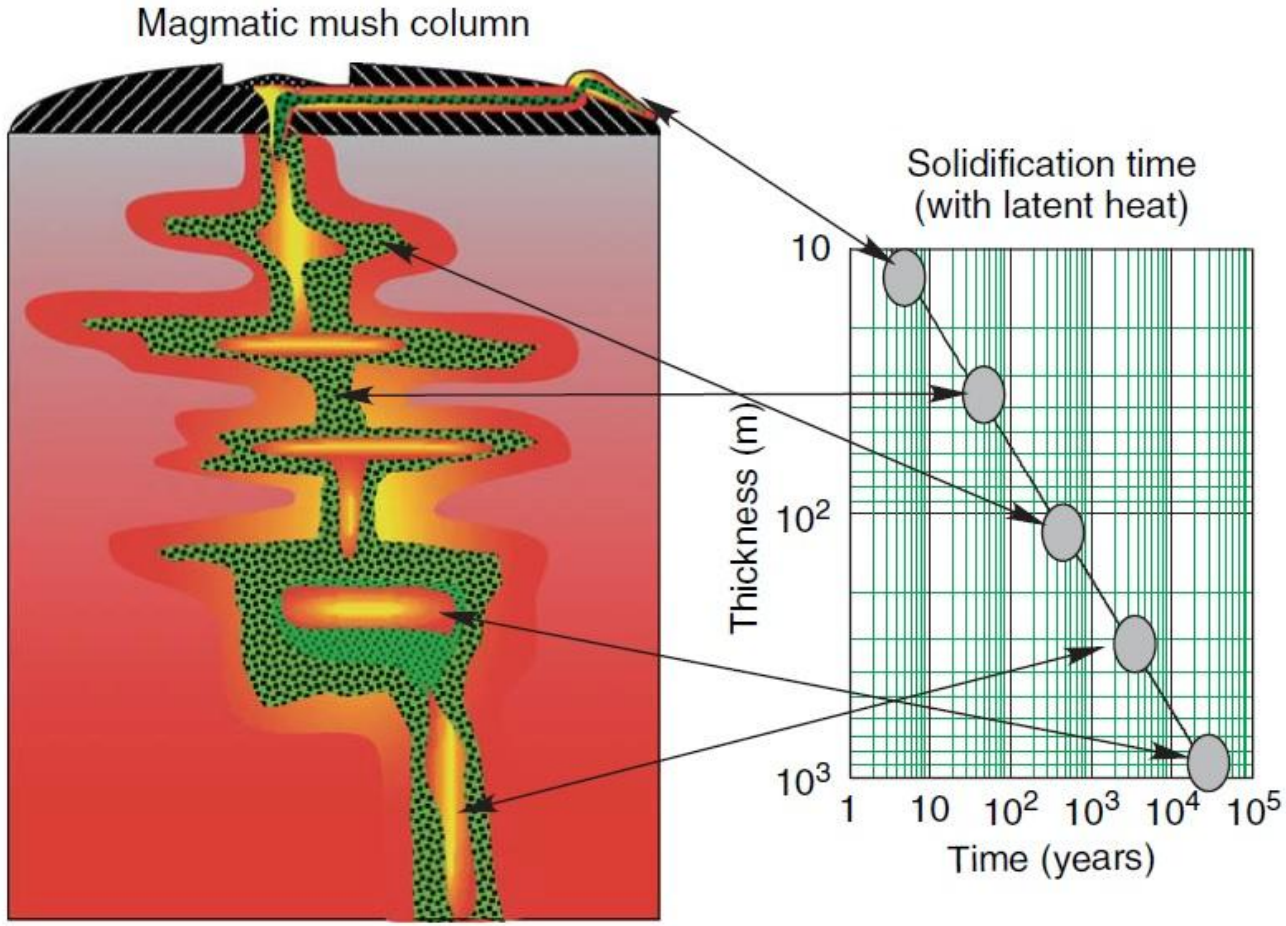

Marsh, 2007, Treatise of Geophysics, vol. 6

- **The thermal timescales for solidification vary throughout the system due to the local thermal regime and the length scale of the system.**

Convection in a magma chamber

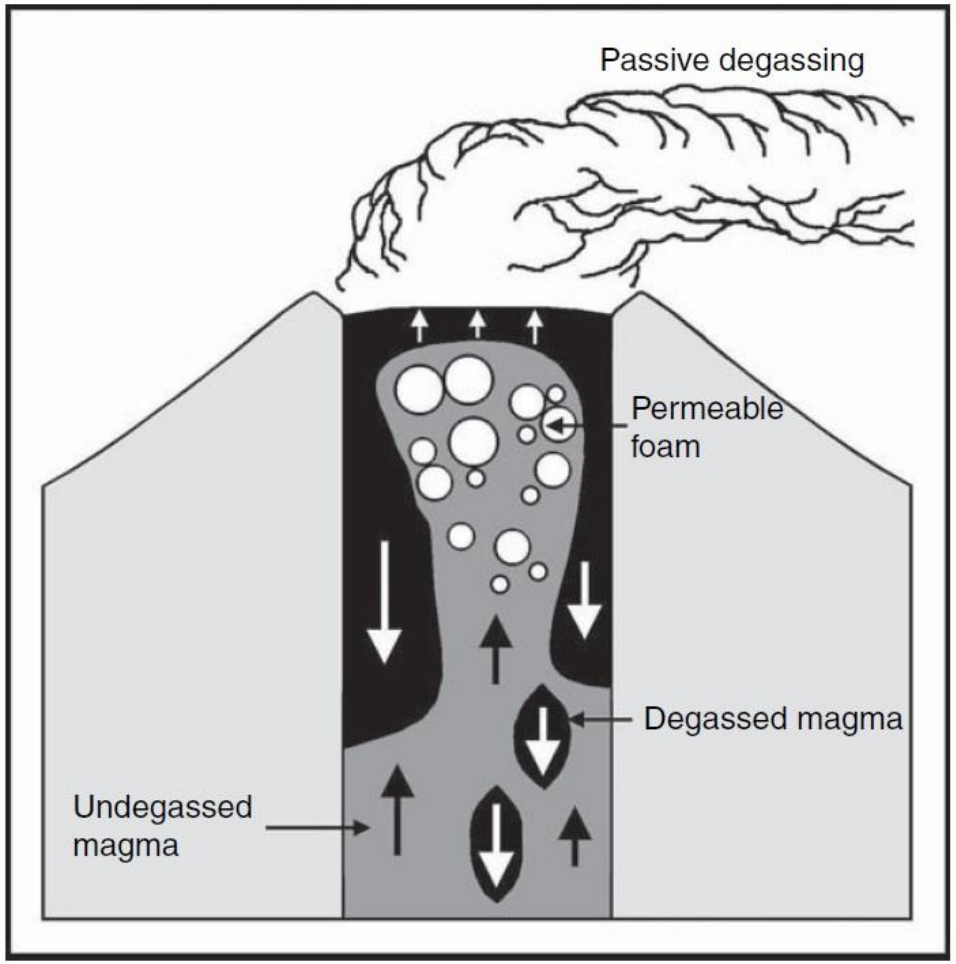

- Gas-rich magma develops a head of foam near the surface. Gas escapes, and the degassing foam collapses, sinking back down through the column, displacing gas rich magma upward.
- Once the process begins, it will be driven primarily by sinking blebs, until the supply of fresh gas rich magma into the conduit becomes too slow to sustain the process.

Magma Upwelling

Magma ascension occurs because of:

- Difference in density (due to *T*) with the hosting rocks (diapirs).
- Migration through fractures generated by magma pressure.

- Fractures move upwards and reach a critical length depending on (1) the elastic properties of the medium (2) fracture size (3) density contrast between the magma and the medium.
- Fractures formation is favored by gases (besides high temperature and water), which would corroder the rocks, reducing the energy required for fracturing the medium.

The rate of propagation of dykes is controlled by the rate of the fracturing at the tip and by the flow rate of magma inside the dyke:

(1) When high energy is needed to fracture the host rock and magma viscosity is low, the rate of propagation is controlled by the rate of fracturing (fracture controlled regime).

(2) When the energy needed to fracture the host rock is low, propagation is controlled by the magma flow rate (magma–controlled regime).

Magma Upwelling causes seismicity:

- Low-frequency earthquakes at volcanoes seem to occur by rupture of relatively ductile material, (either hydrothermally altered rock or of viscous, nearly solid magma).
- Some low-frequency events termed long period earthquakes may related to the re-supply of magma from depth into shallower reservoirs and reflect the time it takes for fluid head to pass through the constriction.
- Volcanic tremor characterized by periods of continuous vibration lasting from minutes to years are induced by magma flow, resonance of a fluid-filled crack or hydrothermal boiling.

Lava Flows

Transition between laminar and turbulent flow can be estimated from the **Reynolds number (R_e)**

$$R_e = \frac{\rho \, v \, D}{\eta}$$

where *v* is the mean velocity, ρ the density and D is the diameter of a circular conduit

Transition between laminar and turbulent flow occurs at values of *Re* between 500 and 2000

For Bingham fluids:

$$R_e \geq 1000 \, B \qquad B = \frac{\tau_o D}{\eta \, v}$$

Hampton Number: **Re/B=** $\frac{\rho \, v^2}{\tau_o} \geq 1000$

with τ_0 the mechanical strength of the material

Only lava with low viscosity can have a turbulent flow (when the ground slope increases the already high velocity of the lava).

$$\eta = \frac{g \, \rho \, h^2 \operatorname{sen} i}{n \, v}$$

where *i* is the ground inclination, *h* and *v* is the thickness and velocity of the lava flow, g is the gravity acceleration, ρ is the density, and n =3 (for thick lava flows) up to 4 (for thin lava flows).

Eruption triggering mechanisms

Internal:

- Intrusion of fresh magma (and its gas) from depth, driven by partial melting and by buoyant forces and/or lithostatic squeezing
- Buildup of gas pressure as magma rises.
- In situ buildup of gas pressure from crystallization, as in 'second boiling'.
- Mixing of fresh magma with pre-existing magma (addition of fresh mafic magma raises *T* of pre-existing magma and decreases the gas solubility).

External:

- Regional earthquakes: They can trigger eruptions through local faulting that relieves confining pressure, shaking-induced bubble nucleation, or in low viscosity hydrothermal water, shaking-induced rise and pressurization of bubbles.
- Unloading, rapidly as by a massive landslide off a volcano's flank, or slowly, as by glacial retreat: Decrease of confining pressure induces exsolution of volatiles and the related chain of increased buoyancy and/or increased internal pressure.
- Earth tides: Some volcanoes show a slight statistical preference to erupt on or around fortnightly tidal maxima (or minima) or near semidiurnal tidal maxima (or minima). These volcanoes have relatively open conduits, relatively low-viscosity magma, and frequent, small eruptions.

Explosive eruptions

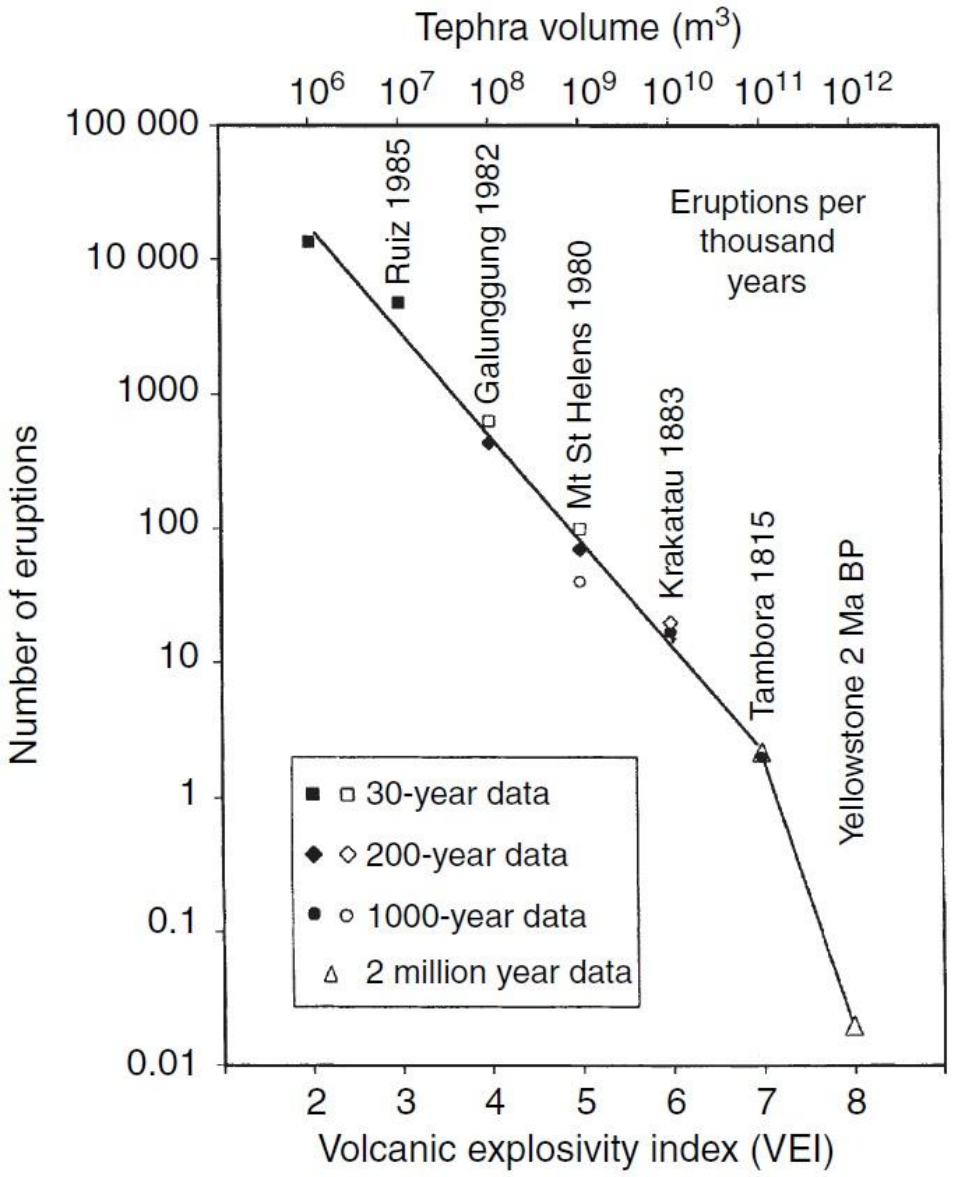

Newhall, 2007, Treatise of Geophysics, vol. 4

- The explosivity of an eruption is an expression of the AMOUNT and RATES of exsolution and bubbles growth.
- The explosivity and eruption is a function of (1) initial gas content and melt and magma viscosity (the latter influences how fast bubbles can expand and how fast dissolved volatiles can diffuse through melt into bubbles); (2) presence or absence of impurities to cause heterogeneous bubble nucleation; (3) presence or absence of a preexisting discrete bubble phase; and (4) effective permeability of the magma, magma foam, and wallrock.
- The volcanic explosivity index (VEI) is based mainly on bulk volume of pyroclastic deposit, maximum column height, and duration of eruption.

Explosive *vs* effusive eruptions

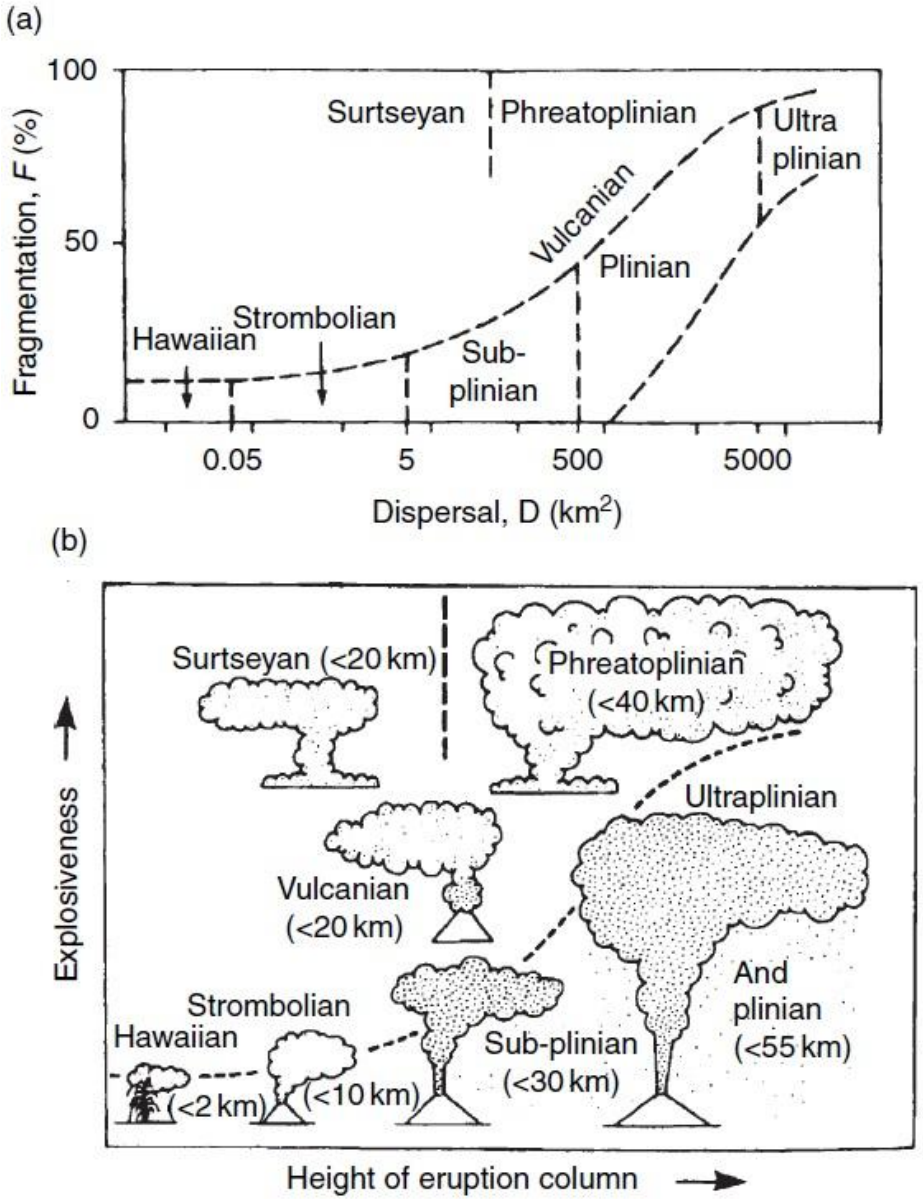

Newhall, 2007, Treatise of Geophysics, vol. 4

A quantitative classification of explosive eruptions is based on two characteristics of their fall deposits:

1. Fragmentation (*F*) = wt.% of pyroclasts <1mm along dispersal axis, where thickness = 0.1 maximum thickness of deposit (0.1 T_{max}).
2. dispersal (*D*)=area enclosed by (0.01T_{max}) isopach line of the tephra fall deposit.

- Ascent rates of 0.5ms^{-1} or higher inhibit degassing enroute to the surface and result in higher explosivity; those of 0.05ms^{-1} or lower encourage enroute degassing and result in relatively low explosivity.
- It has been suggested correlation of magma supply rate to column height and dispersal (*D*), and proportion of erupted magma that is erupted explosively (%tephra) to explosivity and fragmentation (*F*).

Volcanic Eruptions

- The magma starts to rise when the pressure *P* within the magma becomes larger than the lithostatic pressure $P_0 (P>P_0)$.
- Lower pressure are required for the rhyolitic magma, due to their lower density.
- Higher temperature and a decrease of volume of the magma leads to an increase of *P* compared to P_0 (increase in *excess P*).

A change in temperature (*T*) and pressure (*P*) results in a change in volume (V_0):

$$dV = (dV/dP)_T dP + (dV/dT)_P dT \qquad \frac{dV}{V_0} = \frac{1}{V_0}(dV/dP)_T dP + \frac{1}{V_0}(dV/dT)_P dT$$

$$\alpha = \frac{\left(\frac{\partial V}{\partial T}\right)_P}{V_0} \qquad \beta = -\frac{\left(\frac{\partial V}{\partial P}\right)_T}{V_0} \qquad \frac{dV}{V_0} = -\beta dP + \alpha dT \qquad P = P_0 + \frac{\alpha}{\beta}(T - T_0) - \frac{1}{\beta}\frac{\Delta V}{V_0}$$

$$P_T = \frac{\alpha}{\beta}(T_m - T_0) \qquad P_c = -\frac{1}{\beta}\frac{\Delta V}{V_0} \qquad P_c = \frac{1}{\beta}\frac{\Delta \sigma}{\sigma}$$

P_T and P_c are the additional pressure due to the excess temperature (determined by the difference between the magma temperature, T_m and the normal temperature T_0) and decrease of volume during magma formation (a magma has a lower density than when is solid and thus needs more space. This creates an excess of pressure P_c).

$$P = P_0 + P_T + P_c \qquad P - P_0 = P_T + P_c \qquad P\text{-}P_0 > 0$$

Unloading pressure ($\Delta V/V_0$) depends on the volume of the magma chamber V_0 (ΔV must increase for large magma chamber).

Normal Temperature

- The normal temperature T_0 for matter is determined using the condition for the equilibrium line: $V/V_0=1$ ($\Delta V=0$)
- $T > T_0$ will lead to an increase of P compared to the lithostatic or hydrostatic value, whereas $T < T_0$ will lead to pressures below the lithostatic or hydrostatic value.
- $\Delta V = 0$ represents a state of equilibrium and is used to determine the normal temperature T_0.

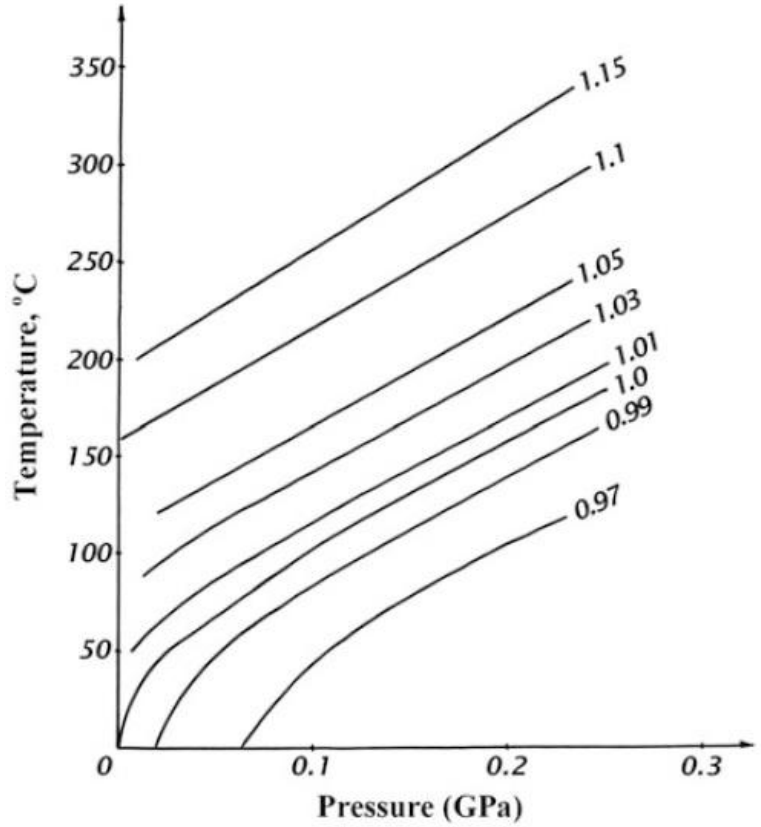

Change in a unit of volume of water under a wide range of P and T

The equilibrium condition $\Delta V = 0$ is represented by the line V/V0 = 1; conditions with $\Delta V>0$ are represented by lines $V/V_0>1$, and $\Delta V<0$ are represented by lines $V/V_0<1$ respectively.

Calculating the lithostatic pressure for different depths and substituting it for P_0 can be used to find the value of T_0 for the rock or mineral at the depth for which P_0 was determined (since for each depth there is only one pair of P_0 and T_0 values, represented by the line of equilibrium).

Density variations due to melting

Changes in densities of some typical magmatic rocks upon melting

Rock	Density of molten rock (in kg/m^3)	Density of solid rock (in kg/m^3)	Relative change of density on fusion ($\Delta\sigma/\sigma$)
Rhyolites[a]	2,170	2,280	−0.0482
Andesite[a]	2,410	2,590	−0.0695
Tholeiite basalt	2,600	2,760	−0.0580
Alkali olivine basalt	2,680	2,830	−0.0530
Diabase[a]	2,640	2,960	−0.1081
Basalt, gabbro	2,600	2,900	−0.1034
Rhyolite, granite	2,300–2,400	2,600	−(0.0769–0.1154)
Diabase[a]	2,603	2,890	−0.0993
Diabase[a]	2,640	2,880	−0.0833
Rhyolite[a]	2,310	2,450	−0.0571
Andesite[a]	2,580	2,830	−0.0883
MORB	2,650	2,950	−0.1017
Mars basalts	2,720	3,130	−0.1310
Komatiites	2,730	3,090	−0.1165
Basalt	2,600	2,800	−0.0714
Silicic melt	2,300	2,600	−0.1154

- The process of magma formation requires a change in volume of about 4.8–13.1 % (the density of magmatic rocks is 10–20 % greater than their corresponding melts).

Further values of density variations: -0.2012 for both diopside and for enstatite, -0.0462 for anorthite, -0.0779 for forsterite and -0.1138 for fayalite.

Thermal expansion coefficient (α) and compresibility coefficient (β)

Thermal expansion coefficient (α) and compressibility coefficient (β) values for some typical magmatic melts

Molten rock	Thermal expansion coefficient (α), 10−51/K	Compressibility coefficient (β), 1/GPa	References
Average silicate melt	3	0.07	McBirney (2000)
Average silicate melt	3	0.07	Best (2002)
Kilauea gas poor magma	–	0.06–0.10	Rivalta and Segall (2008)
Rhyolite[a]	7.1	–	Guillot and Sator (2007)
Andesite[a]	9.8	–	Guillot and Sator (2007)
MORB[a]	11.1	–	Guillot and Sator (2007)
Mars basalts[a]	12.3	–	Guillot and Sator (2007)
Komatiites[a]	13.1	–	Guillot and Sator (2007)
Rhyolite	10.1	–	Nelson and Carmichael (1979)
Rhyolite	3.8	–	Lange and Carmichael (1987)
Rhyolite	5.3	–	Ghiorso (2004)
Andesite	8.1	–	Nelson and Carmichael (1979)
Andesite	5.5	–	Lange and Carmichael (1987)
Andesite	6.0	–	Ghiorso (2004)
MORB	10.6	–	Nelson and Carmichael (1979)
MORB	6.4	–	Lange and Carmichael (1987)
MORB	7.0	–	Ghiorso (2004)
Komatiites	4.7	–	Courtial et al. (1997)
Komatiites	9.7	–	Ghiorso (2004)
Komatiites	8.1	–	Lange and Carmichael (1987)
Peridotite	6.2	0.05587	Suzuki et al. (1998)
Peridotite	5.9	0.05649	Suzuki et al. (1998)
Basalt	–	0.1	Rivalta and Segall (2008)
Mount St. Helens Magma	–	0.28[b]	Mastin et al. (2008)
Magma, Soufrière Hills Volcano, Montserrat	–	0.758[c]	Voight et al. (2010)

[a] At a temperature of 1,800 K and low pressure
[b] Magma contains ~1.2 % bubbles
[c] Saturated magma plus exsolved gas

$$\frac{\Delta P}{\Delta T} = \frac{\alpha}{\beta}$$ (e.g., or the average silicate melt ratio α/β = 0.43 MPa/K)

Average values of this ratio for basaltic and rhyolitic magmatic rocks are 1.571 and 0.943 MPa/K

- **Presence of gases and water in magma significantly increases β**
- **Both α and β depend on the magma composition and its *T* – *P* conditions.**

Solidus/Liquidus Temperature for igneous rocks

Melting point/solidus temperature (in K) and liquidus temperature (in K) of most typical magmatic rocks for dry and wet conditions at pressures of 0.1 MPa and 1 GPa

Rock	Melting point or solidus temperature of dry rock at 0.1 MPa/1 GPa	Melting point or solidus temperature of wet rock at 0.1 MPa/1 GPa	Melting point or solidus temperature of saturated rock at 0.1 MPa/ 1 GPa	Liquidus temperature of dry rock 0.1 MPa/1 GPa	Liquidus temperature of wet rock 0.1 MPa/ 1 GPa
Granites	1,233/–	1,233/953[a]		1,569/–	
Granite	1,223/1,333		1,223/893	1,293/–	1,293/983
Granite	1,153/1,333		1,153/893		1,293/993
Andesite	1,263/1,343		–/903	–/1,513	1,473/1,213
Tholeiite basalt	1,353/1,413	1,303/913		1,483/1,533	1,463/1,463
Basalt	1,353/1,413		1,343/913	–/1,523	–/1,333
Peridotite	1,403/1,493		1,403/1,153		
Peridotite	1,518/1,587				
Rhyolite	943–953/–	923/–	923–973/–		
Peridotite	1,363/1,613[b]	–/1,353			–/1,523
Peridotite	1,400/1,700[b]	1,340/1,270[b]			
Basalts	1,525[c]/–				
MORB	1,516–1,624[d]/–				
OIB	1,559–1,645[d]/–				
Picrite	–/1,798				
Komatiite	2,063/–				
Tonalite	1,173/–		1,153/903		1,293/993
Peridotite	1,405/1,535				
Quartz eclogite	–/1,588[b]			–/1,773–1,798[b]	

[a] At 200 MPa
[b] At ~3 GPa
[c] Eruption temperature of most basalts (Schubert et al. 2001)
[d] The parental liquids (Falloon et al. 2007)

- At a depth of about 100 km, peridotite begins to melt at ~1,073 K (with an excess of water), while in the absence of water at ~1,773 K.
- T_s of a granitic melt drops from ~1,233 K with no water to 953 K with a water content increase to ~6.0 wt%.
- The solubility of H_2O in a granitic melt increases from 0 to ~6.0 wt% with an increase of P from 0 to 200 MPa.
- In most cases for water-rich magmas T_s and T_L have a negative gradient of $\Delta T/\Delta P<0$ within a P range of 0–1 GPa. The gradient is usually negative up to a pressure of about 2 GPa and stabilizes at higher values of P and can also starts to slightly increase.

Conditions in forming and rising basaltic magma

P (0-4 GPa), *T* (1600-1900 K), α (8.8 x 10^{-5} K^{-1}), β (0.056 GPa^{-1})

Thermodynamic conditions within forming and rising magma of basaltic composition

Temperature of magma (K)	Lithostatic pressure (P_0) (GPa)	Normal temperature (T_0) (K)	P_T (GPa)	P_C (GPa)	Total P (GPa)
1,600	4	2,818	−1.911	1.00–2.16	3.09–4.25
	3	2,182	−0.913	0.24–1.42	2.33–3.51
	2	1,546	0.085	−0.48–0.64	1.61–2.63
	1	909	1.084	−(1.24–0.12)	1.16–1.96
	0.5	591	1.583	−(1.62–0.88)	0.46–1.20
	0	273	2.082	−(2.00–1.26)	0.08–0.82
1,700	4	2,818	−1.754	1.00–2.16	3.25–4.31
	3	2,182	−0.752	0.24–1.42	2.49–3.67
	2	1,546	0.242	−0.48–0.64	1.76–2.88
	1	909	1.241	−(1.24–0.12)	1.00–2.12
	0.5	591	1.740	−(1.62–0.88)	0.62–1.36
	0	273	2.238	−(2.00–1.26)	0.24–0.98
1,800	4	2,818	−1.597	1.00–2.16	3.40–4.56
	3	2,182	−0.599	0.24–1.42	2.64–3.82
	2	1,546	0.399	−0.48–0.64	1.92–3.04
	1	909	1.398	−(1.24–0.12)	1.16–2.28
	0.5	591	1.897	−(1.62–0.88)	0.78–1.52
	0	273	2.396	−(2.00–1.26)	0.40–1.14
1,900	4	2,818	−1.440	1.00–2.16	3.56–4.72
	3	2,182	−0.442	0.24–1.42	2.80–3.98
	2	1,546	0.555	−0.48–0.64	2.08–3.20
	1	909	1.555	−(1.24–0.12)	1.32–2.44
	0.5	591	2.054	−(1.62–0.88)	0.93–1.67
	0	273	2.553	−(2.00–1.26)	0.55–1.29

$$P = P_0 + \frac{\alpha}{\beta}(T - T_0) - \frac{1}{\beta}\frac{\Delta V}{V_0}$$

$$\Delta P_T = \frac{\alpha}{\beta}(T_{02} - T_{01}) \qquad P_c = \frac{1}{\beta}\frac{\Delta\sigma}{\sigma}$$

T_{02} and T_{01} = normal T of magma at two different depths

Total *P* does not consider the unloading of pressure caused by the increase of magma volume as it rises through the conduit (ΔV_c= 0.179 GPa and 0.143 GPa per 1 % of increased volume for basaltic and rhyolitic magmas, respectively) and the erupted magma volume (ΔV_E, equal to the real volume of a magmatic eruption by a volcano).

- ***P_c* is positive at large depth** (> 2GPa), where the melt cannot expand.
- ***P_T* increases with decreases depth**, since T_0 of magma lowers with decreases depth (at pressure >2 GPa the effect of β overcomes that of α).
- At *T* ~1900 K and *P*=2 GPa the total pressure exceeds the lithostatic pressure of ~0.08 GPa, but it is not sufficient for rising (to overcome the friction of magma or its small expansion).
- In cases of rock with a very large difference of density between its solid and molten states (σ ~0.1212), the excess in pressure would be high enough for the magma to begin rising from depths with a pressure of 4 GPa or lower.
- For volcanoes as high as 2, 3, 4, and 5 km, the minimal additional *P* for the basaltic magma rising to the surface would be 0.051, 0.076, 0.101, and 0.127 GPa, respectively.

Conditions in forming and rising rhyolitic magma

P (0-1 GPa), T (1000-1500 K), α (6.6 x 10^{-5} K^{-1}), β (0.07 GPa^{-1})

Thermodynamic conditions within forming and rising magma of rhyolitic composition

Temperature of magma (K)	Lithostatic pressure (P_0) (GPa)	Normal temperature (T_0) (K)	P_T (GPa)	P_C (GPa)	Total P (GPa)
1,500	1	1,333	0.16	0.72–1.86	1.88–3.02
	0.7	1,012	0.46	0.53–1.67	1.69–2.73
	0.5	803	0.66	0.40–1.54	1.56–2.70
	0.3	591	0.86	0.27–1.41	1.43–2.57
	0	273	1.16	0.08–1.22	1.24–2.38
1,200	1	1,333	−0.13	0.72–1.86	1.59–2.73
	0.7	1,012	0.18	0.53–1.67	1.41–2.55
	0.5	803	0.37	0.40–1.54	1.27–2.41
	0.3	591	0.57	0.27–1.41	1.07–2.28
	0	273	0.87	0.08–1.22	0.95–2.09
1,000	1	1,333	−0.31	0.72–1.86	1.41–2.55
	0.7	1,012	−0.01	0.53–1.67	1.22–2.36
	0.5	803	0.19	0.40–1.54	1.09–2.21
	0.3	591	0.39	0.27–1.41	0.96–2.10
	0	273	0.69	0.08–1.22	0.77–1.91

- P_c is positive at large depth, where the melt cannot expand
- P_T increases with decreases depth, since T_0 of magma lowers with decreases depth.
- For volcanoes as high as 2, 3, 4, and 5 km, the minimal additional pressure for them to reach the craters would be 0.043, 0.064, 0.085, and 0.107 GPa, respectively.
- The excess P is much higher than within basaltic magmas (rising magma is favored), making rhyolitic magmas more destructive (caldera formation).

Excess of Pressure due to Temperature

$$P_T = \frac{\alpha}{\beta}(T - T_0)$$

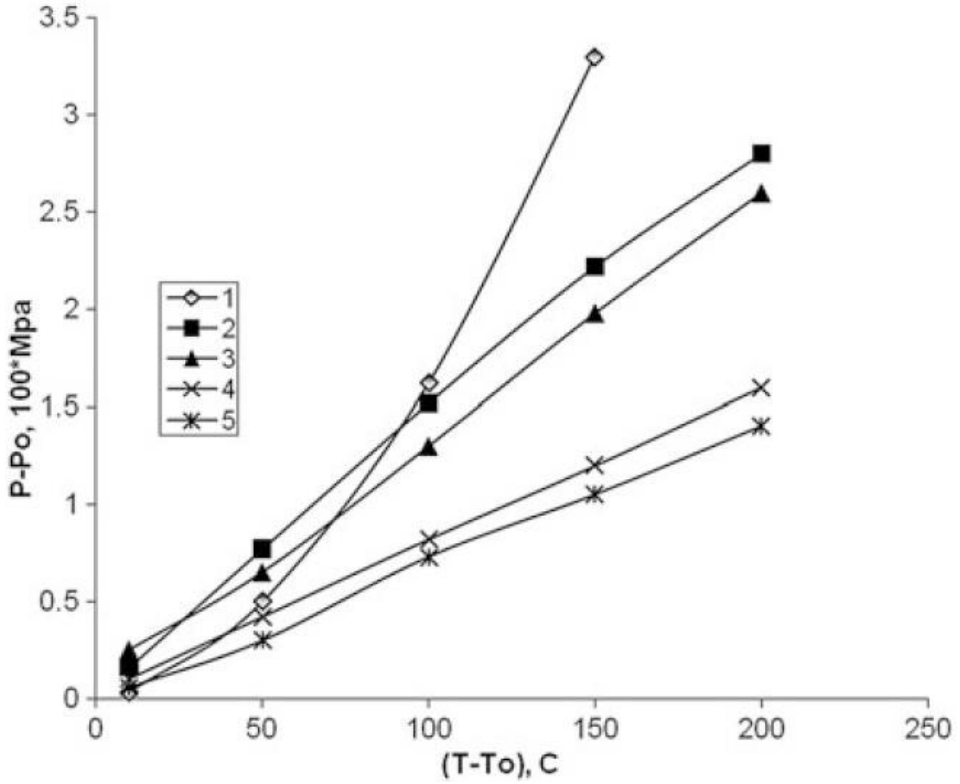

1 wet clay, 2 limestone, 3 granite, 4 sandstone, 5 basalt

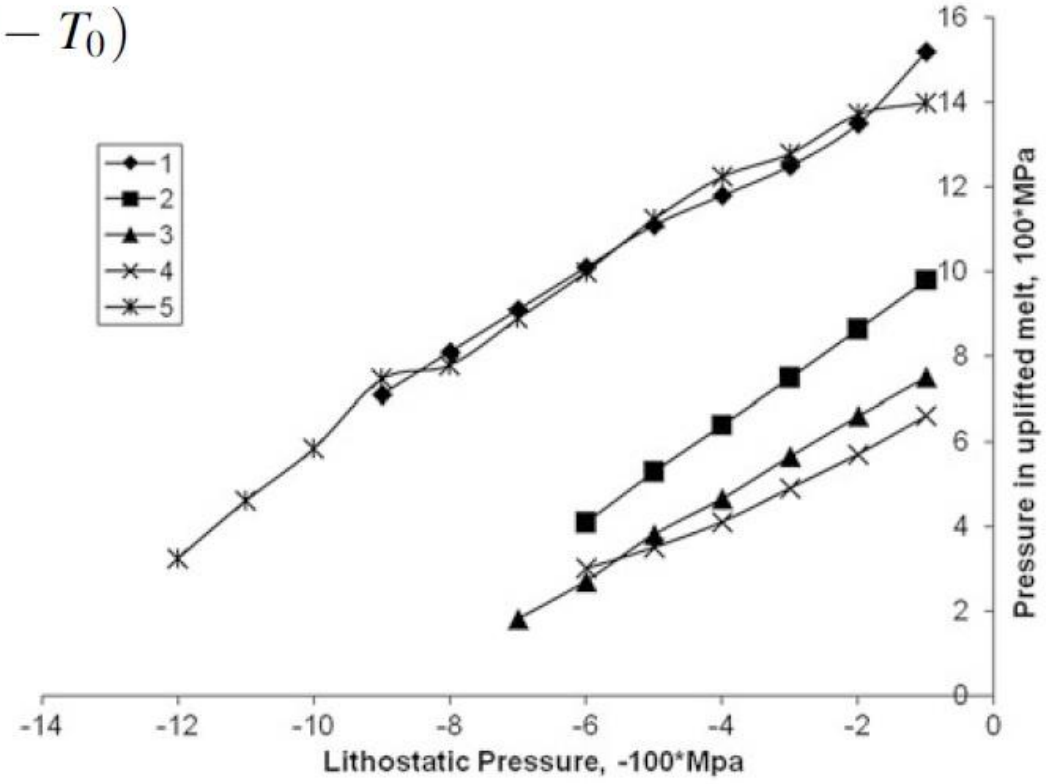

1 gabbro, 2 granite, 3 basalt, 4 diorite, 5 diabase

- Temperatures in excess of 100 K generate greater *P* increases in wet clays than in other rocks because of the large value of α_{water} (other rocks have larger viscosity and lower chances to expand).
- Heating of wet clays, salt and/or porous water high pressure results in the formation of mud volcanoes, geysers, fumaroles, etc.
- Additional increase in *P* caused by rising magma (due to the decrease of T_0 with the decrease in depth) is the largest in gabbro-diabase compositions and lowest in basalt-diorite melts.

Unloading/Loading of Pressure

$$P_U = \frac{1}{\beta}\frac{\Delta V}{V_0}$$

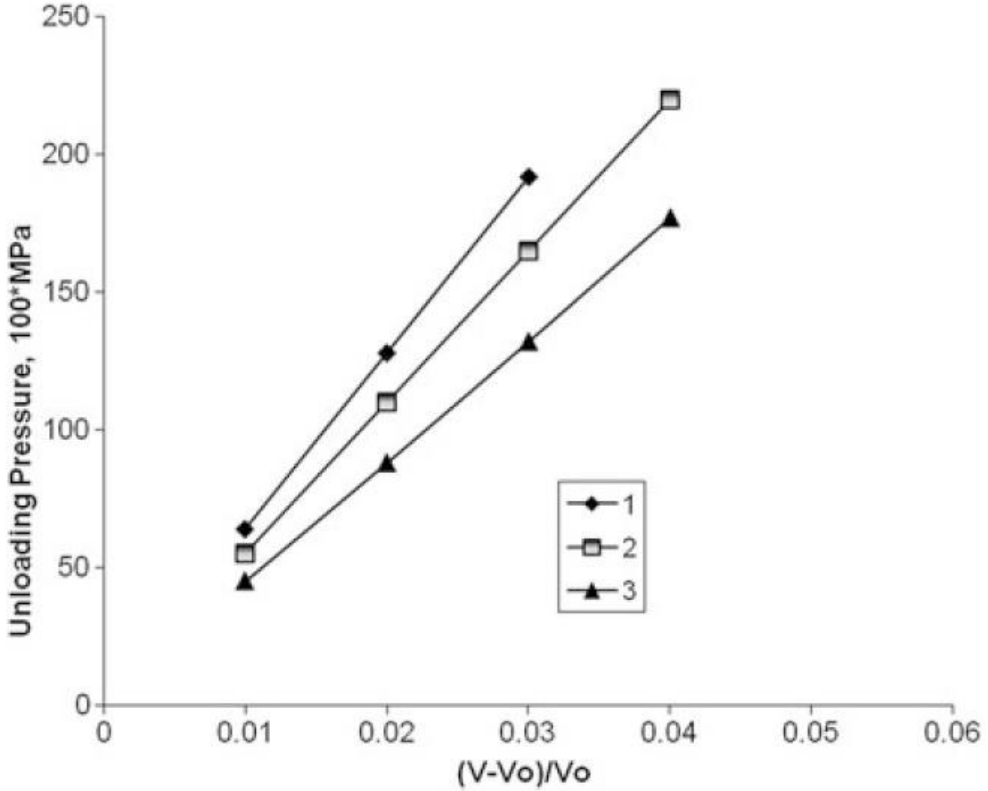

1 limestone, 2 granite, and 3 basalt

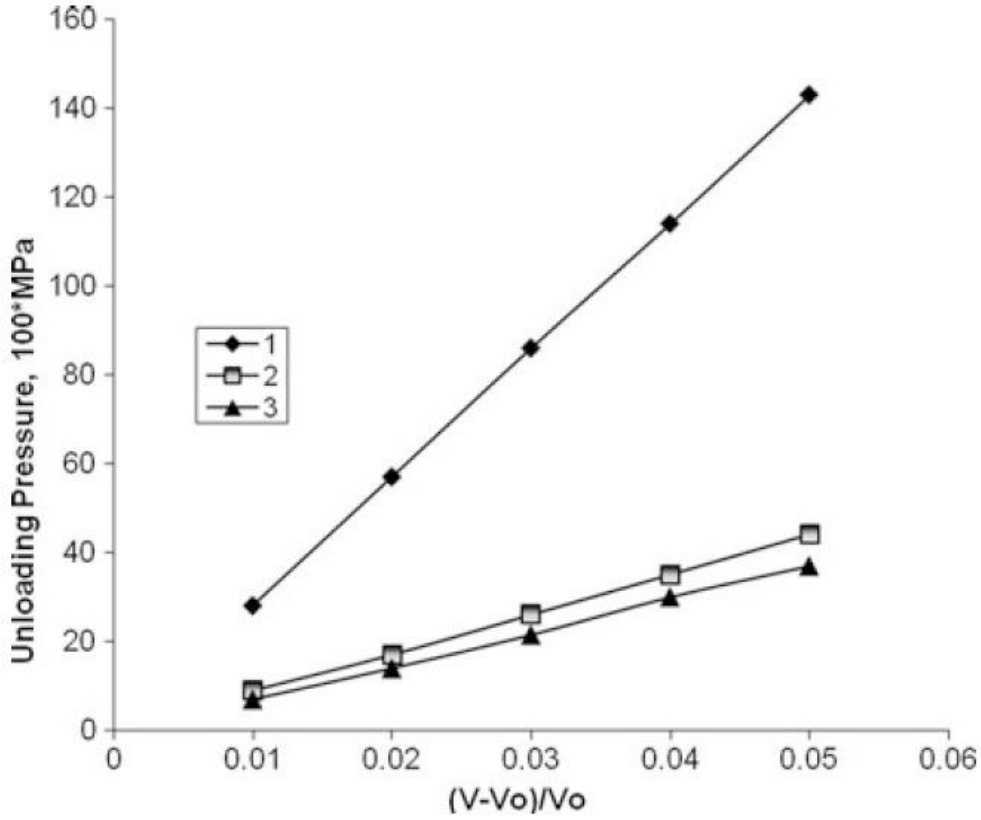

1 sandstone, 2 basaltic melt, and 3 wet clay

- Wet clay and basaltic melt in (mud) volcano eruptions have a relatively slow pressure unloading with increasing volume (they retain high excess pressure during eruption for a longer period).
- In compressional environment wet clay and basaltic melt acquire *P* much slower than granite melt.

Mud Volcanoes

It is a tectonic structure formed during the formation and eruption of significant amounts of water-rich sedimentary rocks (mostly clays and/or silts)

Mud Volcanoes

Thermo-physical properties of clay:

- The high porosity (~45 %) and very low permeability prevents the water from leaving the clay.
- The high water content decreases the clay viscosity to values of 10^6 Pas and favours the transfer of the pressure applied to the clay in all directions.
- The clays have a very low heat condution coefficient and a very high thermal expansion coefficient (α_c) and specific heat capacity. Then, they accumulate large amounts of heat energy, which remains trapped due to their low permeability.

$$a_c \approx K_p \cdot a_w$$

K_p = porosity coefficient and α_w = thermal expansion coefficient of the water (two orders of magnitude higher than for others rocks).

- This increase of volume and pressure is transferred through the plastic clay to all parts of the layers, exerting great pressure on the overburden, which can overcome lithostatic pressure and cause the rise of a diapir, with a mud volcano formation.

Mud Volcanoes

Conditions for mud volcano formation:

- A thick sedimentary cover (several kilometers) and plastic clayey components with an anomalously high formation of pore pressure (greater than the lithostatic pressure) and the presence of thermal water.
- Many mud volcanoes form in regions of volcanic activity (e.g., Pacific Ring of Fire) and are associated to high *T* within the crust (which gives excess *T* under the main plastic clay-rich layer) and regions characterized by serpentinization and salt layers.
- Temperature in a mud volcano chamber is often > 300 °C and causes a large increase of *P*: we should consider that the clay waterproof cap layer has a very small heat conductivity coefficient and high specific heat capacity, which can lead to the accumulation of huge amounts of heat energy below it.
- Clay material can reach the surface, due only to their low density, if the presence of pressure in the chamber is greater than the lithostatic pressure exerted by the weight of the column of clay rocks from the chamber to the surface. This would happen only if volcanoes chamber are 4-5 times greater than its height.
- Mud volcanoes require the presence of huge compressive tectonic forces, which increase fluid pressure, and faults below the thick plastic clay-rich layer, which can act as a pathway for upward migration of overheated fluids. Then, they are often associated to large earthquakes, which favour faults formation.

Thermal waters, Hot springs, Geysers, Fumaroles

- Thermal water is related to the circulation of groundwater in the vicinity of sources of heat within the crust.
- A hot spring is a natural discharge of groundwater with a temperature of about 6.5 C or more above the mean air temperature.
- Reservoir temperatures for hot-water systems are possibly divided into low temperature (<363 K), intermediate temperature (from 363 to 423 K), and high temperature (from 423 to 513 K).
- A geyser is a hot spring with a mixture of steam and water. The boiling point of water at the discharge area is mostly dependent on the atmospheric pressure.

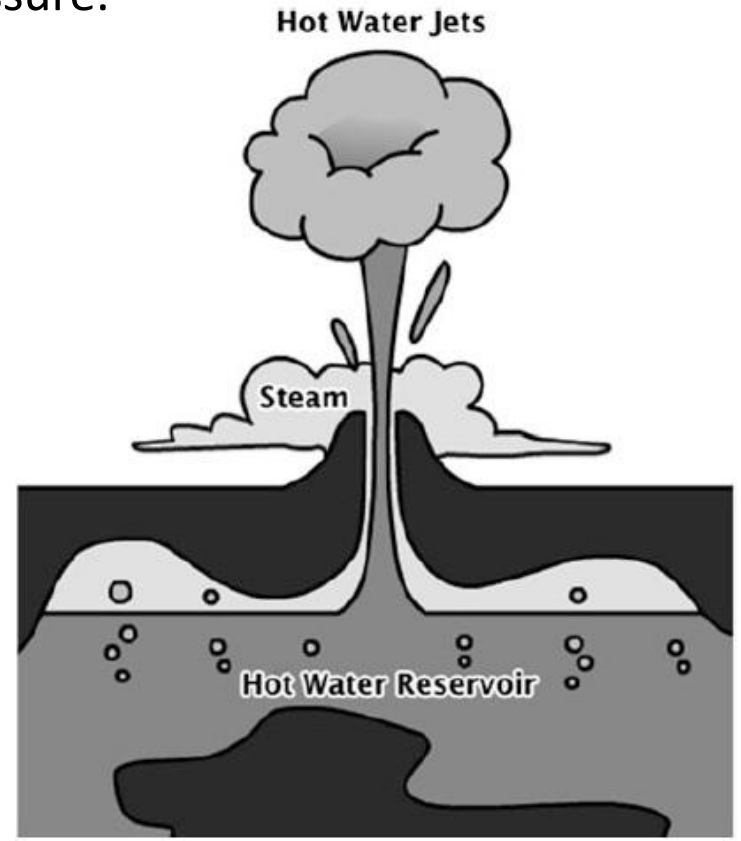

Temperature indicators form groundwater geochemistry

The water solubility of many geochemical compounds (e.g., silica) increases with *T* and their amount can be used to estimate *T*:

$$T = [1315/(5.205 - \log_{10} \mathbf{SiO_2})] \pm 0.5^{\circ}\mathrm{C} \quad (1)$$

Swanberg and Morgan (1979)

$$T = [1533.5/(5.768 - \log_{10} \mathbf{SiO_2})] \pm 2.0 \quad (2)$$

$$T = [1015.1/(4.655 - \log_{10} \mathbf{SiO_2})] \pm 2.0 \quad (3)$$

For sodium (*Na*), potassium (*K*), and calcium (*Ca*):

$$T = [855.6/(0.8573 + \log_{10}(\mathbf{Na}/\mathbf{K}))] \pm 2.0$$

$$T = [846/(0.5964 + \log_{10}(M_{\mathrm{Na}}/M_{\mathrm{K}}))]$$

$$T = [1647.3/(2.24 + \log_{10}(M_{\mathrm{Na}}/M_{\mathrm{K}}) + \beta \log_{10}(\sqrt{M_{\mathrm{Ca}}}/M_{\mathrm{Na}}))]$$

M_X = molar concentration of element X (i.e. moles per litre)
$\beta = 4/3$ for $(\sqrt{M_{\mathrm{Ca}}}/M_{\mathrm{Na}}) > 1$ and $T < 373.15$ K(100°C)
$\beta = 1/3$ for $(\sqrt{M_{\mathrm{Ca}}}/M_{\mathrm{Na}}) < 1$ or $T > 373.15$ K (100°C)
T is in kelvin

***T* range of precision: 125°-250°C** **SiO_2 (ppm by weight)** **T(K)**

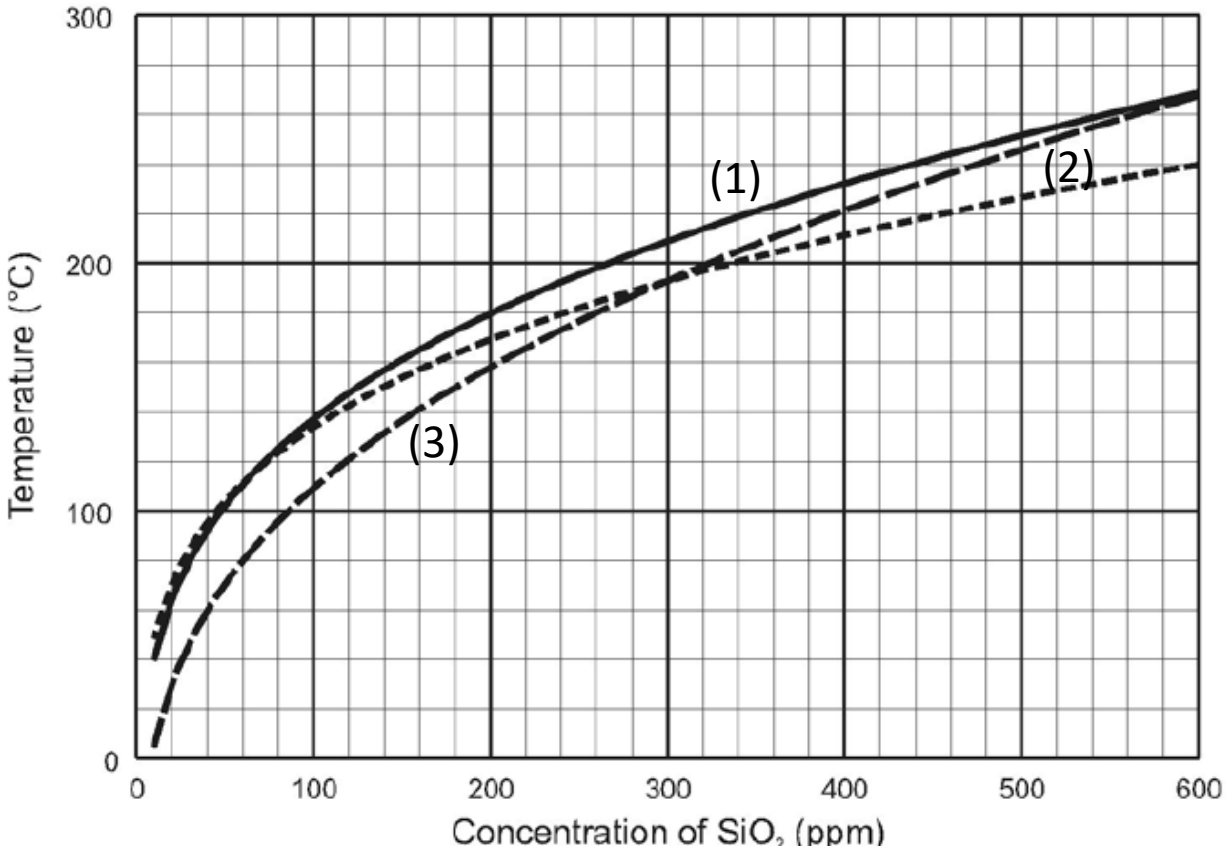

Magma cooling

- Cooling is the driving mechanism for crystallization and differentiation. It determines how, where, and how quickly crystals nucleate and grow.
- Most crystals are generated in the cold thermal boundary layers that develop at the margins of a magma body, where there are strong gradients of temperature, crystal content, and viscosity.

The thermal structure at the margin of a magma body is split in three different parts:

1) The part below the solidus is fully solid and may include a chill phase.
2) The part between the solidus and liquidus (magma is partially crystallized).
3) The part below the liquidus made of superheated magma (its existance depends on the initial conditions).

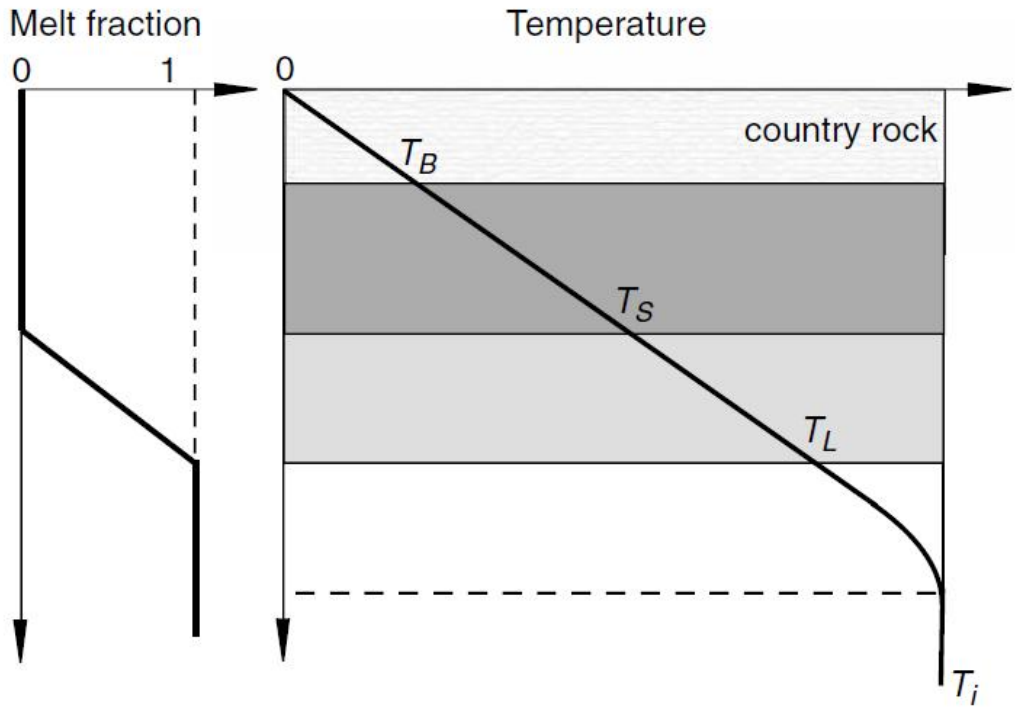

Thermal structure of magma bodies

- The partially crystallized zone, may be treted as an equivalent liquid with properties depending on the crystal content and composition of interstitial liquid.
- This layer is separeted by a rheological transition occurring for a solid fraction of ~55%: above this treshold, crystals are interconnected and immobile (cannot partecipate to covection), below it, crystals are suspended within a continuous liquid phase.
- Depending on the inital melt composition, the interstitial liquid may be less dense or denser than the uncrystallized magma.
- In a magma reservoir convection occurs, since cooling generates a negative density contrast, potentially unstable despite the magma composition ($\Delta\rho = -\rho_i \alpha \Delta T$). For α=3x 10^{-5} K^{-1}, κ=$10^{-6}$$m^2s^{-1}$, ΔT=10 K, η_m=10 Pa s, the upper layer is at least 10 cm and the magma layer 40 cm, to get N_U=2.

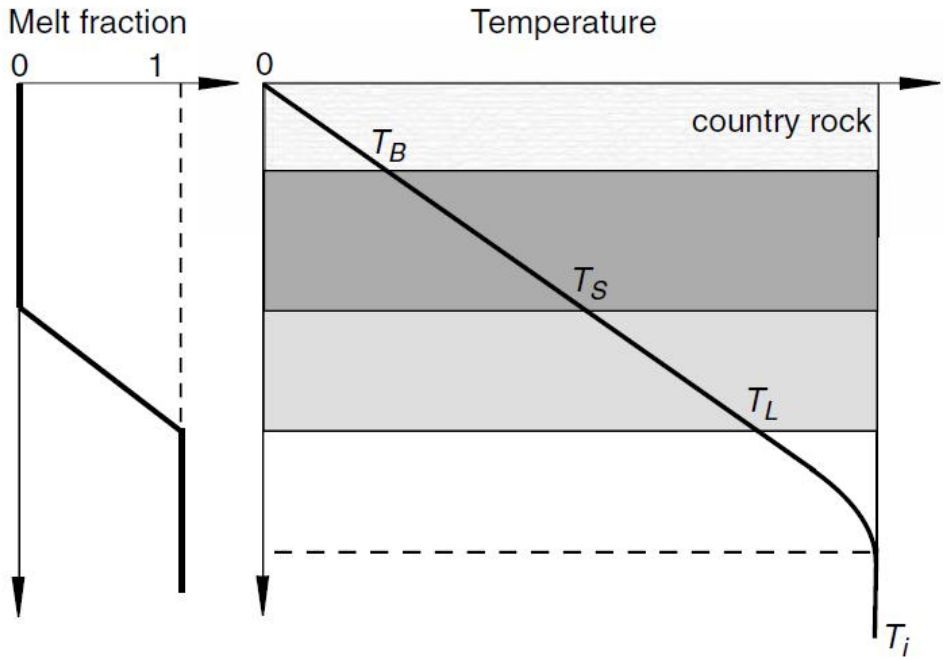

Cooling in a magma chamber

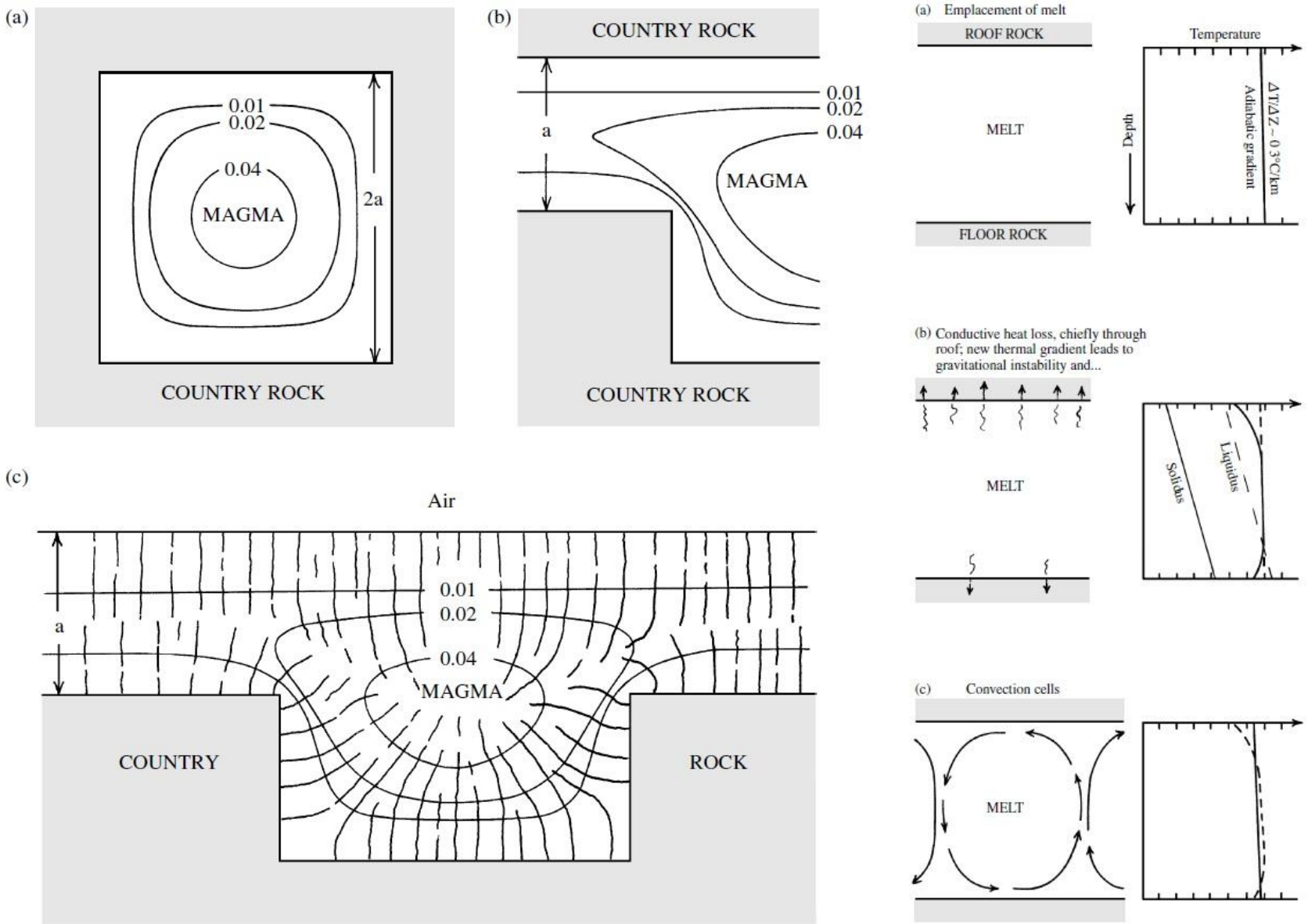

- Since the liquidus temperature of minerals increases about 3 °C/km depth, while the adiabatic gradient in melts is about one order less, crystallization occurs at the base of a uniform melt body of considerable vertical thickness.

Myron, 2003, Igneous and metamorphic petrology 2° Ed.

Cooling in a magma chamber

Thermochemical convection in a crystallizing bottle-shaped calc-alkaline magma chamber

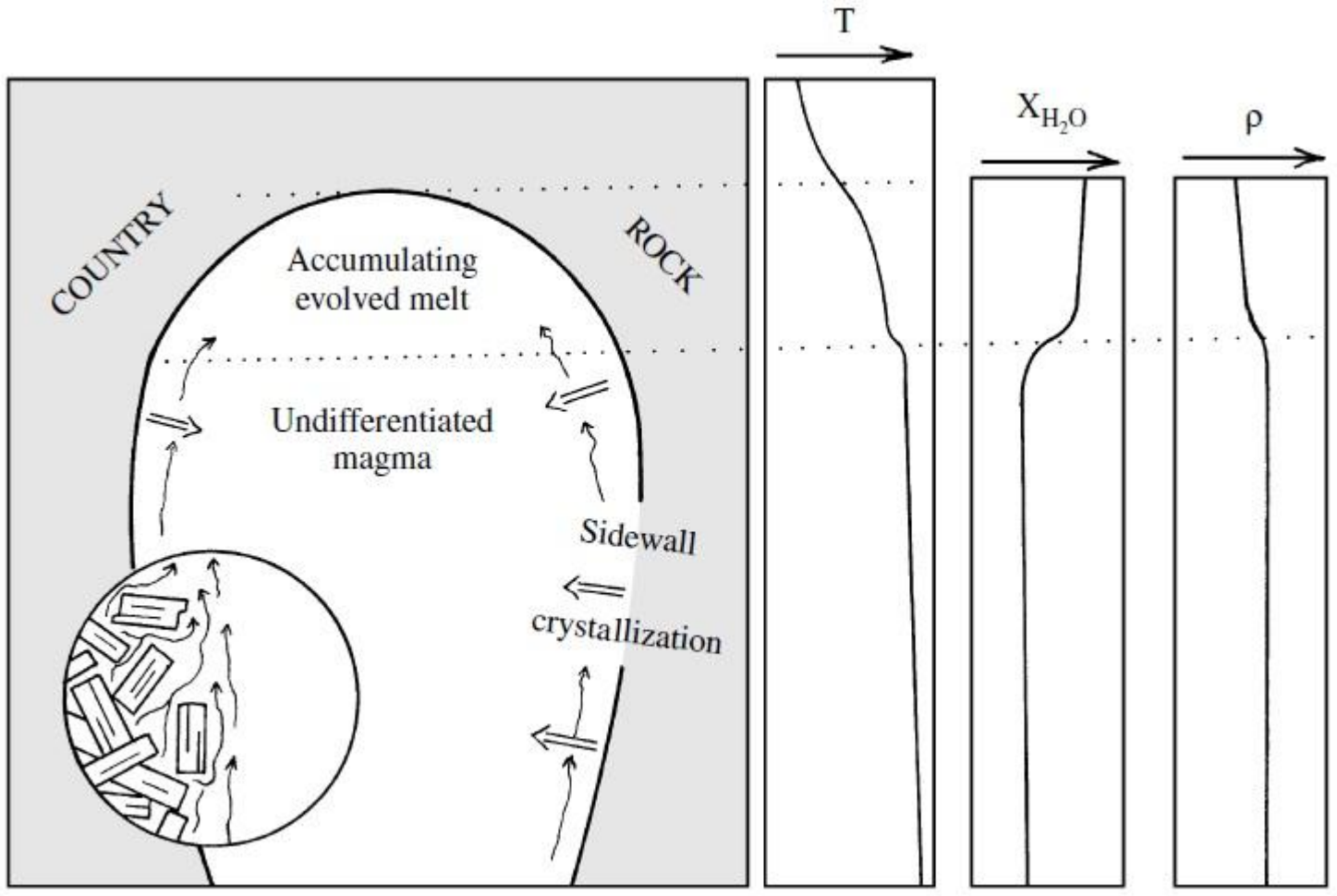

Myron, 2003, Igneous and metamorphic petrology 2° Ed.

- Pronounced compositional stratification can be produced in an initially homogeneous magma chamber, since sidewalls crystallization leads to less dense, silica and water enriched residual melt.
- Convection can be facilitated by hot magma rising from the bottom and/or water coming from the wet wall rock.

Cooling in a magma chamber

Thermochemical convection in a flat slab of crystallizing magma

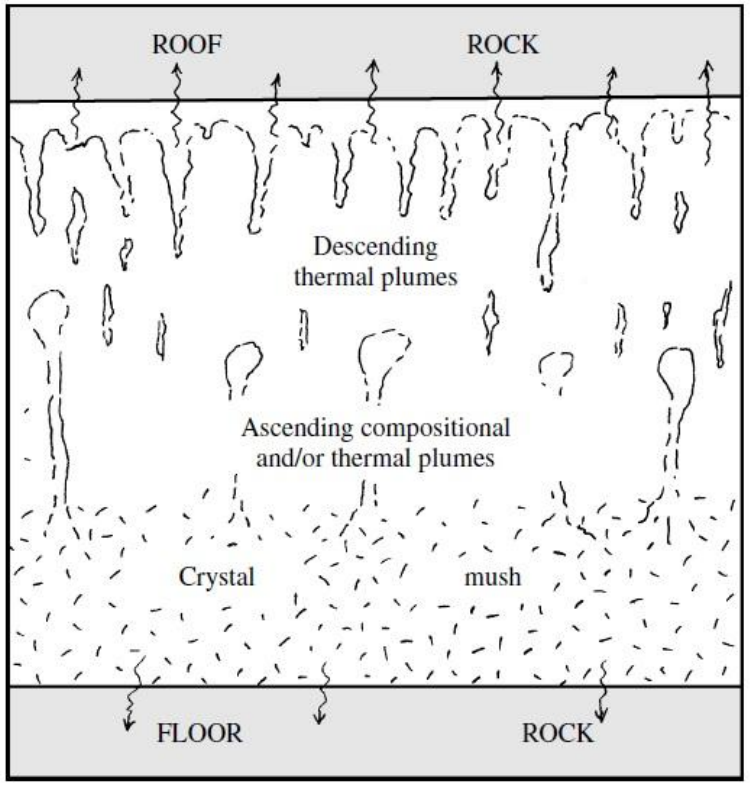

Myron, 2003, Igneous and metamorphic petrology 2° Ed.

- Cooling melt at the roof becomes denser and sinks, while floor crystallization of calc-alkaline magmas could release compositionally buoyant (and possibly thermally buoyant as well, due to the latent heat) residual melt.
- Residual melts from fractionating tholeiitic basalt magmas could be more Fe-rich and more dense.
- Depending on the contrasts in viscosity of different magmas, varying degree of magma mixing and homogenization may occur by ascending and descending plumes.

Partially crystallized magma layer

Kilauea Iki lava lake

The difference in temperature between the lab experiments and the *in situ* partially crystallized lava is < 15 K (crystals and coexisting melt are in local thermodynamic equilibrium).

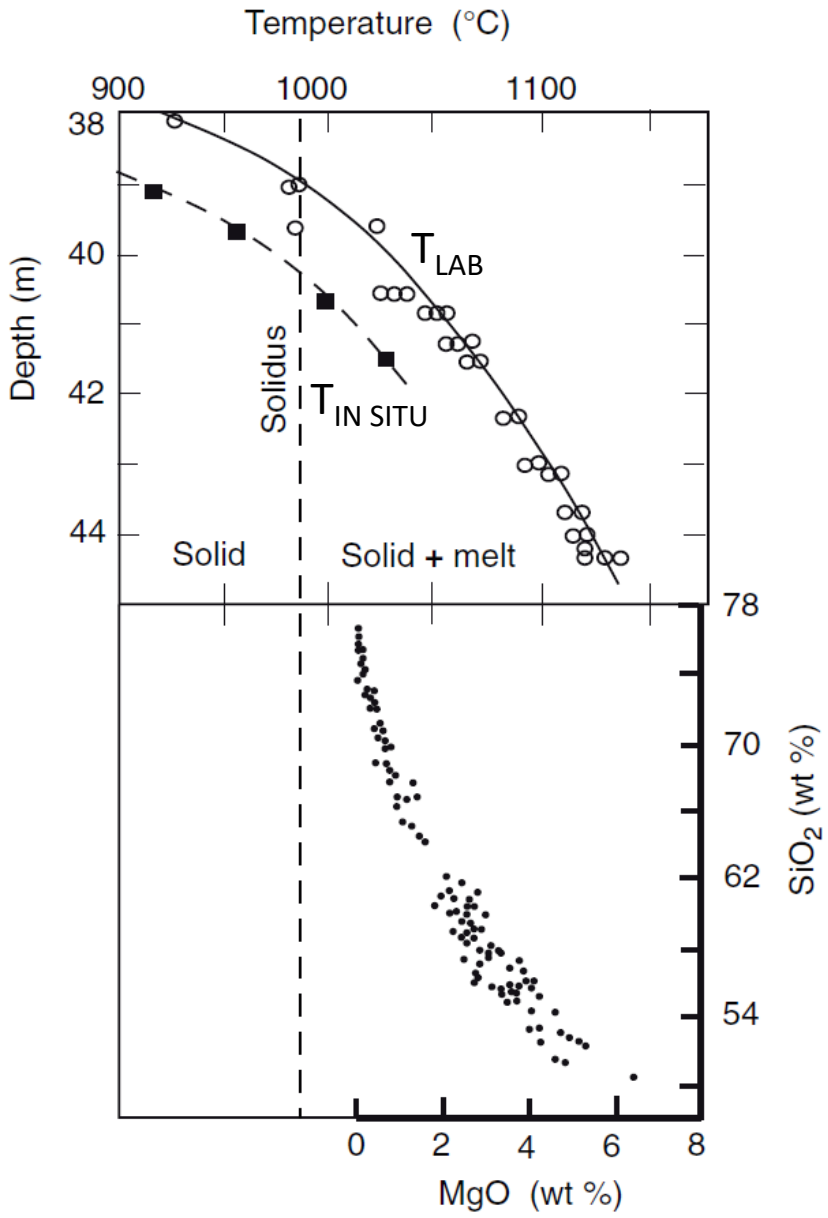

Convection in magmas

Time variation of *T* in the Makaopuhi lava lake, Kilauea volcano, Hawaii, at three different depths

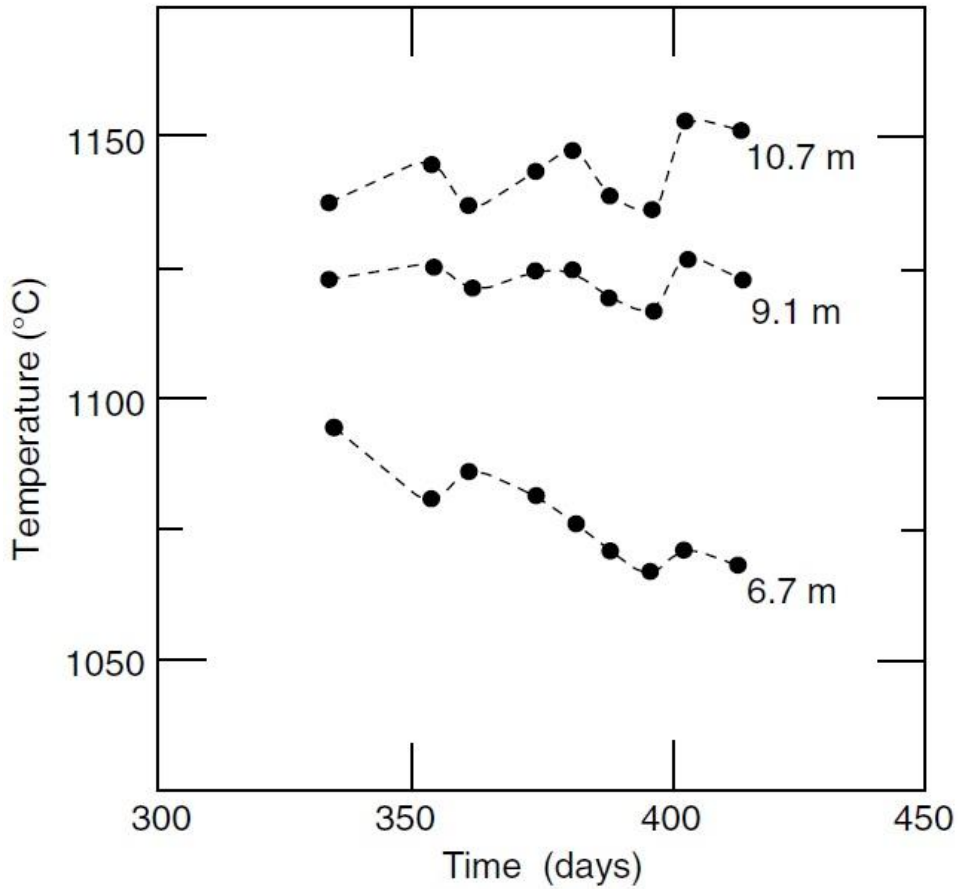

- In magma reservoirs, thermal convection does not modify temperature profiles greatly in comparison with those for purely conductive cooling.

Slopes of solidus-liquidus curves

Anhydrous tholeiite basalt

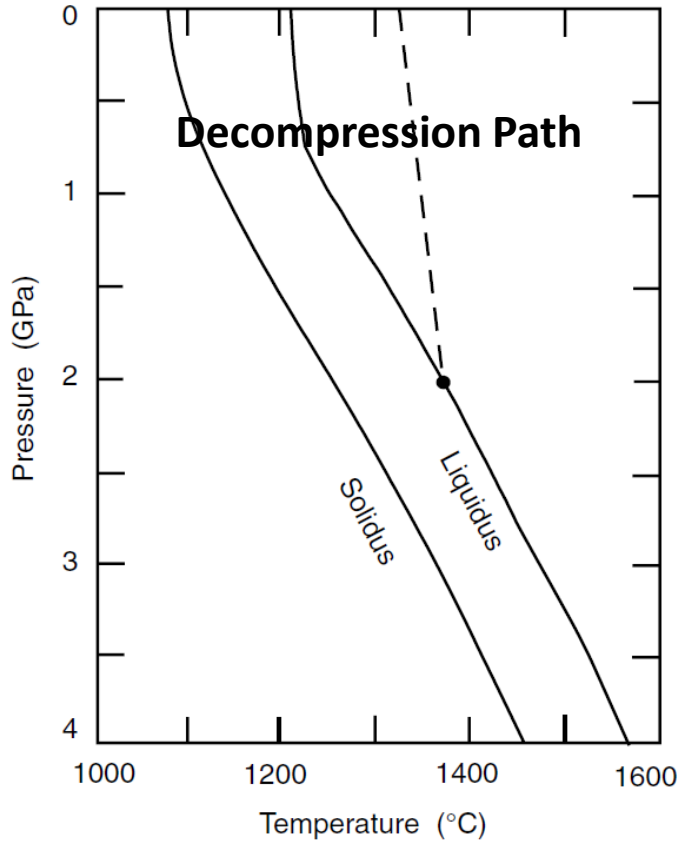

Mount St Helens dacite with 6% water

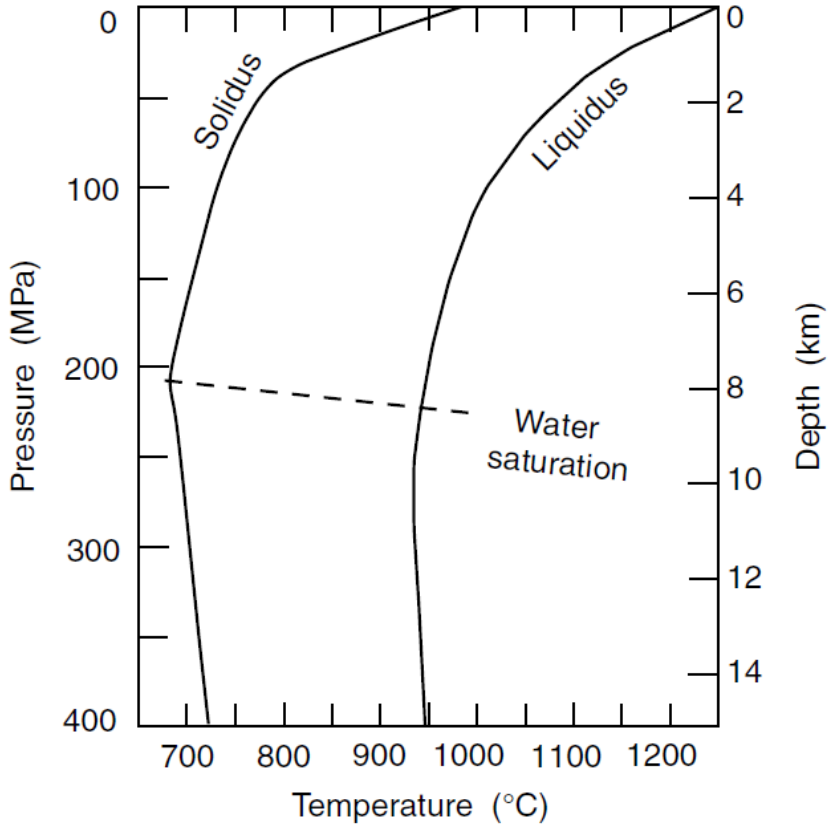

- **At *P*> 800MPa (>25 km) the slope of the liquidus is 3K km^{-1}**
- **At P< 800MPa (<25 km) the slope of the liquidus is 1-2 K km^{-1}** (in association with a change of mineral phase)

- Below the depth of saturation liquidus T< for P< (similar to dry magma)
- Above the depth of saturation liquidus T> for P< (amount of volitiles decrease)

- **At large depth the magma is not water satured and becomes superheated as it rises, as soon as it becomes water-satured its superheat decreases.**
- **The final amount of superheat upon emplacement depends on the amount of heat lost to cold surrounding rocks during ascent and the initial water content (difference between erupted lavas and magmas intruding in the crust).**

Magma cooling during ascent

Melt that rises in a dyke of length *a* and width *d* loses heat to the walls, so that:

$$\rho C_p w a d \frac{dT}{dz} \approx 2qa \qquad q = \lambda \Delta T / \delta \qquad \frac{dT}{dz} \approx \frac{\kappa}{dw} \frac{\Delta T}{\delta}$$

$$\delta \approx 2\sqrt{\kappa t}$$

w=average magma velocity (e.g., 1ms^{-1}), λ =thermal conductivity, ΔT=temperature difference between the wall and the magma, δ=width of the thermal boundary layer that develops, depending on the duration of the flow *t*.

For κ=10^{-6} m^{2}s^{-1} and *t*=1 month δ=1m
For *w*=1ms^{-1}, ΔT=1000K, d=2 m, *dT/dz* ~ 1 K km^{-1} < 1-3 K km^{-1} (liquidus slope)

Anhydrous tholeiite basalt

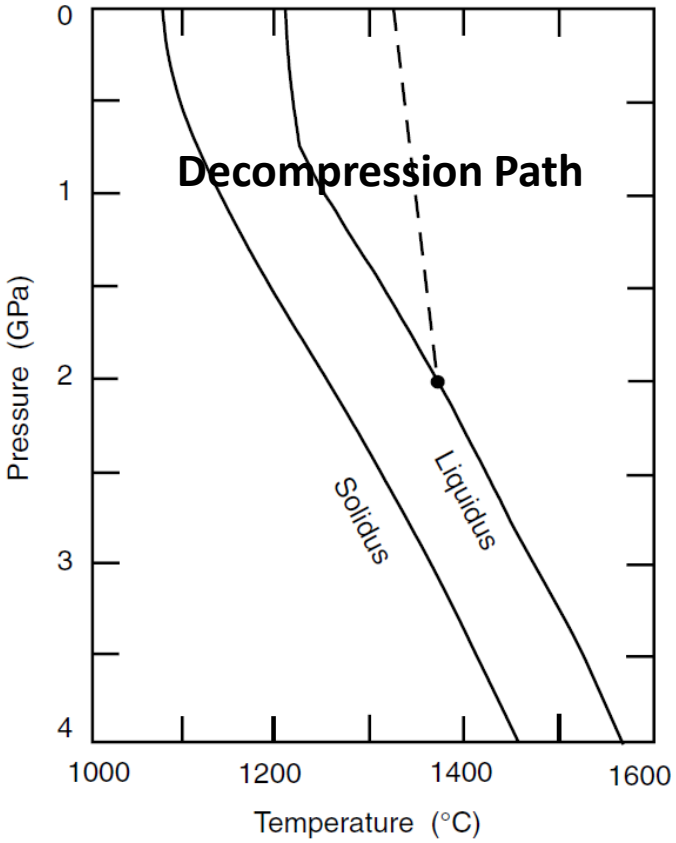

- If the intrusion event last longer (several months or years), the amount of cooling is smaller (no formation of chilled margins of the dykes).
- Volatile undersatured magma is likely to become and remain superheated during ascent, while hydrous satureted magma have lost their superheat and start to crystallize.

Latent heat of fusion

- **Latent heat of fusion: the amount of energy that must be supplied to melt a substance**
- **Transformation from one pahse to another of a single chemical component is accompained by the release or absorbtion of heat (*L=TΔS*), e.g., transformation (melting) of ice in water requires that heat has to be provided to the system (heat absorbtion). The fact that the water has a higher density than that of the ice implies that increasing the presure lowers the melting point of ice:** $dP/dT < 0$

$$\frac{L}{T} = \Delta S = \Delta V \frac{dP}{dT}$$

ΔS=Entropy

Latent heat of fusion for some pure silicate phases, from Spera (2000)

Formula	T_L (K)†	L (kJ kg^{-1})
Water	273	333
SiO_2 (quartz)	1700	157
$CaMgSi_2O_6$	1665	636
$Ca_2MgSi_2O_7$	1727	454
Fe_2SiO_4	1490	438
Mg_2SiO_4	2174	1010
$NaAlSi_3O_8$	1393	246
$Na_2Si_2O_5$	1147	196
$CaAl_2SiO_8$	1830	478

† Melting temperature.

Latent heat release

Importance of the latent heat release is provided by the Stefan number (*St*): it compares the amount of heat released per unit mass of liquid (*L*) to the amount of heat that must be extracted to cool material down at the boundary (T_B):

$$\mathrm{St} = \frac{L}{C_p\,(T_L - T_B)}$$

If *St*<< 1, latent heat does not contribute significantly to the global thermal budget

For L ~3×10^5 JKg^{-1}, T_L-T_B ~ 800 K and C_p10^3 JKg^{-1} K^{-1}, St ~ 0.4 (not negligeble)

Cooling of a pure melt from a horizontal boundary

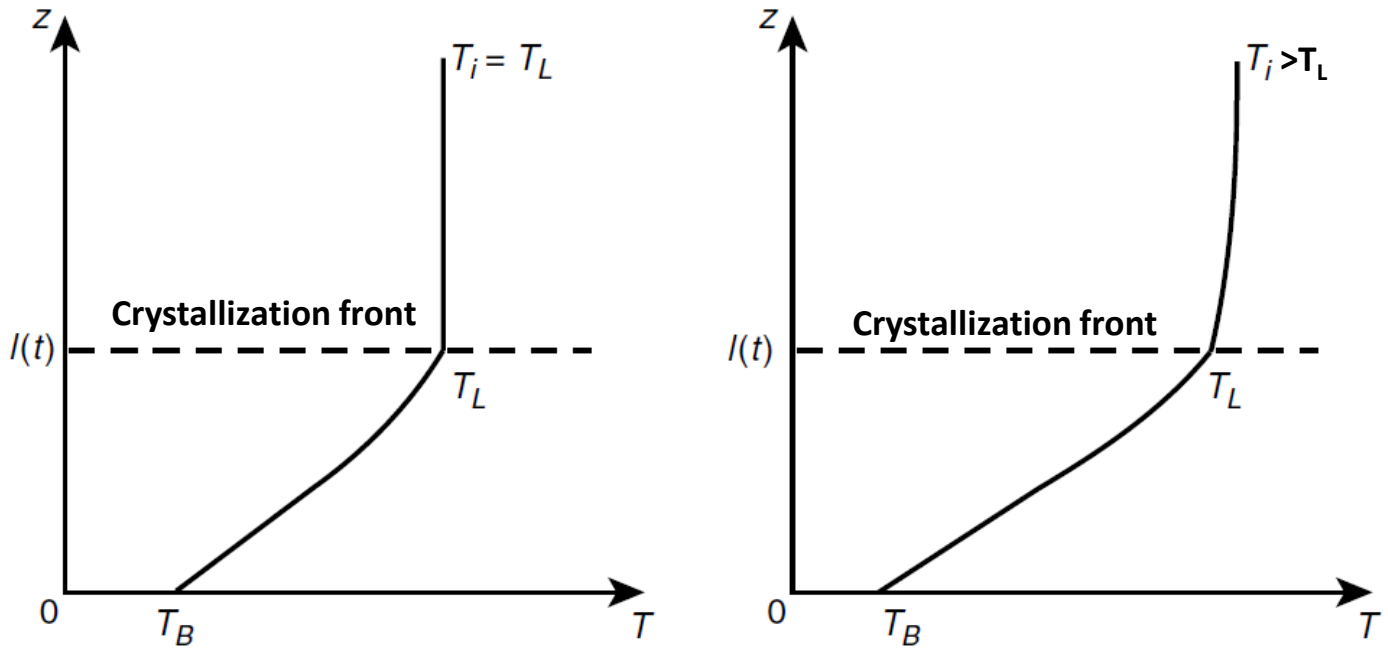

Solidification Front

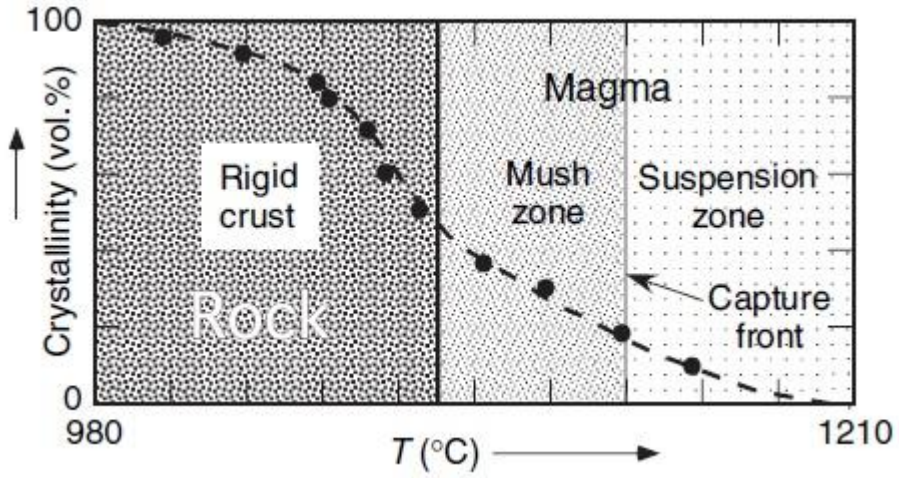

- Near the liquidus, where crystallinity is low (<25 vol.%) and crystals are small, the magma is a 'suspension'.
- In the 'mush' zone the crystals are still separated from one another. This zone persists until the crystallinity reaches about 55 vol.% .
- When crystallinity >55 vol.% tacked together to form a solid framework of some strength. Thus, the magma becomes a rock (dilatant solid) and can no longer flow as a viscous fluid. The remaining melt, (interstitial to the crystals) can still move, but as a porous or Darcian flow.
- With continued cooling and crystallization in the magma below, gases exsolve, increasing pressure.

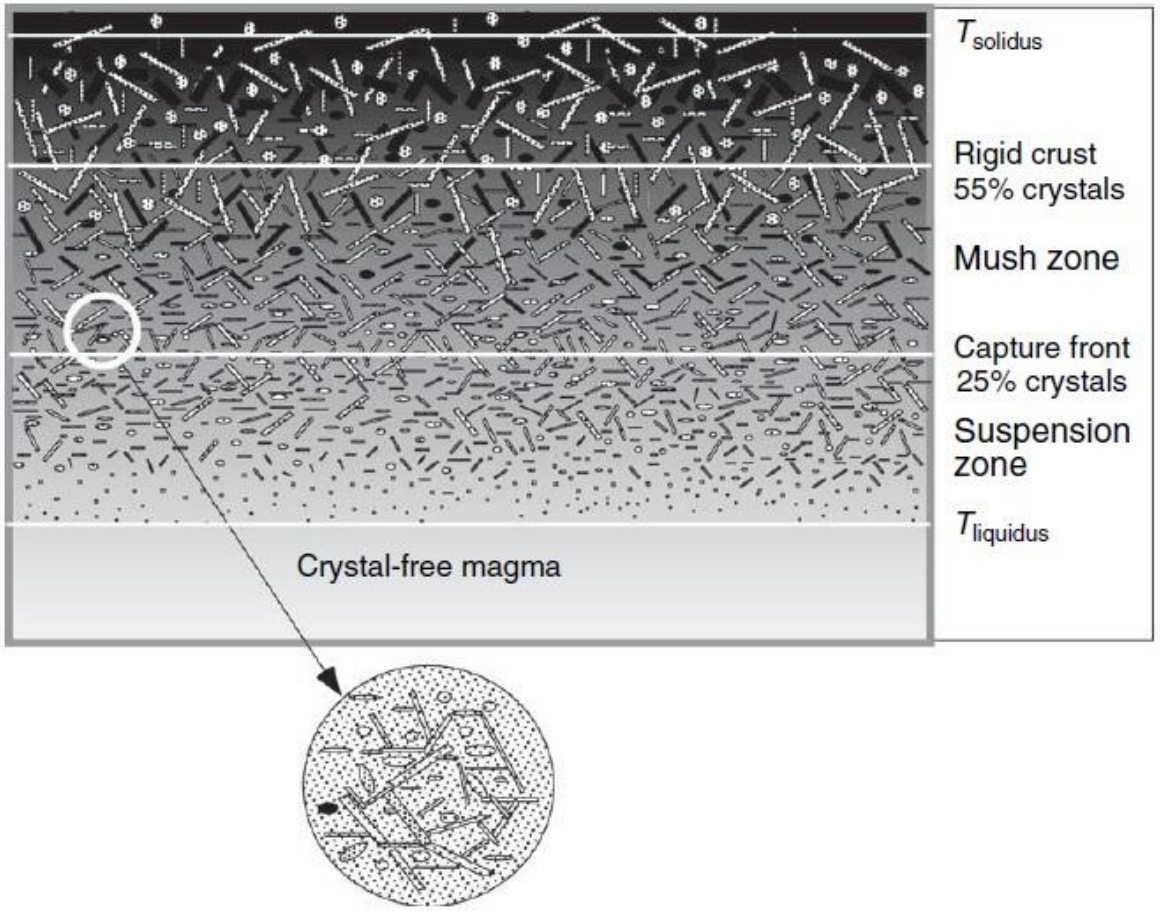

- **A solidification front is an active zone of crystallization that forms the perimeter of all magmas.**
- **Solidification fronts are dynamic, since they continually move in response to the prevailing thermal regime.**

Marsh, 2007, Treatise of Geophysics, vol. 6

Magma Chamber Conditions

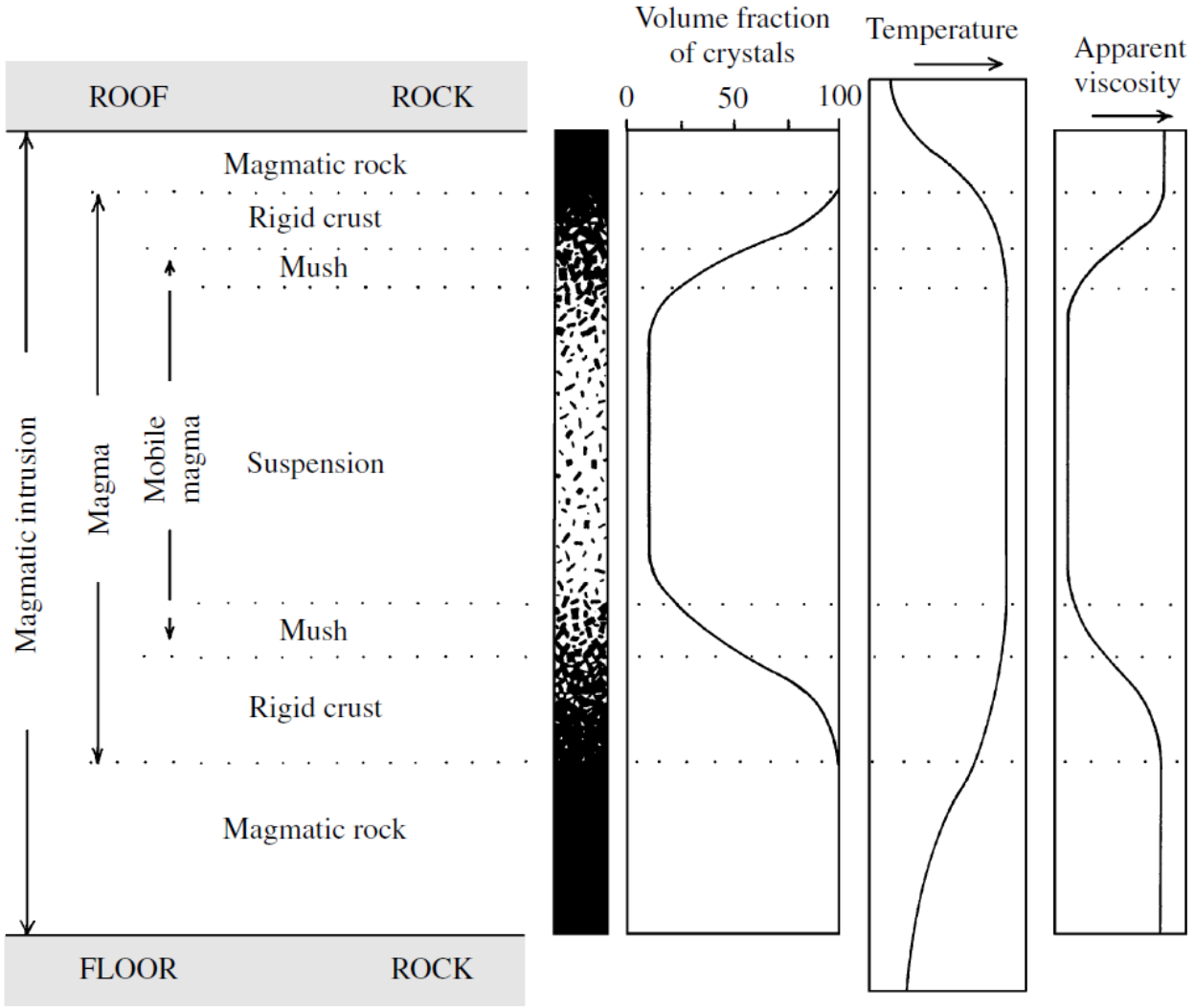

Myron, 2003, Igneous and metamorphic petrology 2° Ed.

- At any time, a magma intrusion consists of different rheological zones: mobile magma, rigid magma (above its solidus), and magmatic rock (below its solidus).

Magma Crystallization

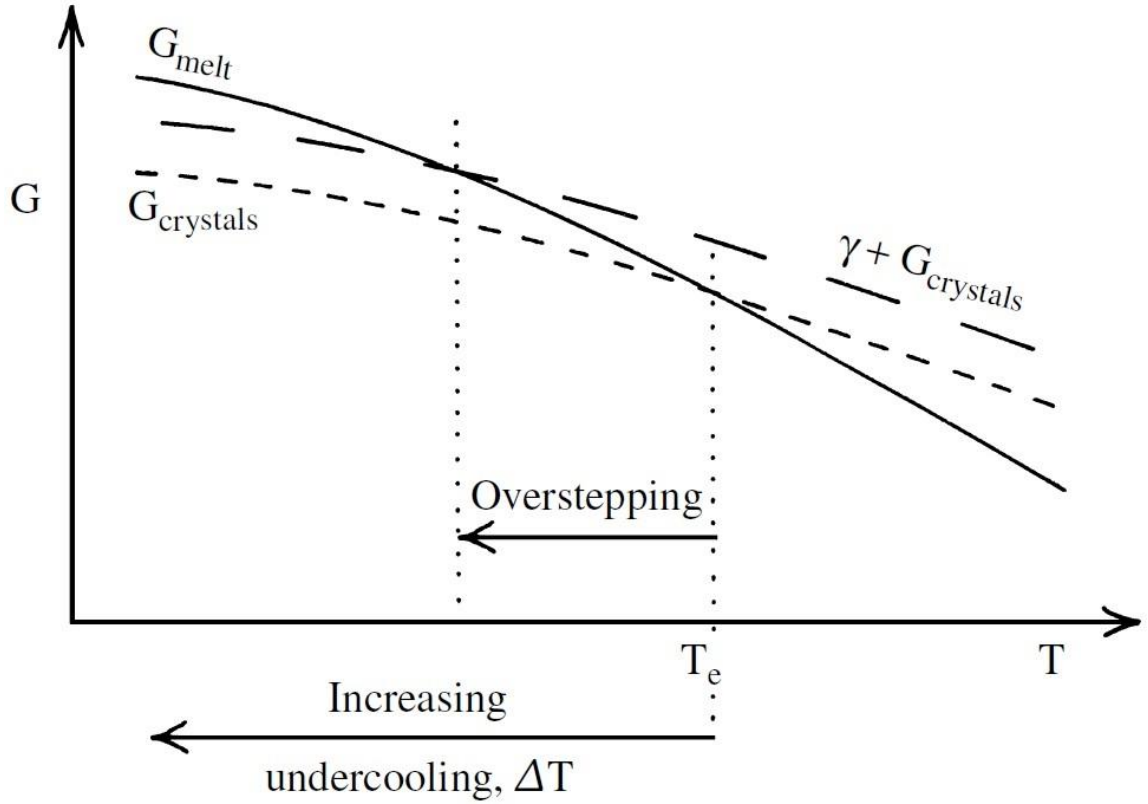

Myron, 2003, Igneous and metamorphic petrology 2° Ed.

- Free energies of melt and crystals are equal and cross over at the equilibrium *Te*. The surface free energy, γ is the energy that must be added to the free energy of the crystal phase for very small crystalline nuclei, because of their large surface area/volume ratio, producing an increase of their total free energy to the dashed line.

Homogeneous Nucleation: the crystal nucleate due to the undercooling.

Heterogenous Nucleation: the crystal readily nucleate on the existing surface in contact with a melt (e.g., magma chamber wall, walls of volatile bubbles, xenocrystals, restite crystals).

Kinetic controls on crytallization

- **When a magma basalt is emplaced at a depth of about 10 km at a *T* of ~ 1200 ° C, coming in contact with the surrounding rocks at *T* ~200 °C, forms a chill zone (sometimes with glass formation) along the margins (initially at T ~700 °C), while crystallization occurs mainly in the inner part during undercooling.**
- **At liquidus, the nucleation and growth rates of crystals are zero, then they increase with increasing undercooling until they reach a maximum and then decrease to zero at large undercoooling.**
- **Crystallization efficiency is sensitive to pre-existing nucleation sites (e.g. presence of xenocrystals) and presence of water dissolved in the melt: in hydrous basalts the amount of solid phases formed is smaller than in the dry ones, at the same cooling rate.**

$$\tau_K = (IY^3)^{-1/4}$$

τ_k= Kinetic crystallization time scale, $\tau_{max}=3x10^5$s
I = nucleation rates (number of nucleus formed per unit volume in unit time), $I_{max}=1cm^{-3}s^{-1}$
Y = growth rates, $Y_{max}=10^{-7}$cm s^{-1}

For olivine: Y= 10^{-11}- 10^{-10} cm s^{-1} and I=10^{-6}-$10^{-5}cm^{-3}s^{-1}$, τ_k ~$4x10^8$s
For plagioclase: τ_k ~10^7s-10^8s

If chilling occurs, cooling is faster than crystallization and conduction is the dominant heat transport and cooling time (τ_{diff}) is:

$$\tau_{\text{diff}} \approx \frac{1}{4}\frac{h^2}{\kappa}.$$

h=thickness of sills/dykes

Avrami Number (Av): ratio of the cooling time to the kinetic time: $\text{Av} = \left(\frac{\tau_{\text{diff}}}{\tau_K}\right)^4$

For Av<1 magma gets chilled
For an intrusion of basalt magma of 1 m τ_{diff} =$3x10^5$s, Av<1

- Crystals are distinguished in **phenocrysts**, representing crystallization at depth under slow, protracted cooling, and **groundmass**, representing the latest rapid phase of cooling.

Growth rate of mineral phases

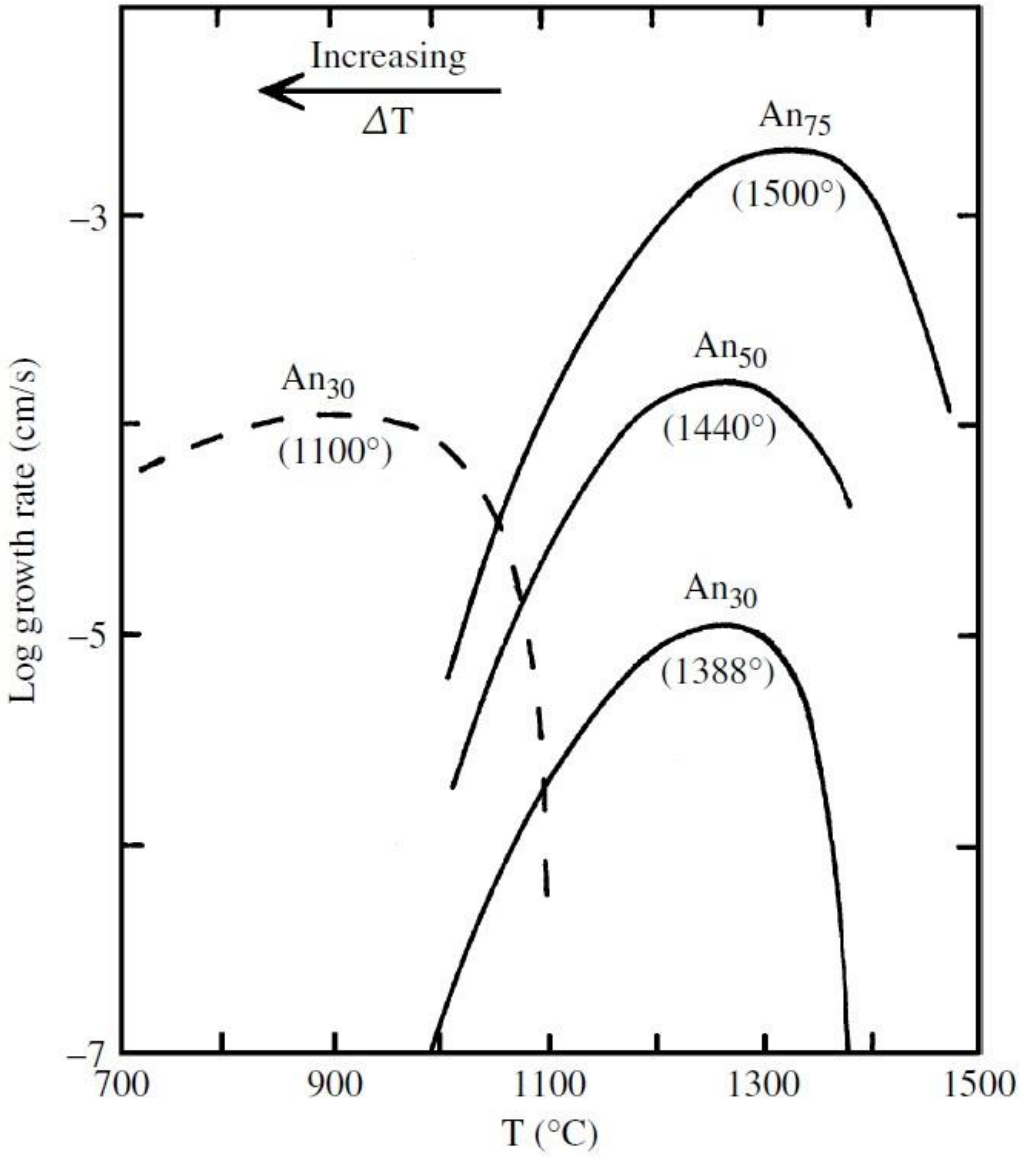

Experimentally determined plagioclase growth rates as a function of degree of undercooling, T, in their equivalent melts. Solid lines are in dry melts at 1 atm. Dashed line is for growth in a water-saturated melt at 2 kbar.

- The rate of crystal growth is related to the degree of undercooling of the system (like nucleation). Increasing undercooling provides a stronger driving force for growth, but with falling T the increasing melt viscosity retards ionic mobility. For this reason, the growth rate is a bell-shaped curve.
- At liquidus, the nucleation and growth rates of crystals are zero, then they increase with increasing undercooling until they reach a maximum and then decrease to zero at large undercoooling.

Myron, 2003, Igneous and metamorphic petrology 2° Ed.

Magmatic rocks texture

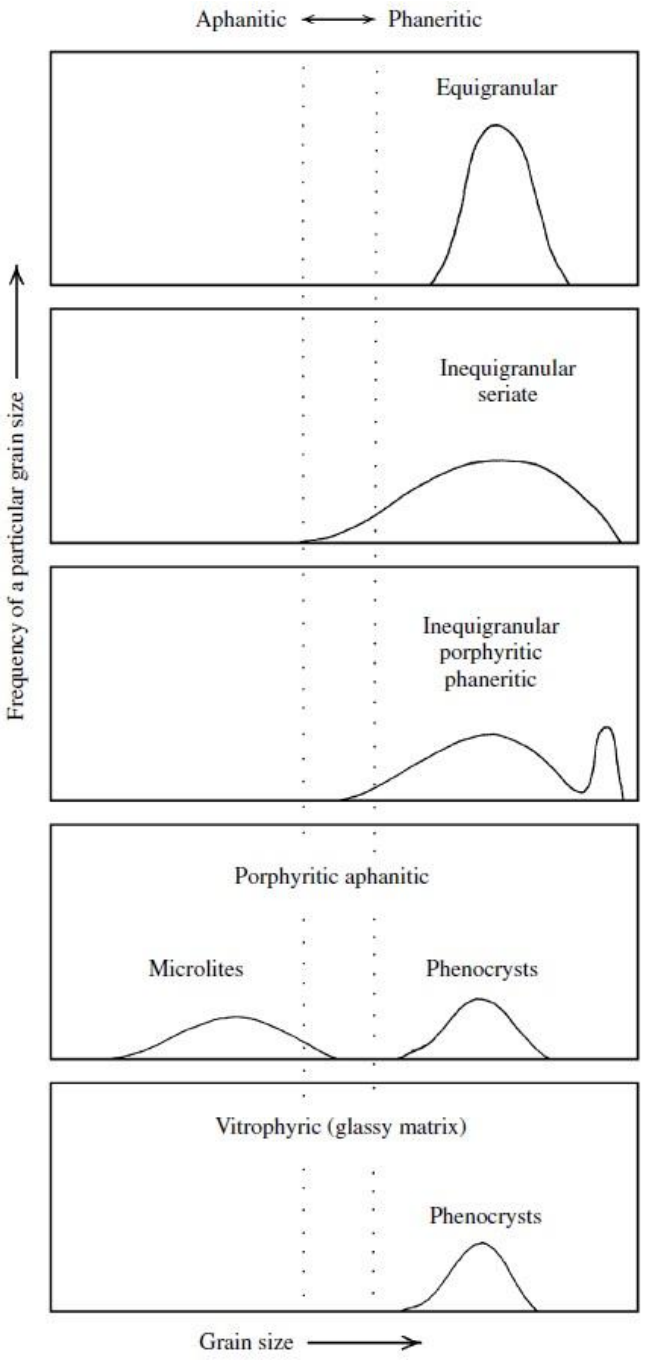

- Phaneritic rocks have an **equigranular** , or simply a **granular**, texture if the grains are of similar size, within an order of magnitude (Each crystalline phase must have experienced similar nucleation and growth rates).
- Other phaneritic rocks have an **inequigranular** texture in that they contain grains of conspicuously variable size. These include rocks of porphyritic texture in which there is a bimodal size population and rocks having **seriate** texture in which grains have a more or less continuously ranging size.
- The more or less continuous variation in grain size probably reflects differing ease of nucleation among the coprecipitating minerals in the slightly undercooled magma (Fe-Ti oxides nucleate readily, alkali feldspar nucleates at the slowest rate).
- Most aphanitic rocks, contain large, more or less euhedral **phenocrysts** embedded in a distinctly finer-grained or glassy **matrix**, or **groundmass (porphiritic texture)**, which imply different nucleation rates for different minerals or two-stage cooling or two levels of volatile concentration.

Myron, 2003, Igneous and metamorphic petrology 2° Ed.

Crystals shape and size

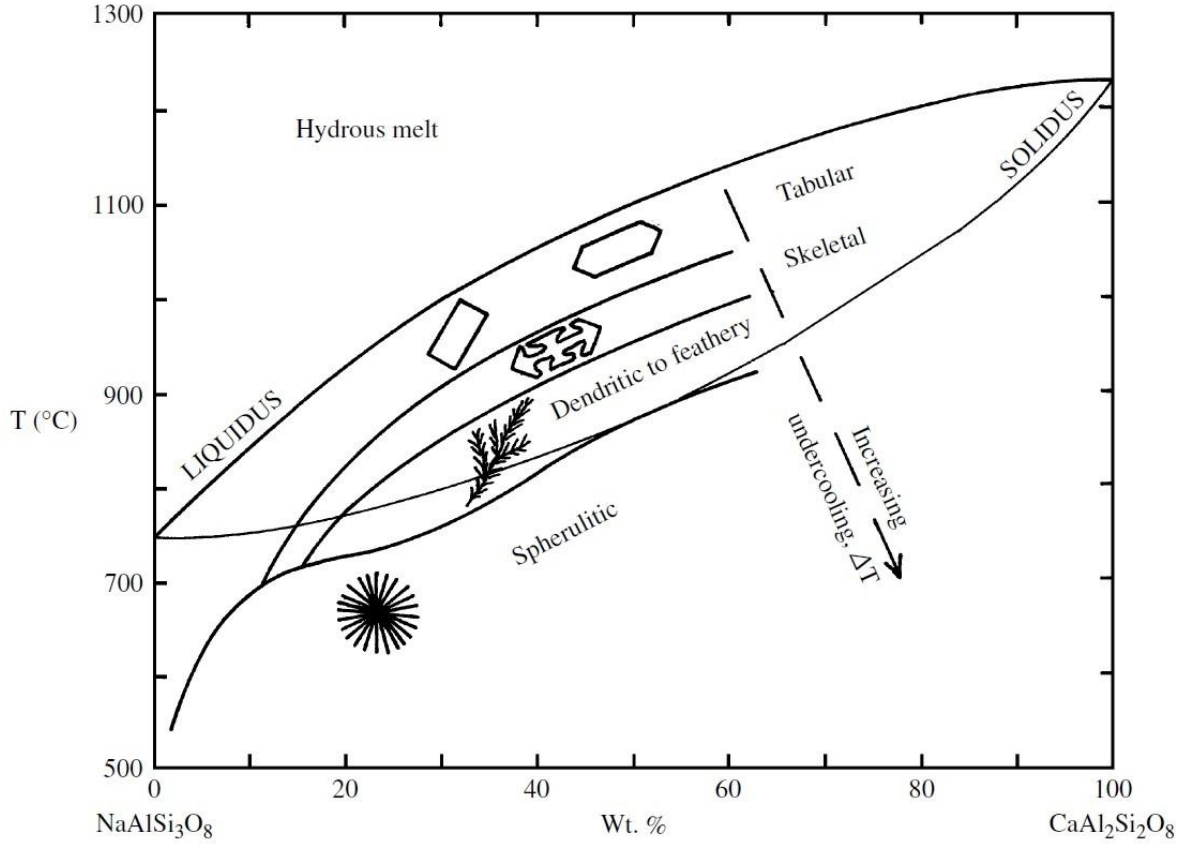

Myron, 2003, Igneous and metamorphic petrology 2° Ed.

- The total energy (sum of the surface energy and Gibbs energy) of progressively smaller volumes of a phase increases as the surface area/volume ratio increases. This means that many small particles are less stable (have greater energy) than one large particle of equivalent volume but lesser surface area.
- Grain shapes vary with respect to the particular mineral, melt composition, and amount of undercooling: $\Delta T/\Delta t$ less than a few degrees/hour, crystals have a euhedral tabular habit. For $\Delta T/\Delta t$ of tens of degrees/hour crystals are hollow, skeletal, and H-shaped forms. For greater $\Delta T/\Delta t$, dendritic, branching, and feathery forms develop. For $\Delta T/\Delta t$ of hundreds of degrees/hour, radiating, 3D sprays of fibrous to needle like crystals called spherulites develop, probably after the melt drops below the glass transition.

Crystals escape

- When a crystal becomes deeply embedded in a solidification front, melt viscosity and hindrance from neighboring crystals increase to the point that escape is not possible.
- The region where this transition occurs marks the boundary between the suspension and mush zones and is called the 'capture front'.
- Crystals outward of the capture front are trapped in the solidification front.

In the leading part of the solidification front, the suspension zone, crystals can settle easily with a rate V_s (Stokes' law):

$$V_s = C_s \frac{\Delta\rho g a^2}{\mu}$$

C_S = constant (2/9) depending on the shape of the crystal
$\Delta\rho$=density contrast,
g = gravity,
a = crystal radius
μ=viscosity

The position of the front, $S(t)$, is: $S(t) = 2b(Kt)^{1/2}$ The rate of advance (V_F) is: $V_F = \frac{dS(t)}{dt} = b\left[\frac{K}{t}\right]^{1/2}$

K=thermal diffusivity b=constant that measures the effect of latent heat relative to the enthalpy of the magma

Equating V_F with V_s we get the minimum size crystal that can escape from the solidification front as a function of time:

$$a(t) = \left[\frac{b}{C_s}\frac{\mu(K/t)^{1/2}}{\Delta\rho g}\right]^{1/2}$$

- The larger the viscosity the larger the crystal must be to escape, while for density contrast it is just the reverse.

Crystals escape

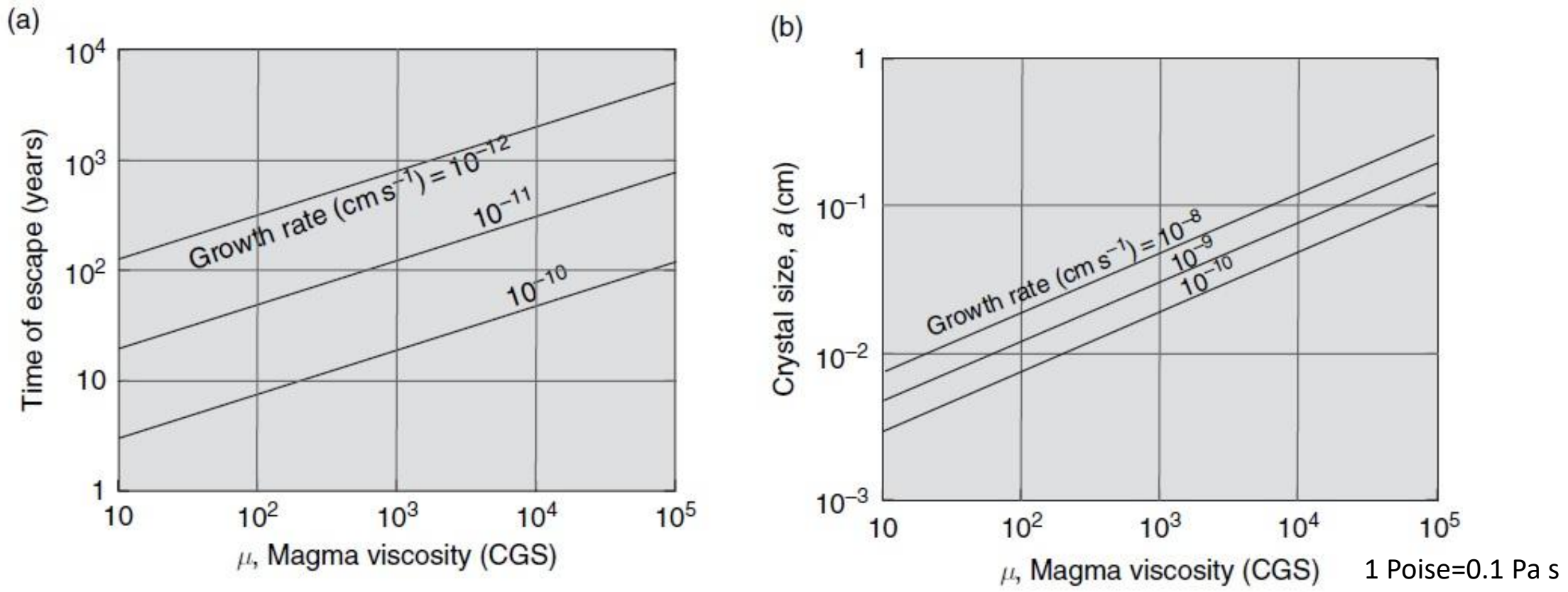

1 Poise=0.1 Pa s

Marsh, 2007, Treatise of Geophysics, vol. 6

- The sooner a crystal can reach the critical size to sink faster than the rate of advancement of the capture front, the sooner it can escape (the time of escape is very sensitive to the growth rate).
- As magma viscosity increases, the time of first escape and the crystal size at escape increase.
- Crystals escaping the crystallization front enter the hottest part of the system and will begin melting and dissolving back into the magma.
- Crystal escape from solidification fronts is much more likely in basaltic magmas once the crystals reach about 0.1 mm in size.

Crystals distribution

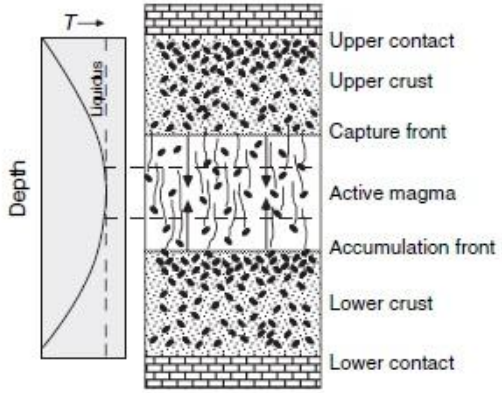

When magma carrying phenocrysts is emplaced, there is a competition between the rate of crystal settling and the rate of solidification.

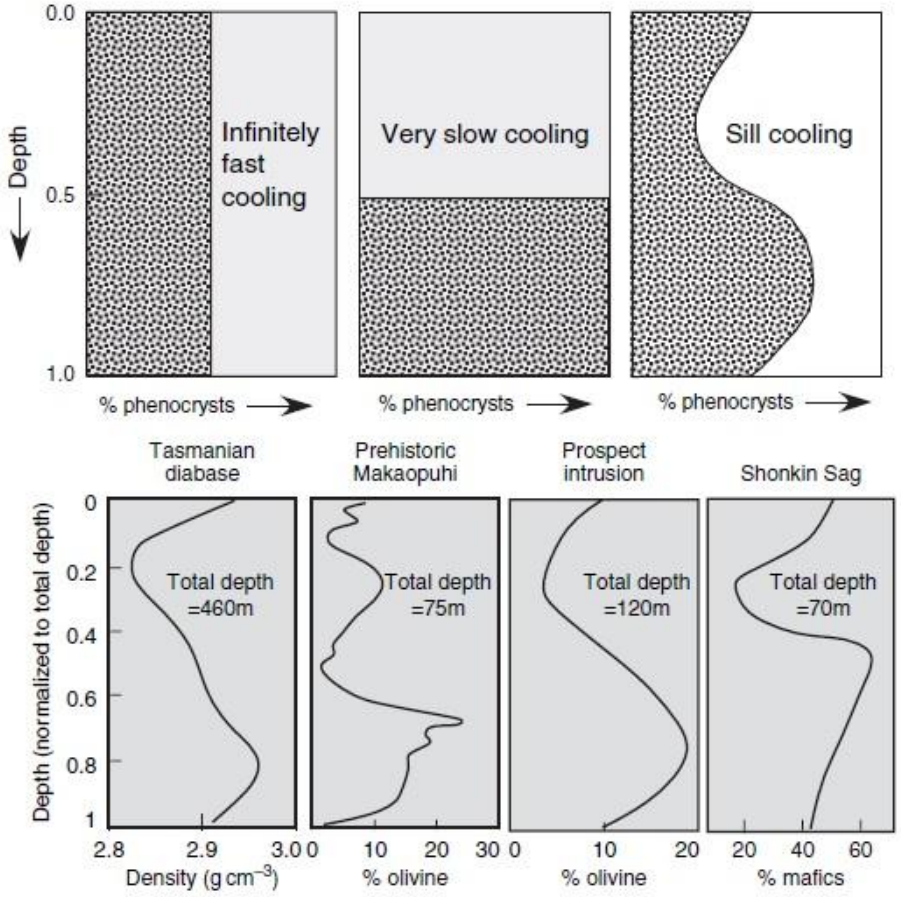

- If the magma could cool instantaneously (very thin sheet of magma) all the crystals would be trapped in place before they could settle any distance at all (uniform crystals distribution from top to bottom throughout the sheet).
- If the body did not crystallize at all (very thick sheet of magma), all the crystals would settle to the floor and form a thick pile.
- In the most common cases, inward advancing solidification fronts from the top and bottom compete with crystal settling.
- Since the rate of solidification front advance decreases inversely with distance into the body, more and more crystals escape capture with depth and all crystals initially in the center of the body settle into the lower rising solidification front (*S*-shaped profile of phenocrystals abundance vertically through the body).

Marsh, 2007, Treatise of Geophysics, vol. 6

Dependence of magma composition and viscosity on crystallization

Separation of crystals from melt causes chemical differentation

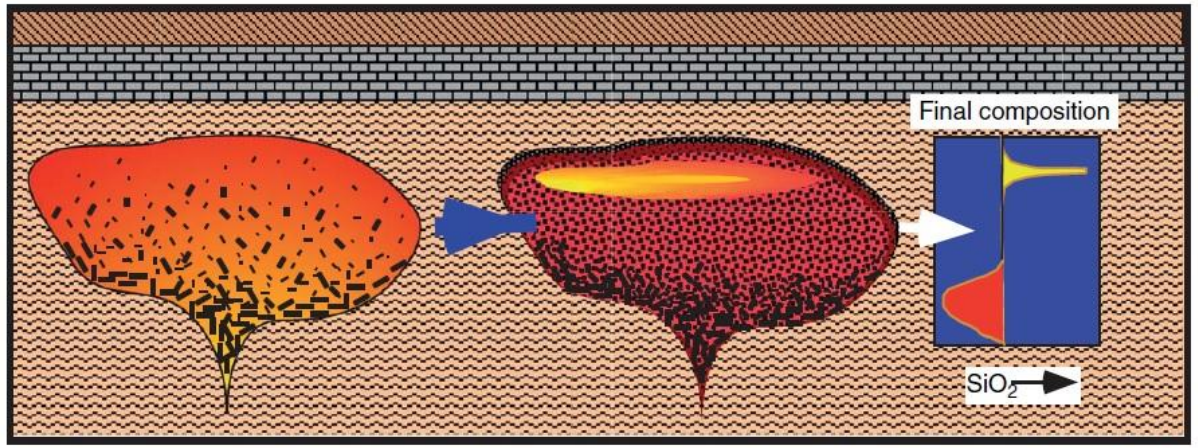

Classical magma chamber

Marsh, 2007, Treatise of Geophysics, vol. 6

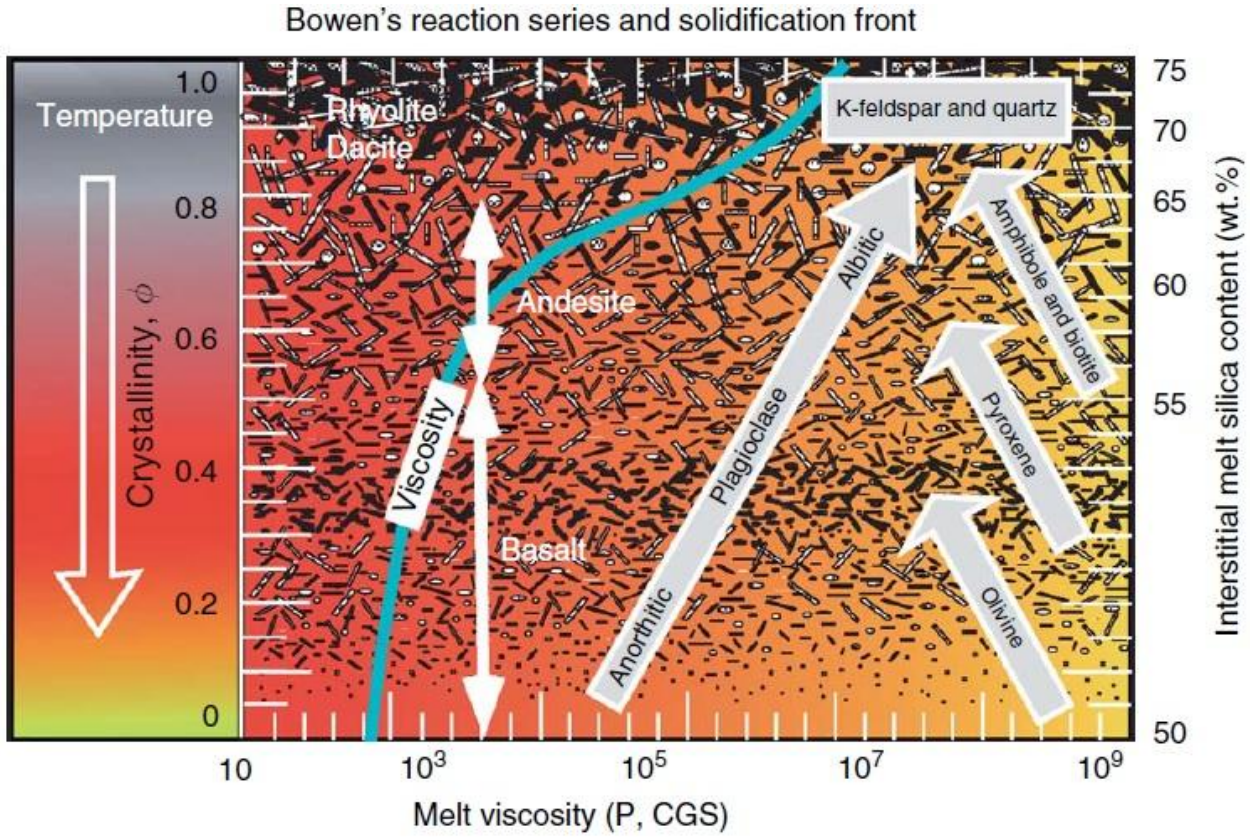

- Crystals already present in the magma favour crystallizzation processes: continual growth of crystals will enhance nucleation
- Once the cooling front arrives, existing nuclei increase in size outward through the solidification front.
- The small crystals combine through aggregation and grain boundary migration into a large, opticalllly continuous crystals (touching grain combine in response to lowering the net free energy).

Dependence of magma composition and viscosity on crystallization

Variations in melt silica content and viscosity with crystallinity

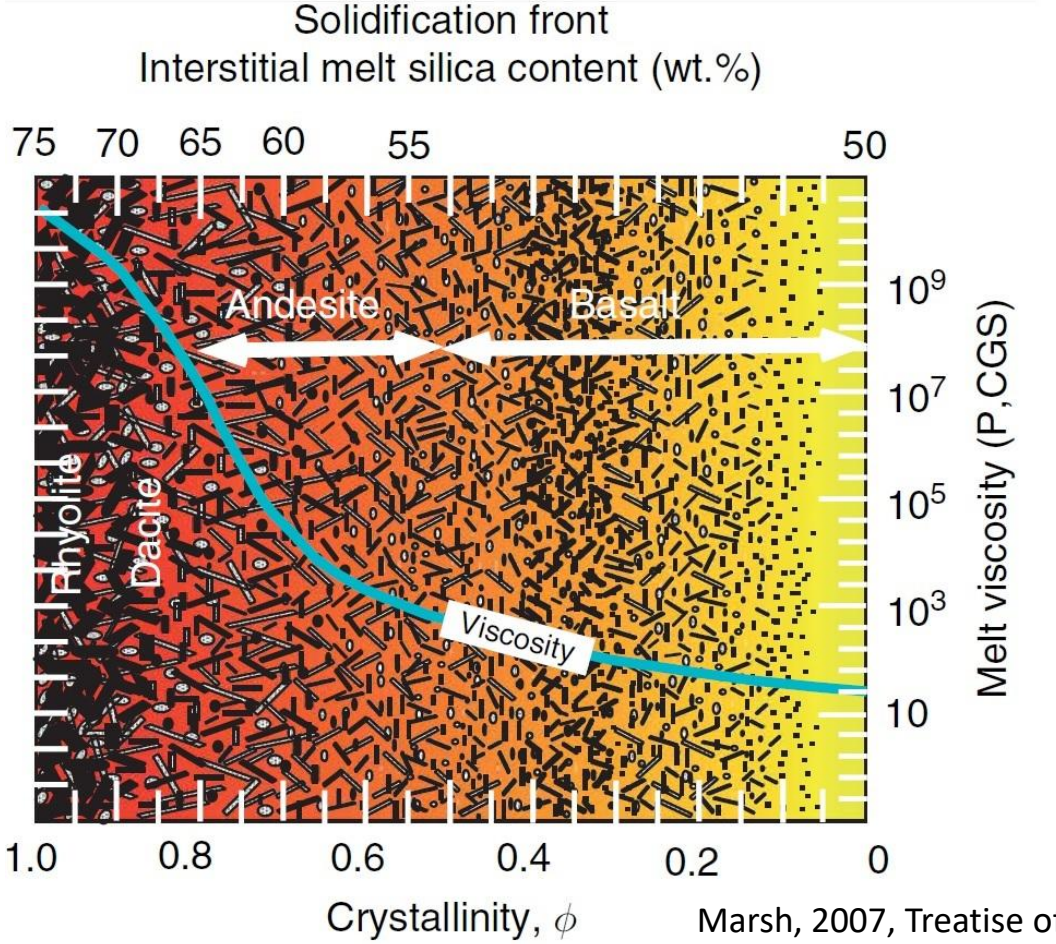

Marsh, 2007, Treatise of Geophysics, vol. 6

- Silica enrichment increases gradually for the first 50 vol.% of crystallization (the increase is only ~5 wt.%).
- Andesitic, dacitic, and rhyolitic melts occur at increasingly higher states of crystallinity, where the separation of melt and solids is increasingly difficult.

Dependence of magma composition on crystallization

Lavas from Kilauea

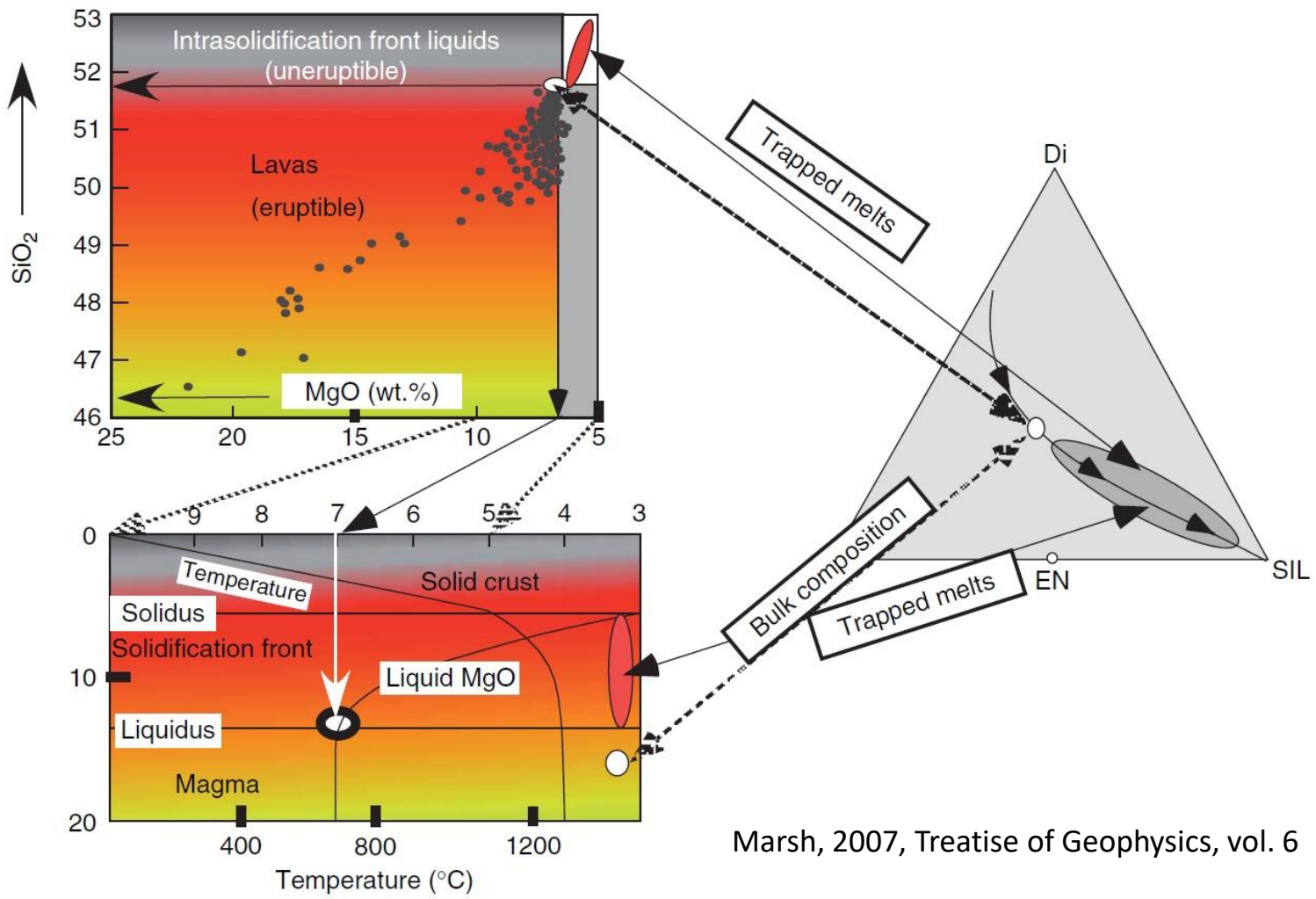

Marsh, 2007, Treatise of Geophysics, vol. 6

- No magma comes from within the solidification fronts (the lavas are generally always just basalts).
- Bimodal differentiation comes from solidification fronts that tear open and form lenses of silicic liquids or silicic segregations.

Differentiation Processes: Solidification front instability (SFI)

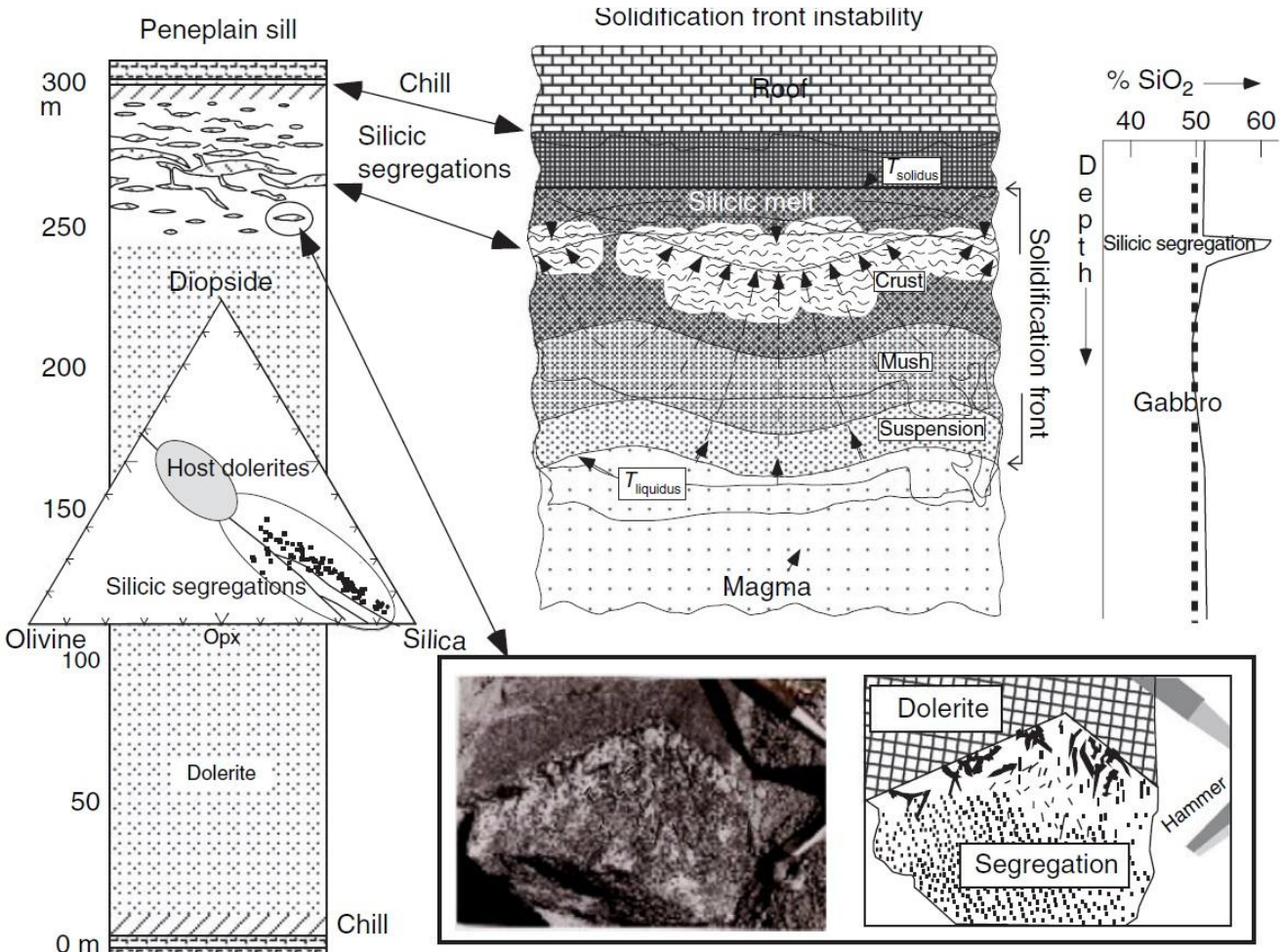

Marsh, 2007, Treatise of Geophysics, vol. 6

- The lenses of silicic materials (pegmatitic segregations, 60–65 wt.% SiO_2) begin thin and small near the sill roof and increase in thickness and length (usually are between 1m and 20–30m).
- A likely mechanism of formation of these lens, having a coarse texture, is by internal failure (e.g., roof failure) or tearing of the solidification front (where there is enough strength to fracture).
- With initiation of tearing, local interstitial melt is drawn into the tears. The melt arriving from lower in the solidification front is slightly hotter and as it cools it forms progressively smaller crystals downward in the segregation.
- To avoid tearing, the local strength of the solidification front must increase proportionally with weight, and strength comes from increasing crystallinity.

Bimodal suite of composition (basaltic and silicic end-memeber): Iceland volcanic rocks

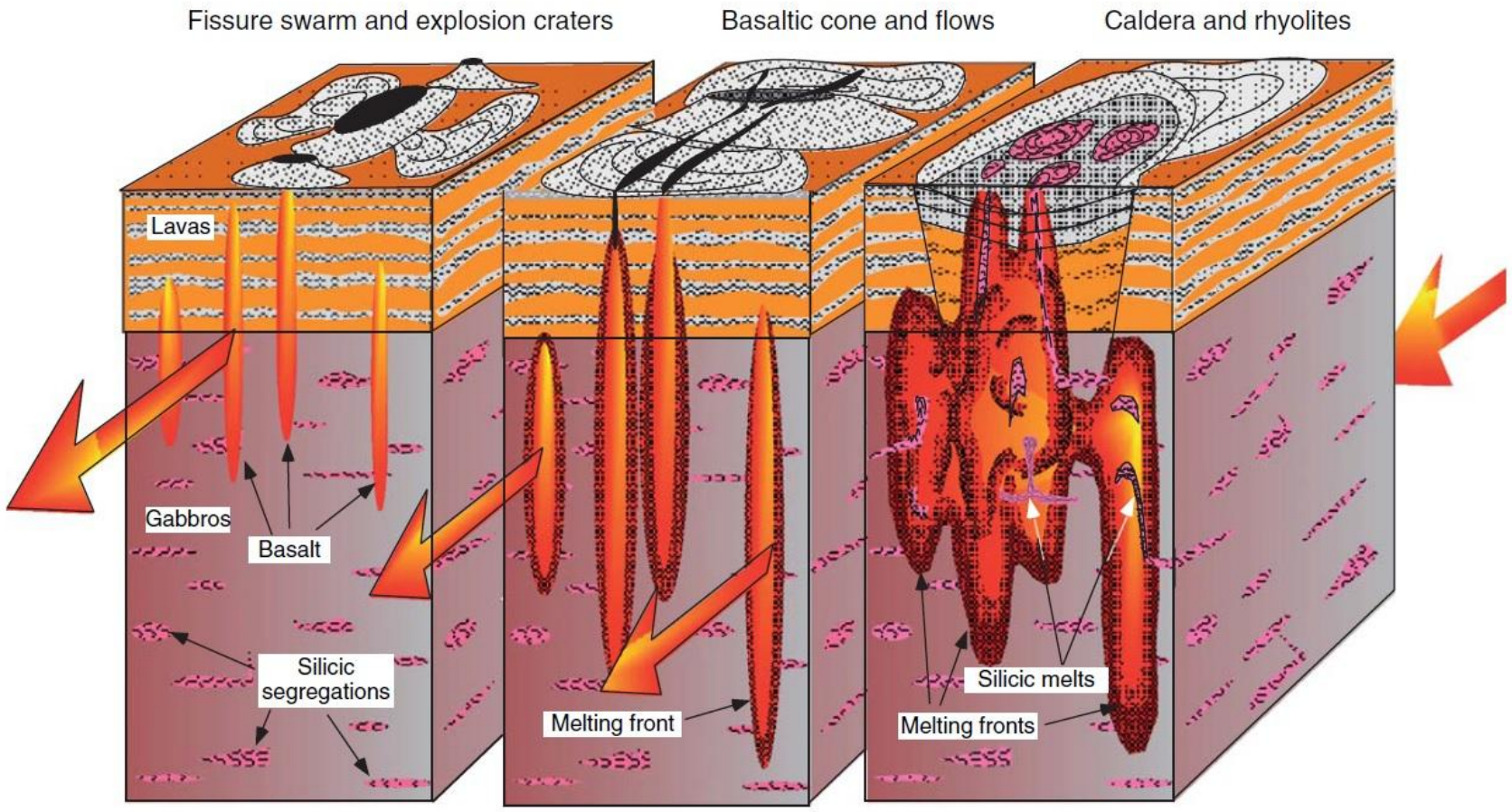

Marsh, 2007, Treatise of Geophysics, vol. 6

- About 18% of the surface rocks of Iceland are highly silicic rhyolites.
- Fissures propagating into older crust bring hot basaltic magma into thin warm crust, which promote progressive wholesale melting via melting fronts propagating outward into the country rock.

Sidewall Uflow

Another means for escape of residual silicic melt from deep within solidification fronts is by upward flow along steep lateral walls

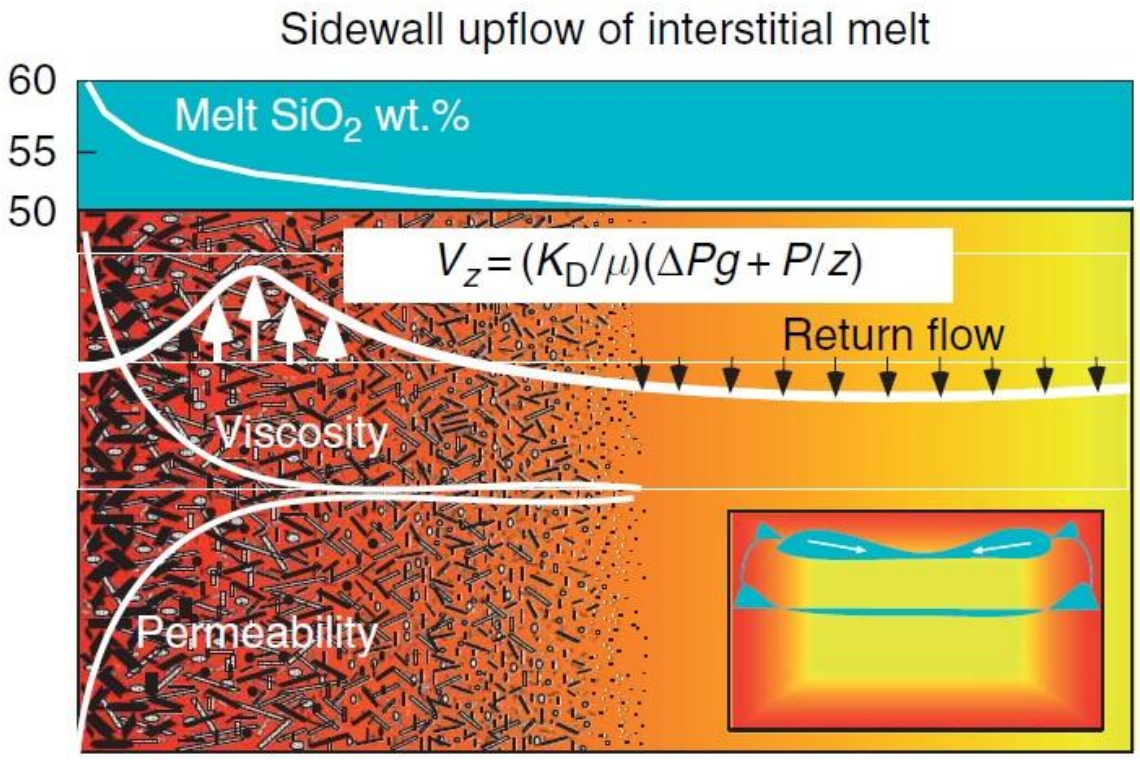

$$V_m = \frac{K_D}{\mu}\left[\frac{\partial P}{\partial Z} + \Delta\rho g\right]$$

Marsh, 2007, Treatise of Geophysics, vol. 6

- Silicic melts can escape if the advance of the solidification front is slow enough (cooling slows with increasing depth) to allow upward flow through the porous solidification front (Darcian dynamics).
- There is an optimum position within the rear of the solidification front where melt is most efficient at flowing upward.

K_D/μ decreases strongly approaching the solidus *T*.

V_m = Darcy velocity, (it measures the melt flux per unit area), K_D = permeability, μ= melt viscosity, *P* is pressure, *z* = spatial coordinate, $\Delta\rho$= density contrast, and *g* = gravity.

Fissure Flushing

Another process to melt flow through the rear of a steep solidification front is the flushing of residual melt from an aging solidification front spanning a fissure or other sheet-like body.

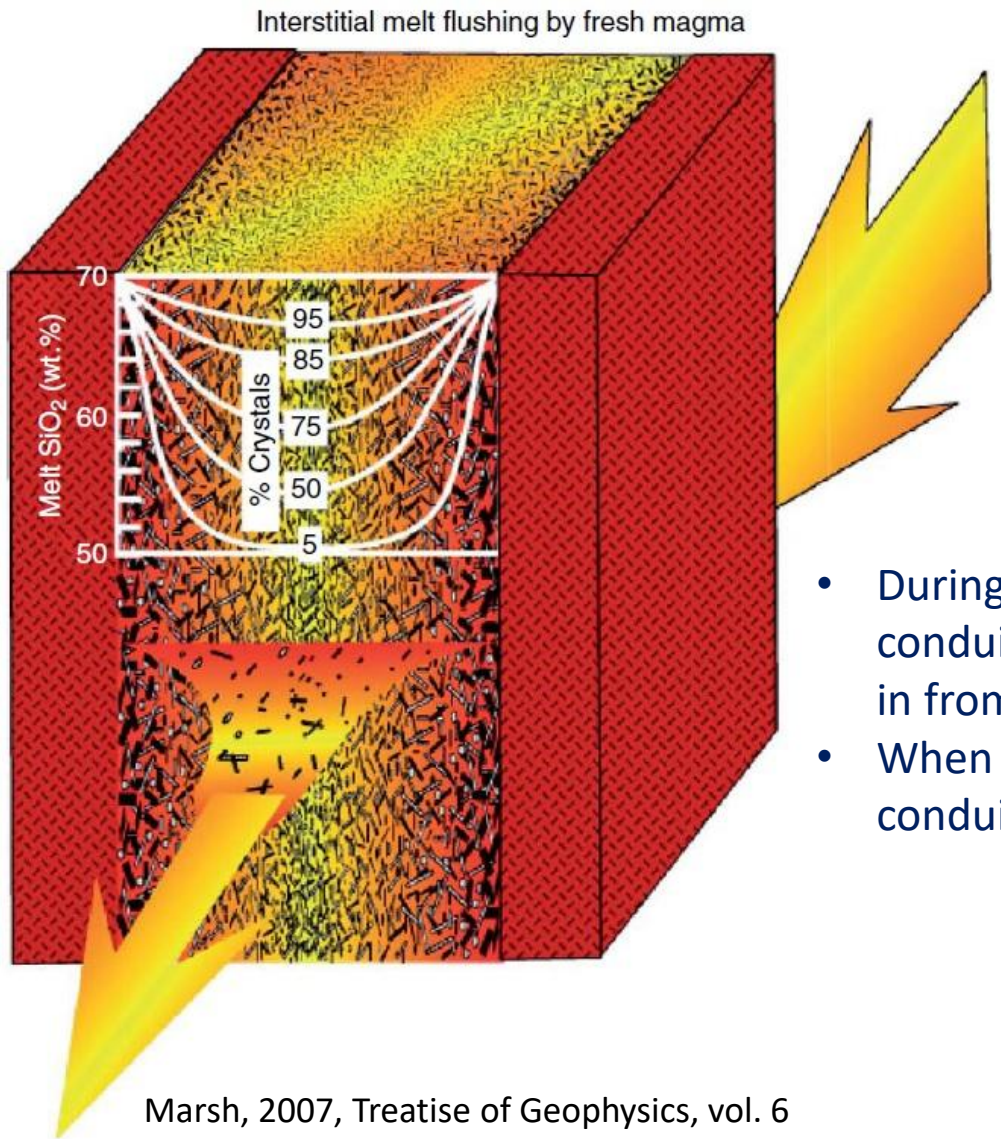

Marsh, 2007, Treatise of Geophysics, vol. 6

- During times of repose in magmatic systems, the driving pressure relaxes, conduit walls press in on the remaining magma, and solidification fronts move in from the lateral walls, meeting each other and forming bridges of crystals.
- When the repose period ends and magma flow resumes, magma coursing this conduit will flush the residual melt from the crystalline matrix of solids.

Superheat Conditions

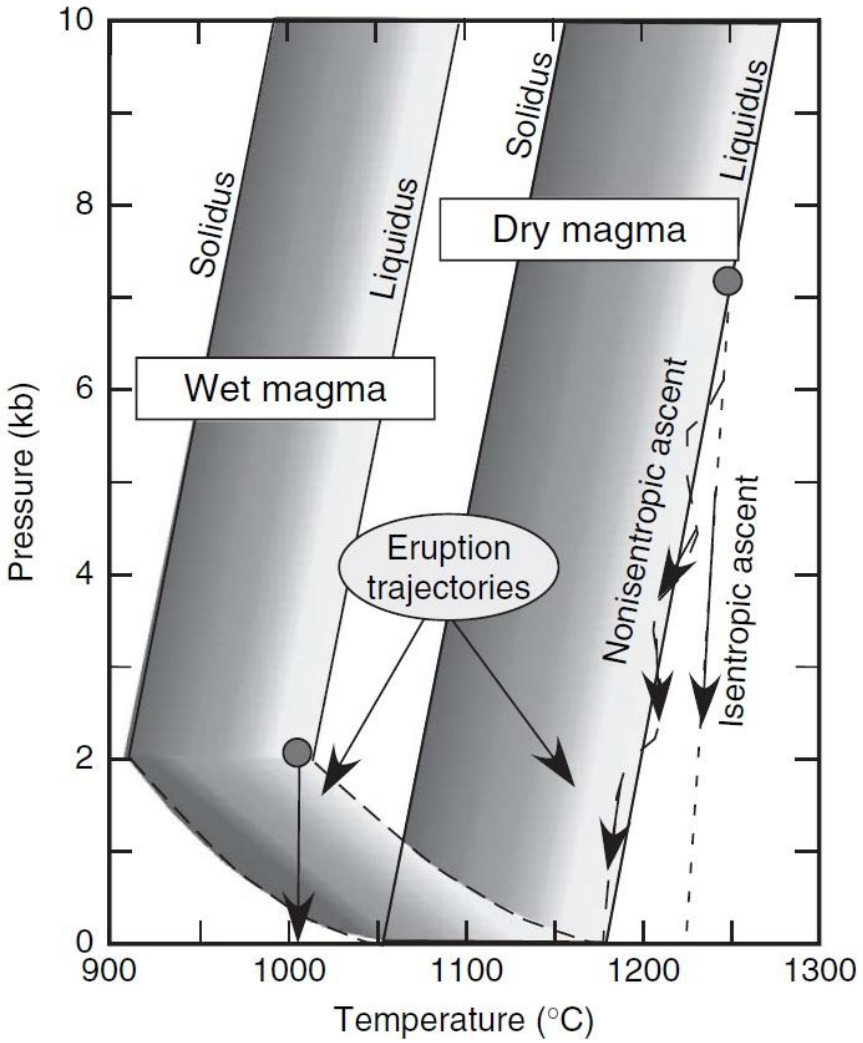

Marsh, 2007, Treatise of Geophysics, vol. 6

- Thermal convection is not a common process in magma chambers.
- For a magma with a very small amount of superheat (~1 °C), *Ra* could be large if *L* is sufficiently large .
- Any amount of superheat will bring on vigorous convection and rapidly bring the temperature back to the liquidus (dissipation of superheat to the wall rock).
- With the loss of superheat, thermal convection ceases, and the process repeats itself on a timescale governed by the rate of ascent.

The time (t) for convection in each layer to start and become fully established is:

$$t = \frac{L^2}{\kappa}\left[\frac{B}{Ra}\right]^{2/3}$$

B = 350

L=thickness of an individual layer

$$Ra = \frac{\alpha g \Delta T L^3}{v\kappa}$$

Ra=Rayleigh Number $Ra=10^{15}$-10^{17}

g= gravity, ΔT is the initial amount of superheat (500 °C), α= coefficient of thermal expansion (5 x $10^{-5}C^{-1}$), L = thickness of an individual layer (e.g., norite 1 km, granophyre 1.5 km), v = kinematic viscosity of the melt layers (norite 10 $cm^2\ s^{-1}$, granophyre 100 $cm^2\ s^{-1}$), κ =the thermal diffusivity (10^{-2} $cm^2\ s^{-1}$).

Modes of Magmatic Cooling: Superheated Magma

Rapid convective cooling

The average temperature (T) in a rapidly convecting layer, strongly cooled from its margins, is:

$$T = T_L + \Delta T_o \left[1 + \frac{t}{\tau}\right]^{-1/b} \qquad \tau = \frac{L^2}{2Cb\kappa'} Ra^{-b}$$

T_L = liquidus temperature , ΔT_0 = amount of superheat, t = time

$Nu=(CRa^b)$ b=1/3 C=0.4 $(\kappa' = K_c/\rho C_p)$

The thermal conductivity (K_c) is of the wall rock and the density (ρ) and specific heat (C_p) are of the magma.

The magma reaches T_L in about 10-100 years

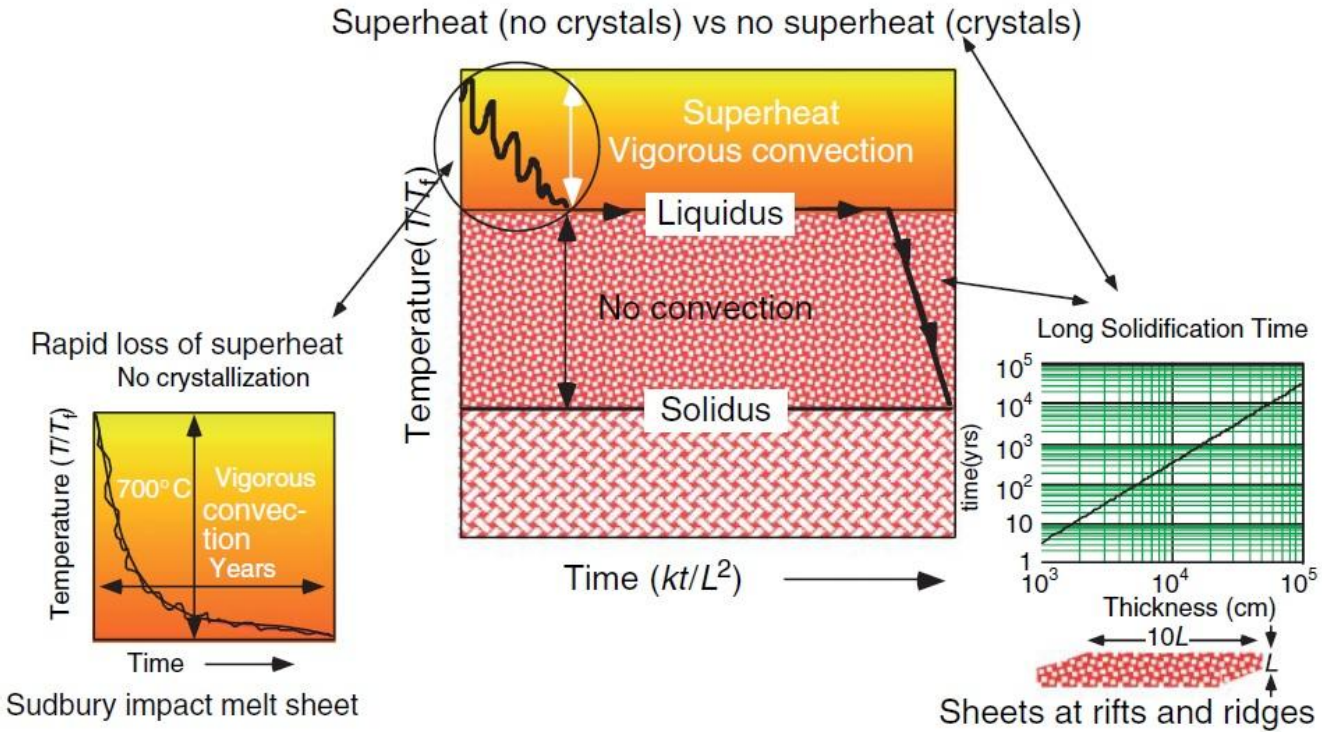

Marsh, 2007, Treatise of Geophysics, vol. 6

Slower convective cooling in conductive medium

(upper and lower layers of country rock are infinitely thick)

$$\frac{T - T_w}{T_m - T_w} = \exp\left(hx + h^2\kappa t\right)\operatorname{erfc}\left(\frac{x}{\sqrt{4\kappa t}} + h\sqrt{\kappa t}\right)$$

x=0

$$\frac{T - T_w}{T_m - T_w} = \exp(4F)\operatorname{erfc}\left(\sqrt{4F}\right) \qquad F = \kappa t/L^2$$

$h=2/L$ *for* $M=\rho' L/2$

The magma reaches T_L in about 10^4 years

T_m = the initial magma temperature, T_w = the initial wall rock temperature, x = the vertical spatial coordinate, and $h=\rho C_p/MC_p'$, where ρ is wall rock density, Cp and Cp' = the specific heats of the wall rock and magma, and M = mass of magma (of density ρ') in contact with a unit area of wall rock.

Arc Volcanism

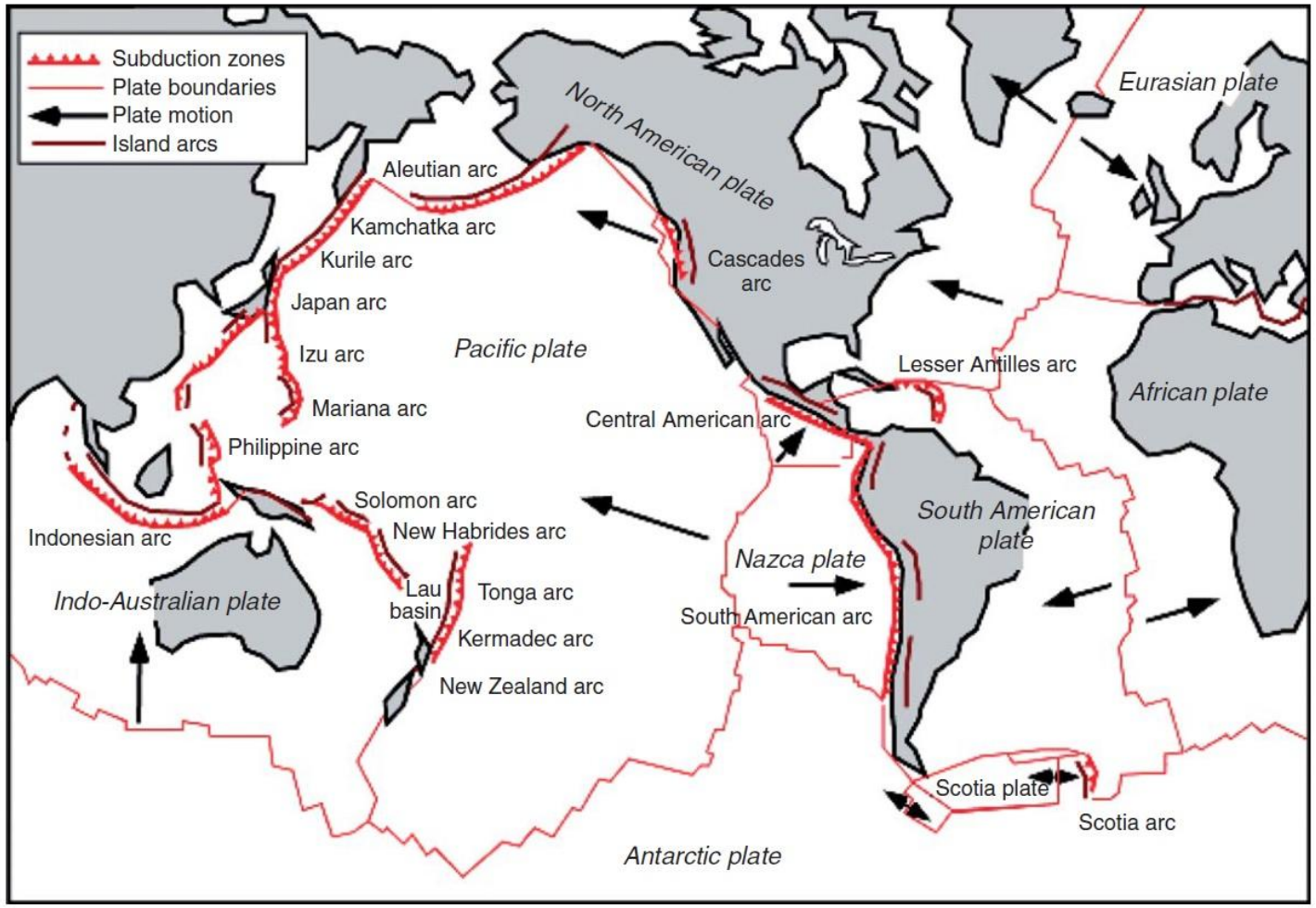

Marsh, 2007, Treatise of Geophysics, vol. 6

- The volcanic centers of the island arcs can remain fixed for long periods of time (1–10 My).
- In arcs a wedge of asthenosphere, sandwiched between the arc lithosphere and the subducting oceanic crust, provides almost any number of end members and combinations from which to get magma.
- The ages of the arcs also vary a great deal from those like the Aleutians that may be as old as 40 Myr to those as a young as the Scotia arc at 3 Myr.
- The detailed structure of the volcanic front of any arc often intimately reflects the structural morphology of the subducting plate (e.g., angle of subduction).
- Arc volcanic fronts are not simple continuous arcs, but are usually segmented into a collection of individual short segments forming a piecewise continuous arc.
- The dominant type of magma emitted depends on the density of the underlying crust: Arcs on continental terrains are dominantly andesitic (i.e., 60 wt.% SiO_2), whereas arcs on oceanic crust are dominated by High-Alumina Basalts (HAB, 50 wt.% SiO_2).

Flows in the mantle wedge of the subduction zones

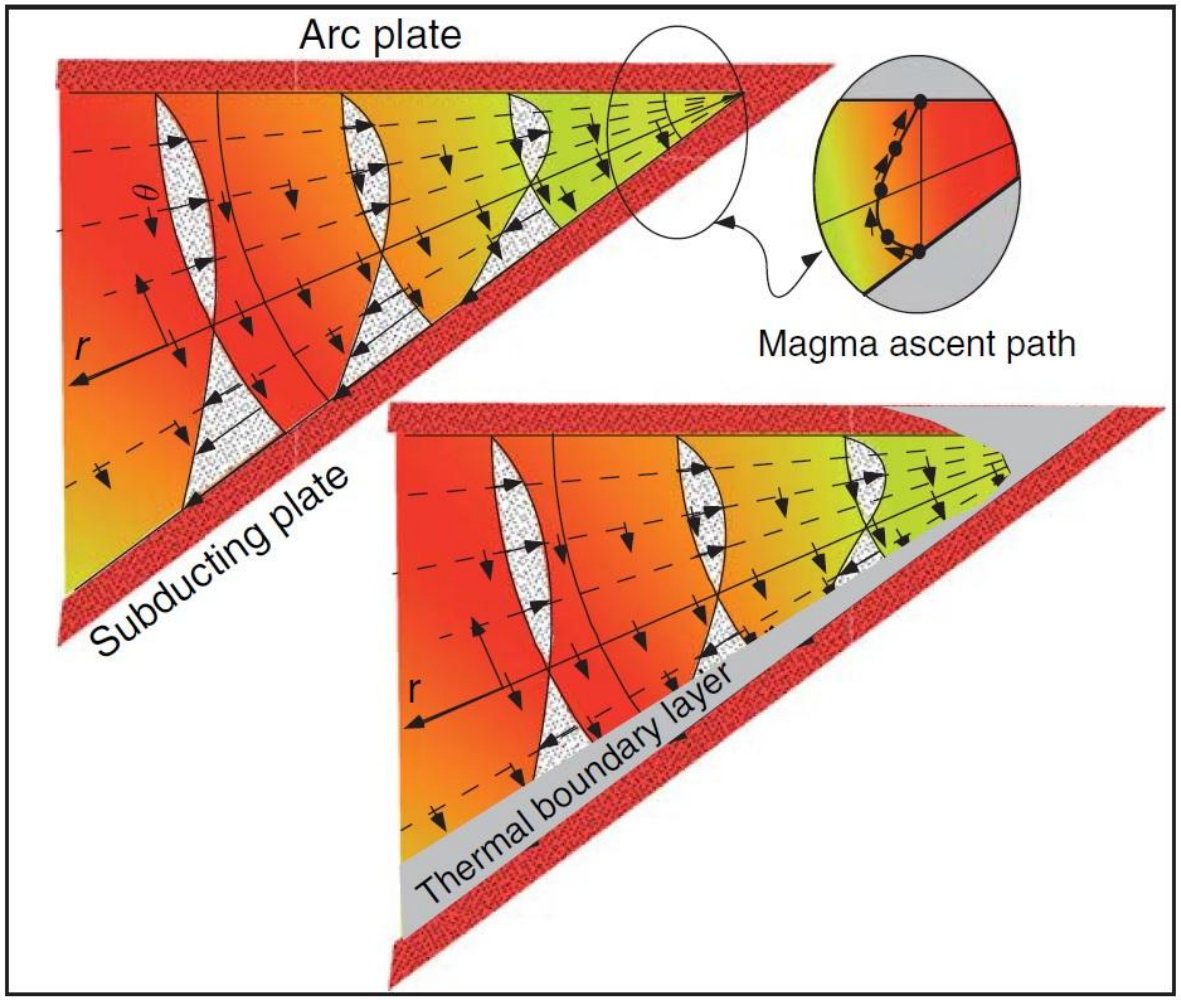

Marsh, 2007, Treatise of Geophysics, vol. 6

- At shallow depths, the subducting lithosphere is in fault contact with the adjacent arc lithosphere. The associated stress field creates a coupling between the two plates (welded together along the lithosphere-to-lithosphere fault contact).
- The depth extent of this contact is 70–100 km or longer in continental terrains, where the lithosphere is older and thicker.
- Below this depth of fault contact, the subducting plate is in contact with the mantle wedge, which adheres to the upper boundary with the arc lithosphere and at the same time is dragged downward by the motion of subduction.
- The flow in the mantle wedge has an upper part, which is essentially a parabolic flow between parallel plates (directed normal to the face of the subducting plate) and the lower half is a shear flow (streamlines parallel to the plate).
- Then, the corner flow continually brings into the wedge region hotter mantle material from greater depths, and this material is continually brought in contact with the subducting plate.
- Consequently, a cold thermal boundary layer develops near the corner and thickens down the plate of thickness δ_T.

$$\delta_T = C\sqrt{K}\left[\frac{x}{V}\right]^{1/2}$$

x= distance from the corner, which is measured by $x=t/V$, t = time, V = subduction velocity, K = thermal diffusivity, C= constant

Hydrothermal flow and magma formation in the subduction zones

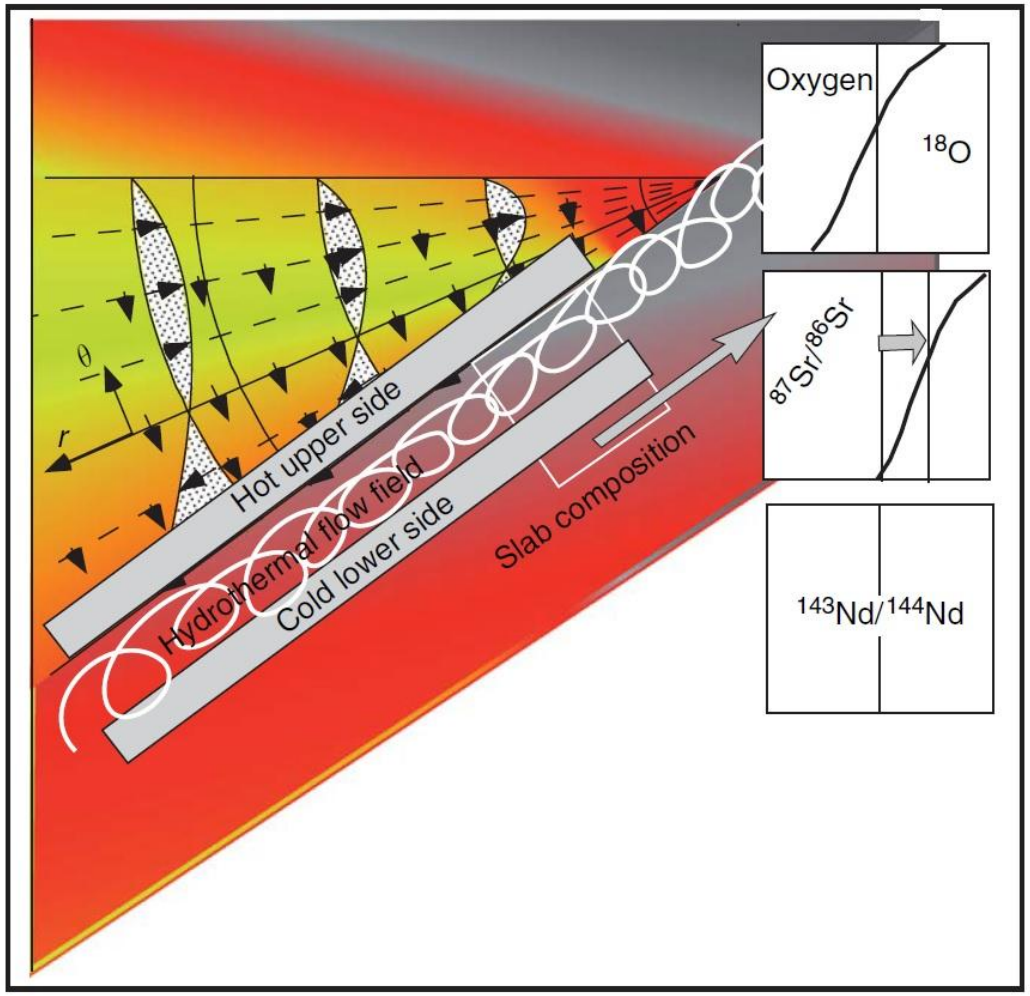

Marsh, 2007, Treatise of Geophysics, vol. 6

- The production of magma are the thermal regime and the transport of hydrothermal fluids.
- For seafloor rocks at 0°C brought up against mantle wedge at 1300°C, the crust interface of the subducting plate would achieve a *T* of about 650°C.
- However, we should consider that the contact between the two slabs extends to some depths (e.g., 125 km) and that frictional interaction produces heat, so that the oceanic crust may be brought to a temperature of about 1350°C and starts to melt.
- As the plate subducts and becomes heated, a new hydrothermal circulation system sets up due to phase transformations associated with dehydration. The form of this flow is horizontal and upward (helical).
- This flow is confined only to parts of the plate where there is sufficient permeability to allow flow (rocks are sealed beyond *T* of ~700°C).
- This flow has a critical effect on the chemical nature of the subducting plate, redistributing the initial amount of ^{18}O and ^{87}Sr and producing the net increase of the ratio $^{87}Sr/^{86}Sr$.

Magma composition of the volcanic arcs

Melt composition as a function of degree of melting at 3–4 GPa produced from:
a) quartz-eclogite subducted oceanic crust and b) pyrolite of the asthenospheric wedge.

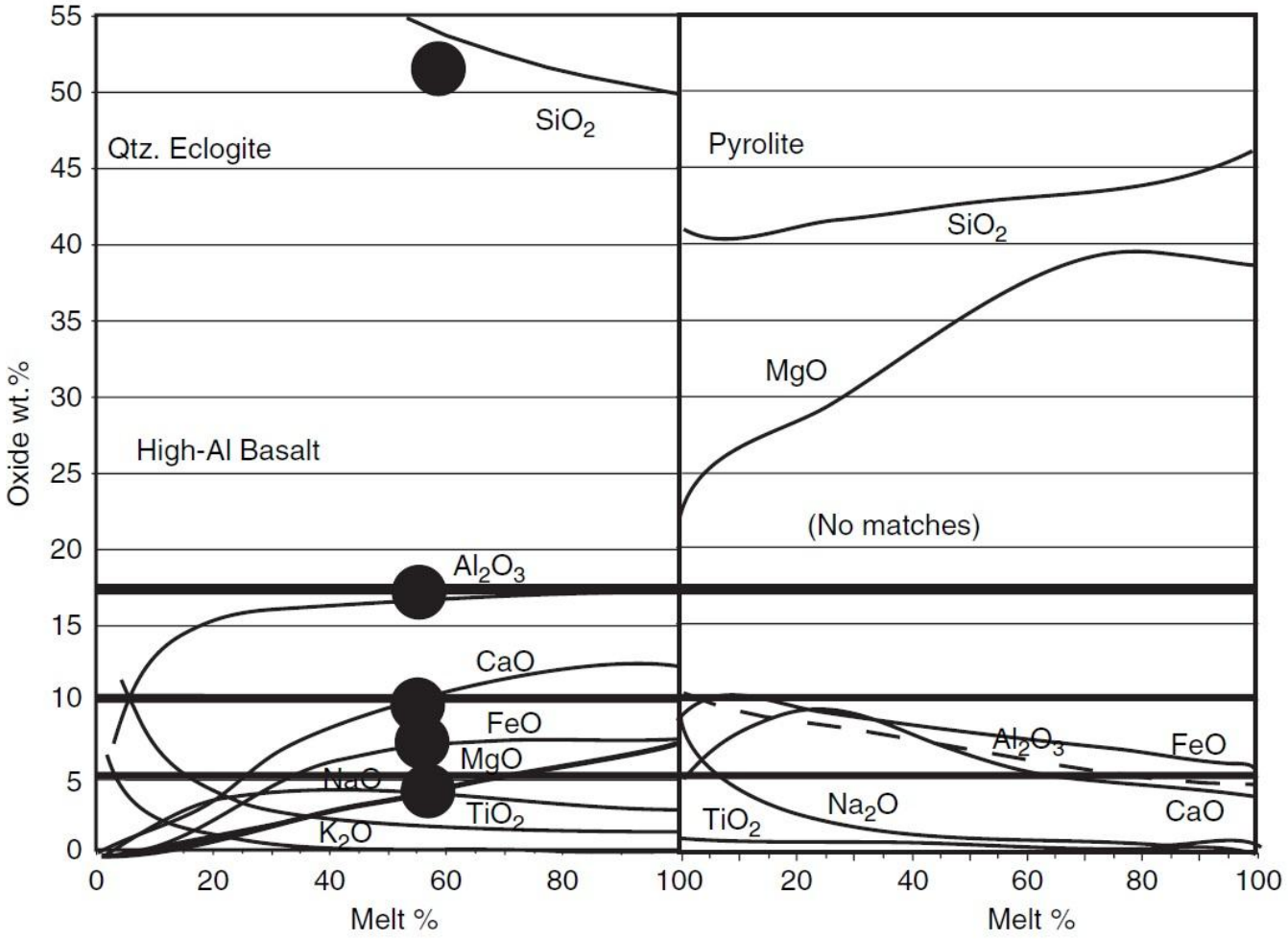

Marsh, 2007, Treatise of Geophysics, vol. 6

- The composition of the predominant basalt found in island arcs has an exceedingly close chemical affinity to subducted MORB.
- No matches are found for melt from the pyrolite wedge material, but matches are almost complete for each of the major elements for slab melting.
- Arc volcanic HABs have a low MgO content (7.5wt.%) and elevated Al_2O_3 content (16–20 wt.%).

At *P* of 2–3GPa, the MORB mineral assemblage of plagioclase, olivine, clinopyroxene transforms to quartz, garnet, jadeitic pyroxene (a quartz-eclogite rock).

The straight horizontal lines show the composition of typical HAB of island arcs (Aleutians) and the large dots show matching points between the observed HAB and the calculated melts.

Volcanic eruptions

- Explosive behaviour of highly viscous magma is due to the fact that different gases in superctitical conditions can be trapped and delivered along with the magma to the surface.
- The most active volcanoes (> 450) and the most powerful eruptions (> 85%) are located within the Pacific Ring of Fire.
- The most powerful eruptions result in caldera formation, whose products are represented by rhiolites and dacites, which have much lower melting point and higher viscosity than basaltic magma (which often do not reach the surface).

Yellowstone Caldera

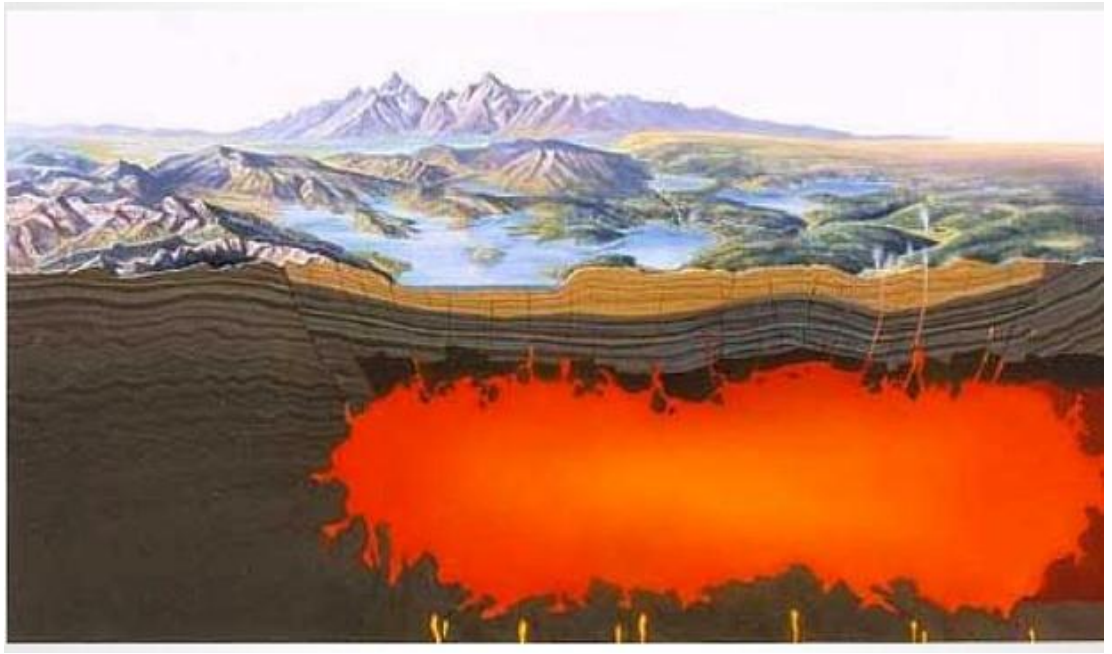

- The **Yellowstone caldera**, about 80 km long and 50 km wide, is the youngest of three nested and overlapping calderas, and is filled with younger rhyolitic lavas. The calderas were formed during three episodes of magmatic eruptions about 2 million years ago (~2,500 km^3 Huckleberry Ridge Tuff), 1.3 million years ago (~280 km^3 Mesa Falls Tuff), and 0.6 million years ago (~1,000 km^3 Lava Creek Tuff).
- The formation of hydrothermal features around the Yellowstone Lake area is related to convective meteoric hydrothermal fluid circulation above a cooling magma chamber.
- The total fluid discharge from all thermal features of Yellowstone National Park averages an astounding ~3,091 L/s and temperature ~345 K.
- Yellowstone National Park has the largest number of geysers in the world (> 400)

Kamchatka Peninsula

- **The Kamchatka Peninsula is located in the Pacific Ring of Fire and is one of the most volcanically active regions on Earth. There are about 300 volcanoes and about 30 are still active.**
- **The largest Holocene eruption in the Kuril–Kamchatka resulted in an estimated tephra volume of 140–170 km^3 with the formation of a caldera.**

Kamchatka Peninsula

Kamchatka has a great geothermal potential, characterized by thermal waters (used for heating) and geysers (more than 200 in the Valley of Geysers).

Mutnovsky Volcano

Site, feature	Temperature on surface (in K)	Power (in mW)
Active vent	>973	700
Northeast crater	578	400
North Mutnovsky springs (east group)	371	19
North Mutnovsky springs (west group)	383	9
Dacha springs	371	73
Pereval springs	369	9
Upper Zhirovskie springs	369	18
Voinovskie springs	366	8
Vilucha springs	363	12

Valley of Geysers

Geyser	Temperature (in K)	pH
Pervenets	371–372.6	8.35
Troynoy	371	8.5
Sakharniy	371	8.74
Sosed	371	8.2
Konus	371	8.2
Maliy	371	8.74
Bol'shoy	371	8.74
Schel'	371	8.74
Velikan	371	8.74
Zhemchuzhniy	371	8.74
Fontan	371	8.74
Dvoynoy	371	8.74

Iceland

Iceland located on the Mid Atlantic Ocean Ridge has about 130 volcanoes. Over the past 500 years, Iceland's volcanoes have erupted roughly a third of the total global lava output.

Iceland

- Geothermal gradients as high as 400 K/km were recorded in volcanically active areas.
- Hot springs are found throughout Iceland (but rare in the eastern basalt area). There are about 250 low-temperature geothermal areas (regions with temperatures ~ 423 K at depths ~1,000 m), with a total of about 800 hot springs, with an average temperature of water in a hot spring 348 K.
- Waters from hot springs and wells at Hveravellir geothermal field have a temperature in the range of 369–385 K and a pH of 9.32–9.44.

Area/system	Number of production wells	Average production (in kg/s)	Reservoir temperature (in K)
Svartsengi (SW-Iceland)	10	380	513
Laugarnes (SW-Iceland)	10	160	400
Reykir (SW-Iceland)	34	850	343–370
Nesjavellir (SW-Iceland)	11	390	553–613
Hamar (N-Iceland)	2	30	337
Laugaland (N-Iceland)	3	40	368
Krafla (N-Iceland)	21	300	483–613
Urridavatn (E-Iceland)	3	25	348
Gata (S-Iceland)	2	17	373
Bjarnarflag (Namafjall field)	–	12.5	553
Reykjanes (SW-Iceland)	–	–	548–583
Theistareykir (NE-Iceland)	–	–	613–653
Húsavík (NE-Iceland)	–	–	393–403

New Zeeland

New Zealand is one of the most active regions in the Pacific Ring of Fire

Almost all of the highly active geothermal fields in New Zealand, are located within the geologically young Taupo Volcanic Zone, which has shallow reservoirs/aquifers (500–1,500 m depth) containing boiling or near-boiling water/ fluids (523–573 K).

Thermal characteristics of geothermal fields, thermal and pH characteristics of waters in the Taupo Volcanic Zone

Geothermal field	Maximum reservoir temperature (K)	Water temperature on discharge (K)	pH
Atiamuri	438–473	338–346	7
Broadlands (Ohaaki)	581	371	<3–8
Golden Springs	–	313–333	6.5–7
Crater Lake (Ruapehu)	–	308–371	<3
Horohoro	>433	352	8.5
Kawerau	>588	371	6.5–7
Mokai	597–599	371	<2–7.6
Orakeikorako	538	338–371	7–9.2
Orakeikorako	–	313–363	2–3.5
Mangakino (excl. Whakamaru or Ongaroto)	527	371	8.5
Moutohora	–	371.5	<4
Reporoa (excl. Golden Springs)	513	371	<3–8.7
Rotokawau (Rotokawa) (Rotorua)	428	320–323	6.5–6.7
Rotokawa (Taupo)	593	313–363	2.5–5.5
Rotorua	523	363–371	<2–9
Taheke	–	313–372	2–5
Tarawera	–	293–371.6	7–8.7
Tauhara (excl. Wairakei)	552	335–371	2–8
Te Kopia	514	318–378	<2–7.5
Tikitere (Hell's Gate, Ruahine Springs)	503	313–371	2–7.6
Tokaanu	523	371	3.5–8.7
Tongariro	523	343	<2.5
Waihi (see Tokaanu)	523	371	6.6–7.9
Waimangu (and Rotomahana)	543	328–371	<3–9
Waiotapu	568	371	1.8–8
Whakaari (White Island)	1,073	573–773 gas	
Ketetahi	–	327–411	2.0–6.5
Waikite Valley	–	371	8–8.7
Wairakei	544	371	<3
Whangairorohea	–	311	7.4
Okataina	–	312	7
Longview Road	–	306–365	3.7–6
Opaheke (Opateketeke)	–	318–371	3–8
De Bretts (Terraces)	–	323–353	7.8
Waiora Valley	–	371	3
Ngatamariki	563	–	–
Rotoma	493–523	–	–

Japan

- Japan, another segment of the Pacific Ring of Fire, is a very seismically and volcanically active region and has one of the highest potentials for geothermal energy in the world, due to the large number of hot springs.
- The main water reservoirs in the Kuju-Beppu Graben are at least 500 m deeper (at 1,000–2,000 m), and they have a water temperature of about 30–80 K lower (493 K) than those in the Taupo Volcanic Zone in New Zeelend.

Japan

Hot spring	Temperature on discharge (in K)	pH
Kannawa Ishimatsu	373	7.7
Kannawa Chinoike	333	2.4
Myoban Yamadaya	340.5	1.7
Kanegawa Shinoyu	329.6	8.2
Old-City Kinura	328.6	7.4
Hotta Hotta	348.5	6.2
Kankaiji Jizouyu	323	6.9
Nasu	318.2–346.1	1.5–1.7
Takao	307	5.6
Sandogoya	365	2.6
Nikko-yumoto	328.2–342	6.0–6.8
Yunohanazawa, Hakone	306–350.2	2.0–2.6
Ashi-no-yu	313–314	6.4
Kowakudani	334	8
Ubako	318	5
Kusatsu	330–338	1.5–1.6
Isobe	288.5	6.6
Ikao	317.2	6.2
Tanigawa	315.3	8.2
Tateyama	315	1.2
Arima	334–364.3	6.0–6.6
Hakone Springs:[a]		
Zone I	322.7	2.9
Zone II	330.5	8.1
Zone III	364.5	7.7
Zone IV[a]	338.5	8.4
Zone IVb	329	8
Ground water	286.1	7.2
Obuki[b] (Tamagawa springs)	369–372	1.22–1.42
Owakudani	309.3–369	2.48–4.25
Azuma	320–373	Neutral
Zao	338	Neutral
Hijiori	357	Neutral
Akakura	347	Neutral
Akayu	336	Neutral

[a] Zonation of Hakone spring area after (Oki and Hirano 1974)
[b] Fluctuation of temperature (1962–2000) and pH (1959–2000) after (Yoshiike 2003)

- Analysis of 3,686 hot springs in Japan showed that they belong to relatively low-temperature geothermal fields with a reservoir temperature of 533 K.
- One of the largest hot spring fields in Japan is the Beppu Geothermal area. The source of heat for the high *T* manifestations is related to the middle-to-late Pleistocene Yufu volcanic formations (~0.32 Myr) and lava domes younger than 100,000 years.
- Japan has the highest number of hot springs in the world, but very few geysers, due to the greater depths of the main thermal sources than in active geyser regions, as well as the much lower temperatures at shallow depths than in these areas.

Rate of discharge of hot springs

- None of most powerful hot springs on the Earth comes close to the average discharge rates of the most powerful non-thermal springs on the Earth (> 2,800 L/s).
- Non-thermal springs require higher flow rates and the presence of more permeable aquifers than those in warm or hot spring waters.
- Low flow rates ensure more lengthy contact of water flowing through the aquifer provides better heating conditions for the spring water (larger temperature).

Rate of discharge of some hot springs and hot spring systems

Spring or system of springs	Average rate of discharge (in L/s)	Magnitude of spring
Yellowstone National Park, USA:		
Total for all thermal features in the Park	3,091	–
Upper Geyser Basin	696	2
Lower Geyser Basin	662	2
Midway Geyser Basin	252	3
Mammoth Hot Springs	57	3
Shoshone Geyser Basin	66	3
Heart Lake Geyser Basin	104	3
West Thumb Geyser Basin	47	3
Kamchatka Peninsula, Russia:		
Paratunka geothermal field	221	3
Esso geothermal field	168	3
Anavgay geothermal field	34	3
Springs in vicinity of rivers Goryachaya and Zholtaya	80–110	3
Taloviye	6	5
Krayevedcheskie	7	4
Verkhne-Schapinskie	40	3
Valley of Geysers, Kamchatka Peninsula:		
Total for the basin	300–315	2
River Geysernaya	3,340	–
Podskalniy	5	5
Bolshoy	3	5
Geyser Velikan	2.4	5
Deildartunguhver, Iceland	180	3
Hveravellir, Iceland	35–40	3
Gata, Iceland	10–22	4
Thorleifskot, Iceland	70–80	3
Yamagata prefecture, Japan, total of 140 springs	916	–
Zao, Yamagata prefecture, Japan	92	3
Bepu Geothermal Area, Japan, Total	579	2
Obuki, Tamagawa springs, Japan	166	3

Oceanaic Vents

- Hot springs in oceanic areas or vents have a temperature ranging from 623 K in the axial zone of ridge to 293 K far away.
- Extra-hot vents are divided into **'black smokers'**, emitting hydrothermal fluids with temperatures mostly within the range of about 573–673 K, containing dissolved metals and **'white smokers'**, with temperatures of 523–573 K, with almost no metals in the ejected fluids.

Temperatures of discharged fluids for some black and white smokers

Vent type and location	Temperature of water (in K)	References
Black smokers:		
Mid-Atlantic Ridge:	613–663	Petersen et al. (2000)
TAG at 26°N	636	Fouquet et al. (1998)
TAG at 26°08′N	583–593	Pedersen et al. (2010)
Loki's Castle, 73°30′N and 8°E	573–673	McCaig et al. (2007)
low-angle detachment fault at 15°45 N	600–654	Herzig et al. (1998)
Black smoker complex (TAG-1) at 26°N	~638	German et al. (2010)
Rainbow hydrothermal field at 36°14′N 5°S	680–737	Haase et al. (2007)
East Pacific Rise:		
Galapagos Rift, 21°N	623	Köhler et al. (1994)
East Pacific Rise	603–678	Tivey (2007)
9–10°N	656	John et al. (2008)
Site #7 at 12° 49′N	653	Graham et al. (1988)
Site #10 at 10°58′N	620	Graham et al. (1988)
Central Indian Ridge:		
Kairei vent field at 25°19.239S, 70°02.429	579–638	Van Dover et al. (2001)
Edmond vent field at 23°52.689S, 69°35.809E	up to 655	Van Dover et al. (2001)
Juan de Fuca Ridge:		
Middle Valley in the area of active venting	up to 633	Turner et al. (1993)
'Sully' and 'Puffer' vents	628–633	Crone et al. (2006)
Izena Hole, Mid Okinawa Trough	593	Sakai and Nozaki (1995)
White smokers:		
Mid-Atlantic Ridge:		
TAG at 26°08′N, the Kremlin area	533–573	Herzig et al. (1998)
East Pacific Rise:		
Galapagos Rift, 21°N	543	Köhler et al. (1994)
9–10°N	480	John et al. (2008)
Site #9 at 11°14′N	~543	Graham et al. (1988)
Site #3 at 12°51′N	>483	Graham et al. (1988)
Juan de Fuca Ridge:		
Middle Valley in the area of active Venting	457–553	Turner et al. (1993)
Northern Okinawa Trough	551	Sakai and Nozaki (1995)

Phlegrean Fields

- Volcanism and hydrothermal activity at the Phlegrean Fields has been active over the past several hundred thousand years and is associated with Quaternary extension along the Eastern Tyrrhenian Margin.
- The Phlegrean Fields consist of two nested calderas, resulting from the interaction between regional and local tectonics. The formation of the larger, outer caldera has been related to the Campanian Ignimbrite eruption (37.000 years ago, with 80 km^3 of material), while the inner caldera formed during the eruption of the Neapolitan Yellow tuff (12.000 years ago, with 10 km^3 of material).
- Most eruptive activity has occurred during two periods: from 10.000 to 8.000 years ago and from 4.500 to 3.700 years ago, while in the last 2000 years there was only one eruption occurred in 1538 which gave the birth to Monte Nuovo.

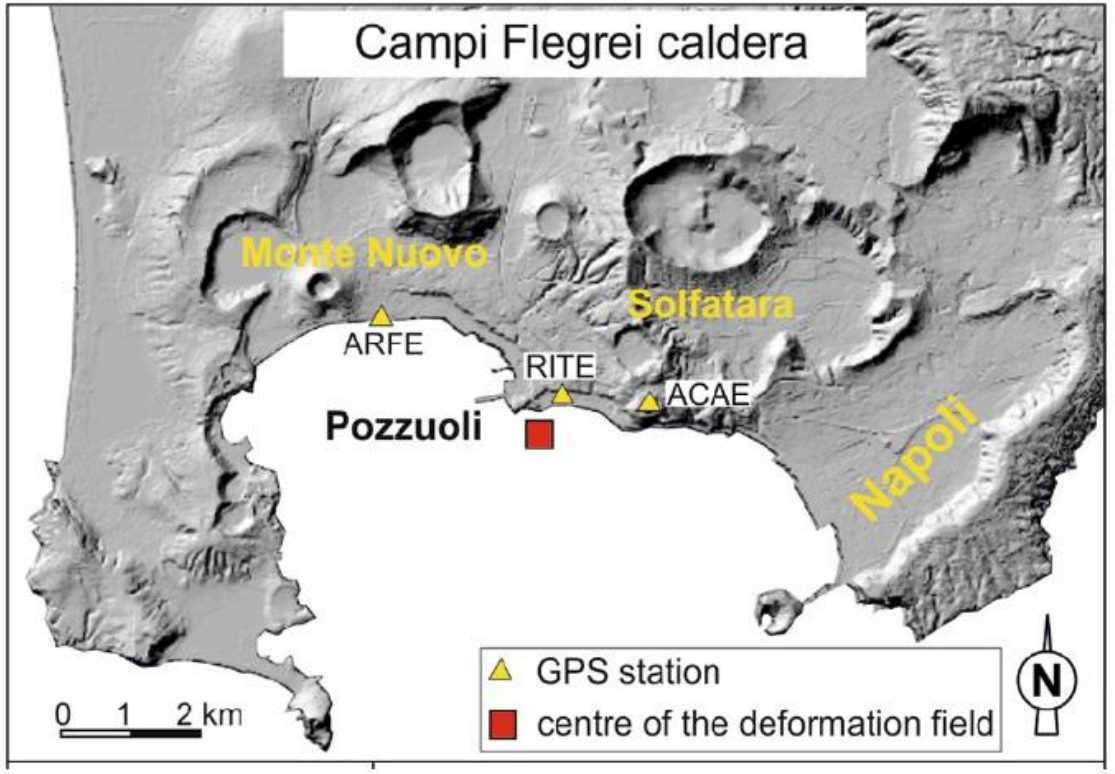

Phlegrean Fields

- During its history, the Phlegrean Fields have alternated phases of uplift and subsidence over a range of timescales. In the last century, there were two major uplift and seismic episodes (‘bradyseisms’) (1969–1972 and in 1982–1984, respectively). These episodes have produced a total vertical displacement of 3.8 ±0.2m and have been accompanied by thousands of shallow earthquakes.
- Since 1985, Phlegrean Fields have been slowly subsiding, which has been interrupted by a few minor uplift events. In 2005, there was new inflation, with a consequent vertical displacement (e.g.,~23 cm by June 2014). This last stage was accompanied by weak seismicity, by a strong increase in fumarolic activity, and by compositional variations in the fumarolic effluents.

Monitoring network

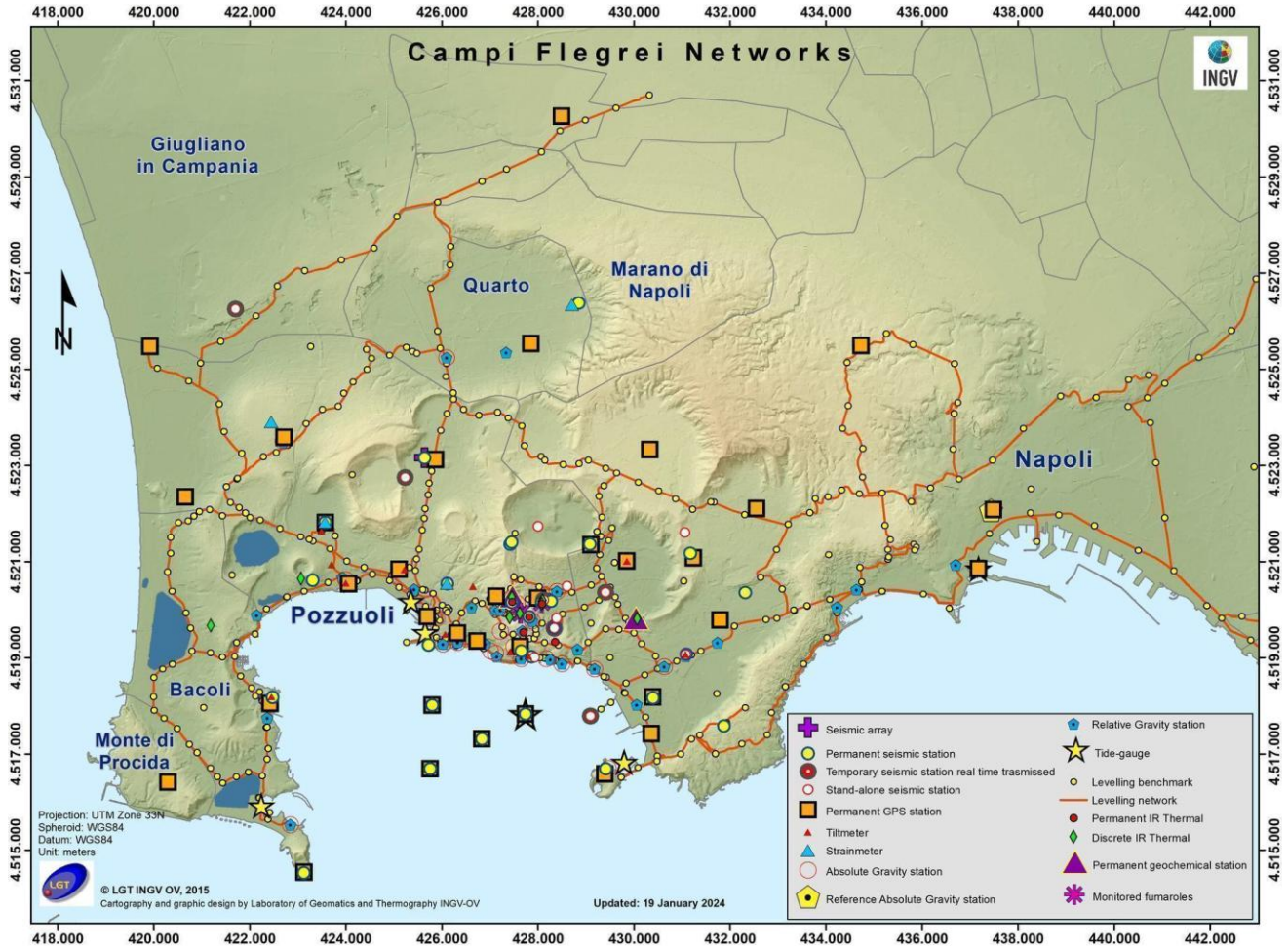

Phlegrean Fields

15000 - 10600

9600 - 9200

5500 - 3800

- After the last caldera collapse the volcanism was intense, frequent and clustered in three epochs of activity separated by long periods of quiescence and preceeded by large ground deformations.
- The majority of the 72 eruptions were explosive with different magnitude and fed by vents active in a large part of the caldera floor.

Phlegrean Fields

Vertical movements history at Serapis Temple in Pozzuoli.

Black circles: constraints found from radiocarbon and archaeological measurements.

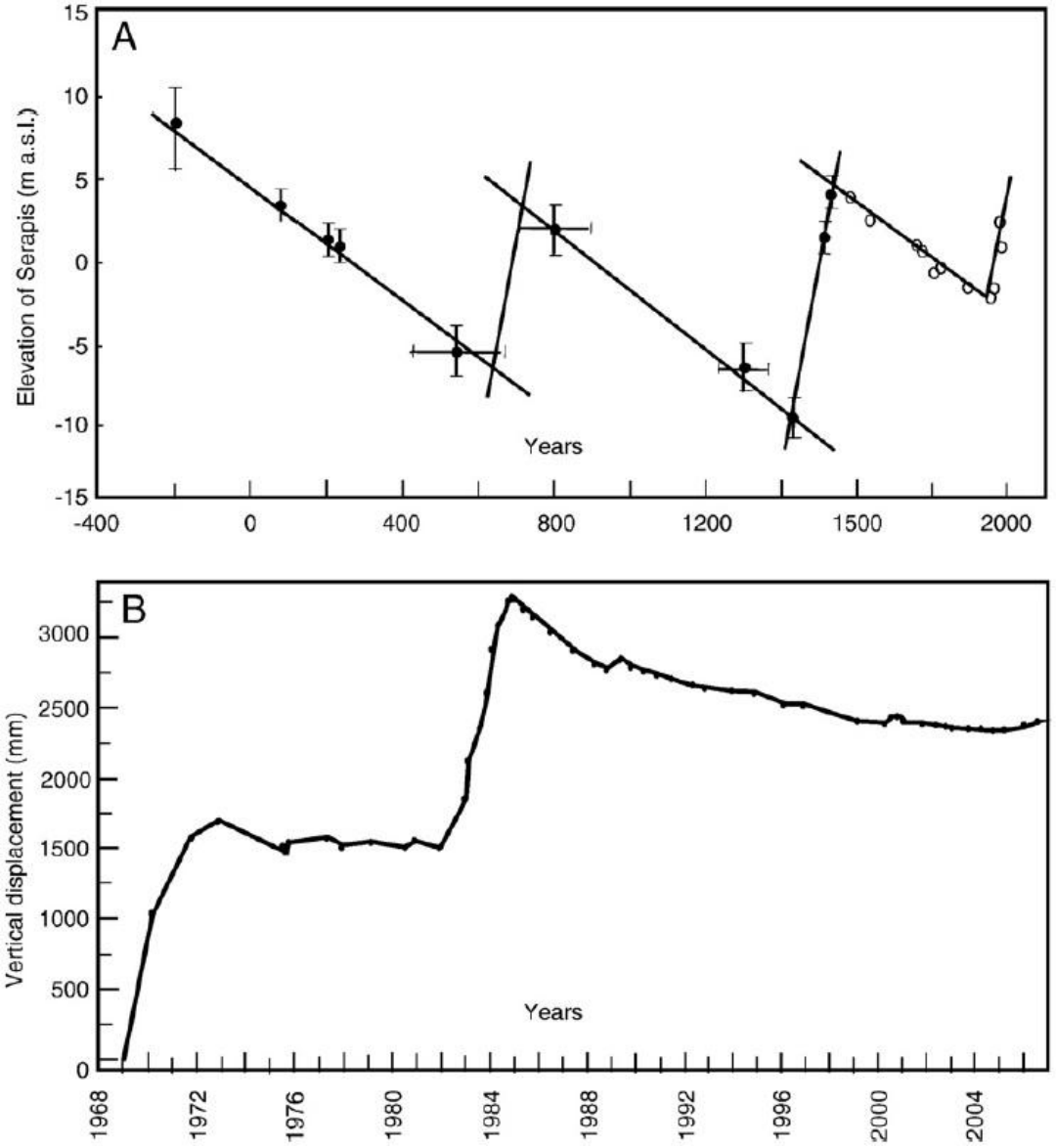

Serapis Temple

Vertical ground displacements as recorded at Pozzuoli Harbour by levelling data (1969–2006).

Phlegrean Fields

Horizontal and vertical ground deformations since 2023

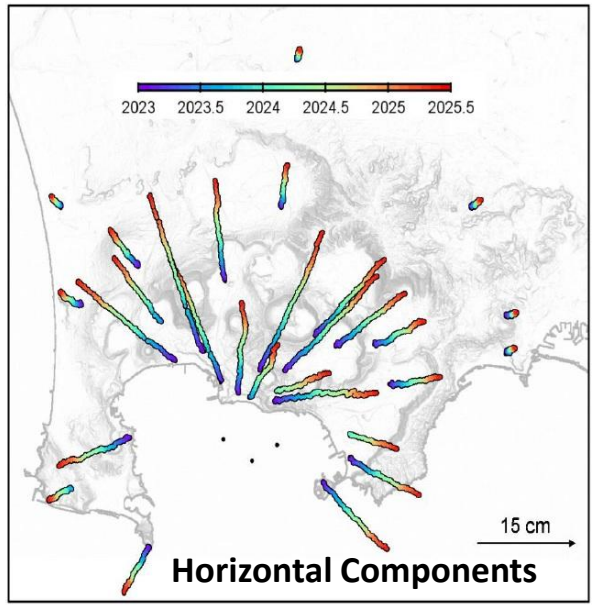

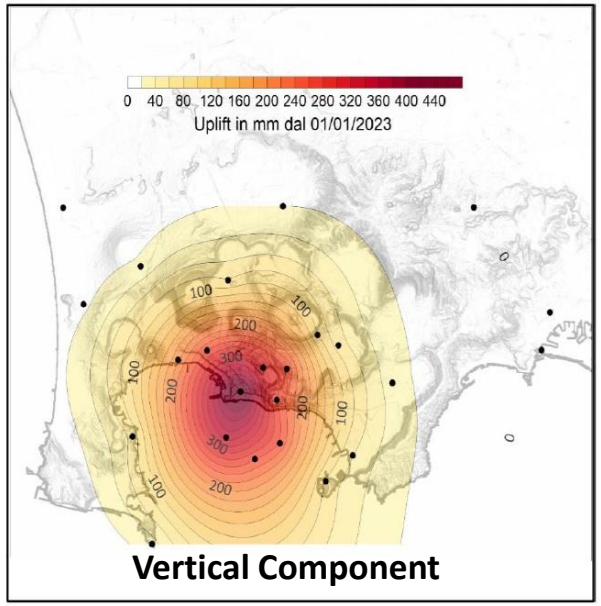

Ground temperature measured over 61 fixed points

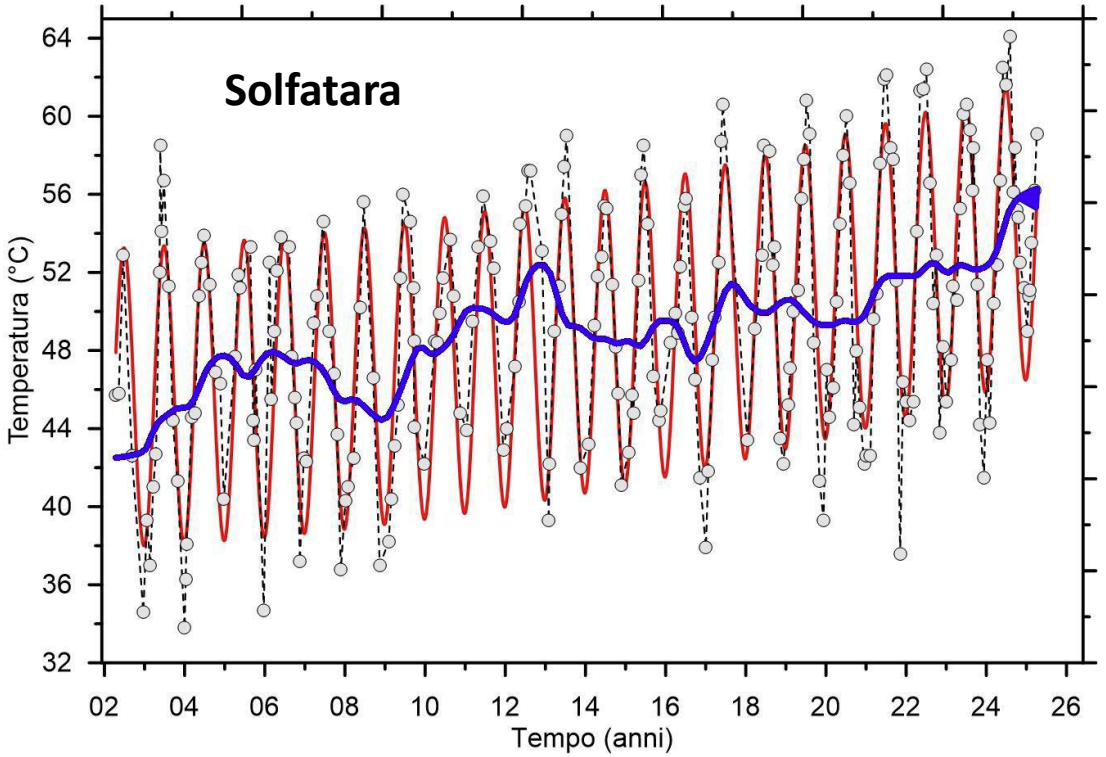

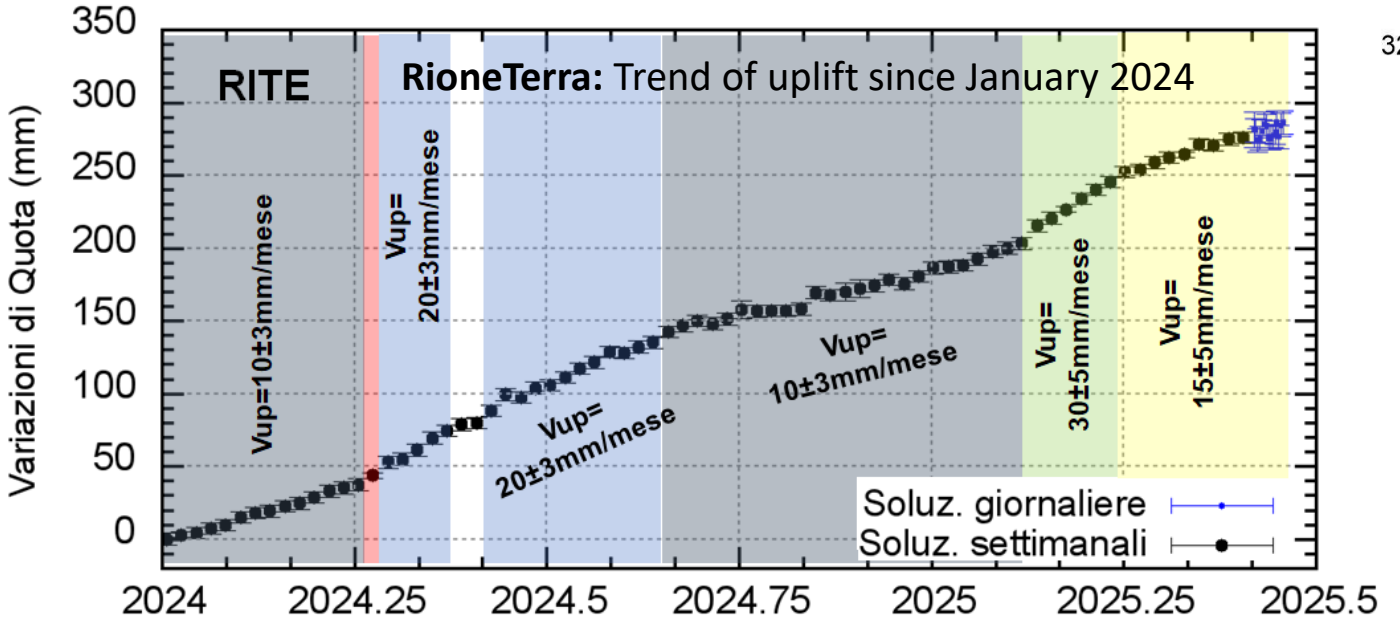

Phlegrean Fields

Surface Temperature

Landsat 8

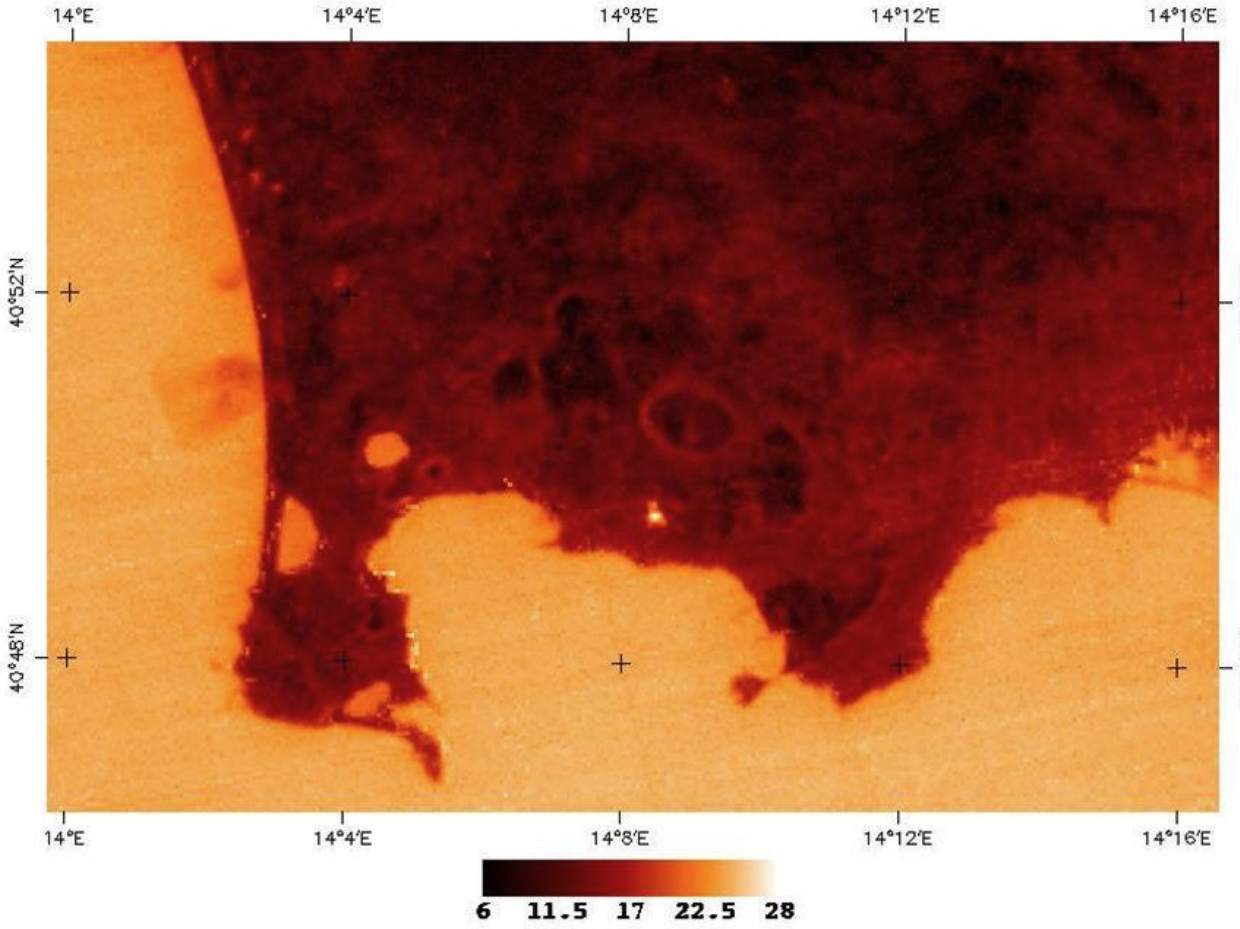

ASTER

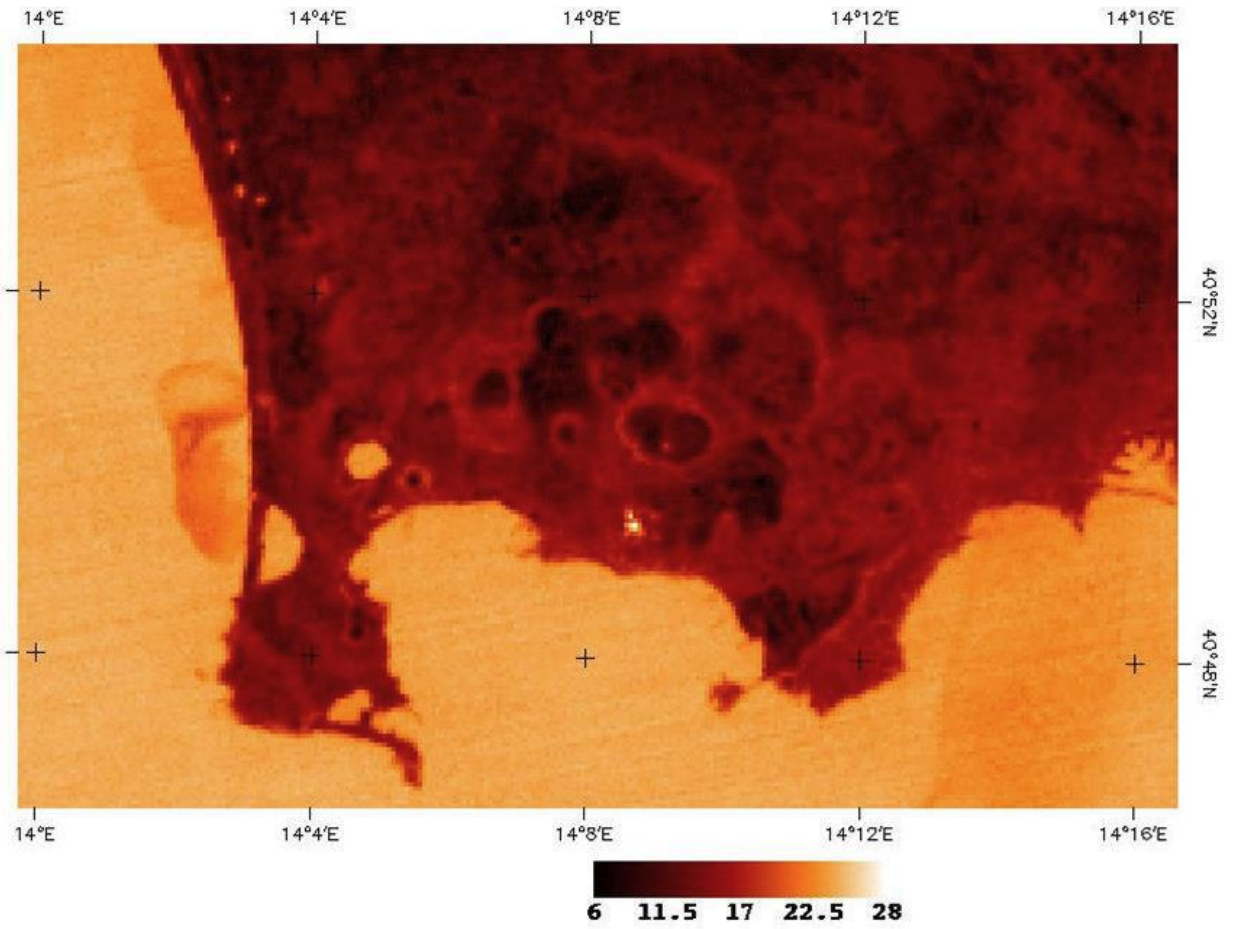

Phlegrean Fields

Models of CF bradyseism fall into three main categories:

- **One scenario relates ground surface deformation (GSD) directly to emplacement of a fresh batch of magma at shallow depth.**
- **A second class of models also involves fresh magma input (recharge) to trigger bradyseism not in response to pressurized magma, but rather due to the injection of magmatic fluids into overlying crust.**

In the second case:

- Injection of high temperature magmatic fluid into the shallow hydrothermal reservoir system induces fluid overpressures that may cause the host rocks to **inflate** depending on the mechanical properties of the local crust.
- **Subsidence** results from a decrease in the flux of magmatic fluid entering the hydrothermal system or as a response to rapid permeability increases and hence pore pressure decreases.

Phlegrean Fields

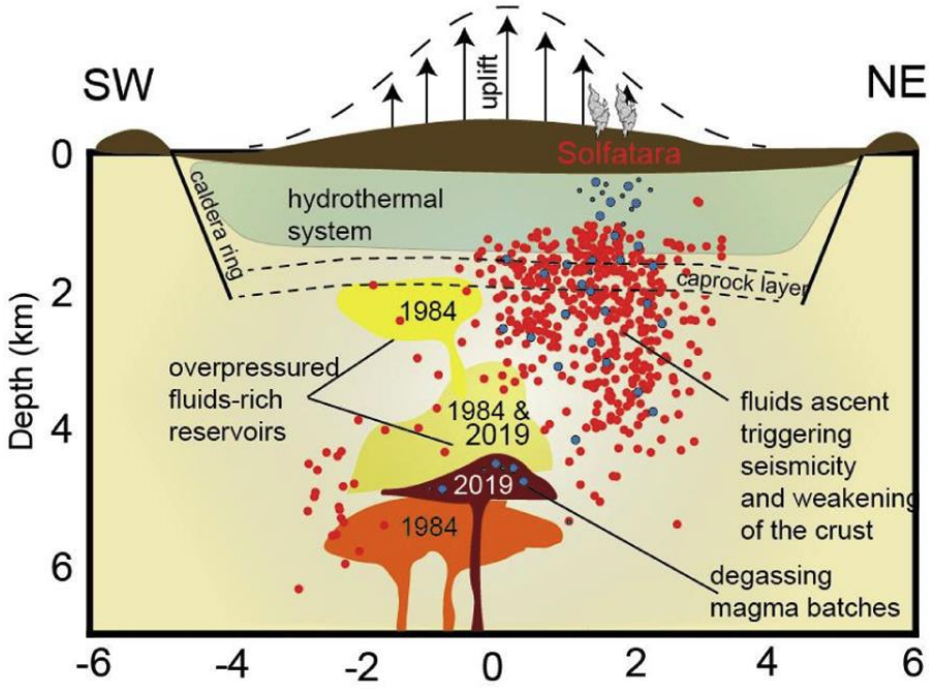

Giacomuzzi et al. 2024

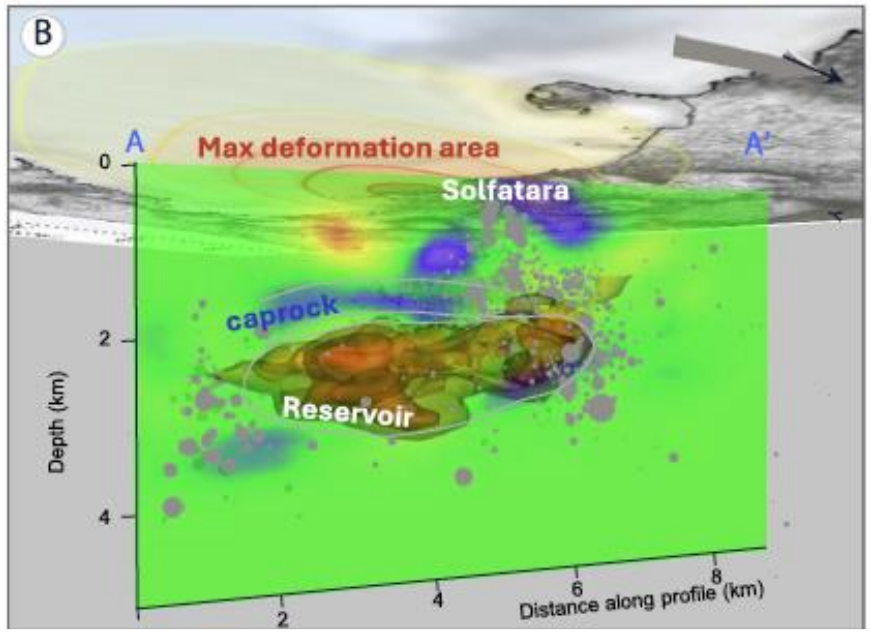

De Landro et al. 2025

- The magma is absent in the first 4 km
- The central reservoir appears to have been recharged by magmatic fluids during the 1982–1984 unrest and, after a period of possible degassing, also during the current unrest.

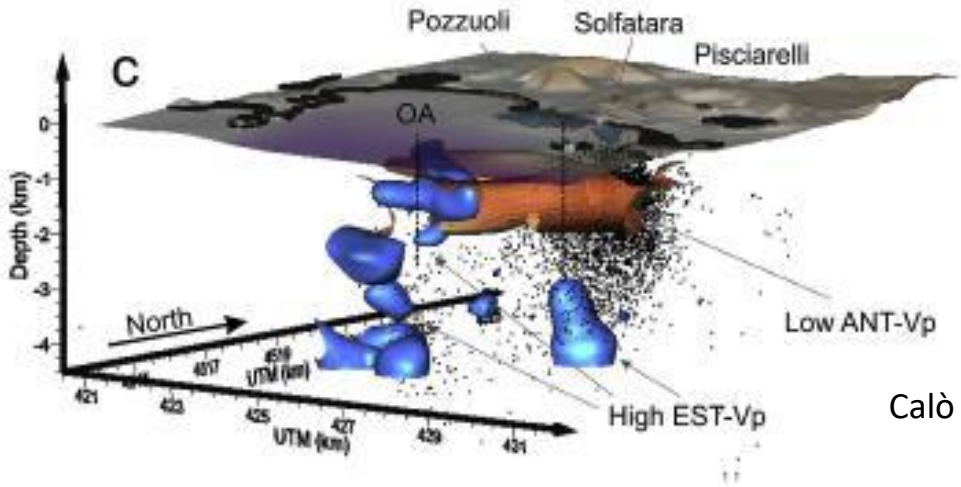

Calò and Tramelli 2025

Phlegrean Fields

Comparison between ground deformation and geochemical signals

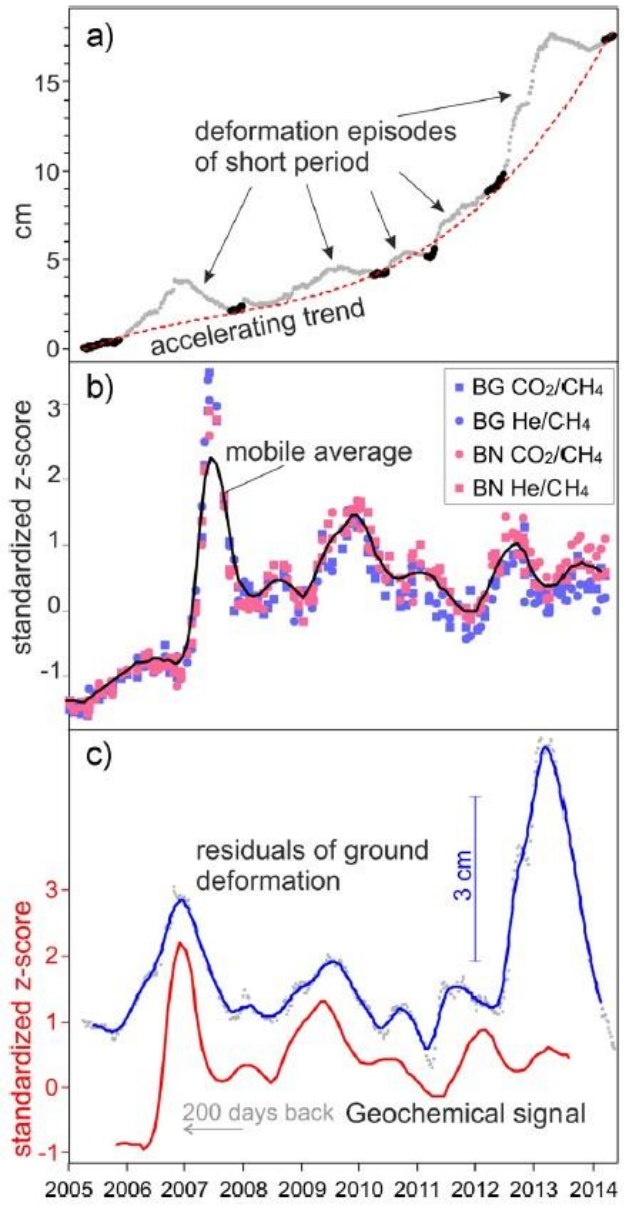

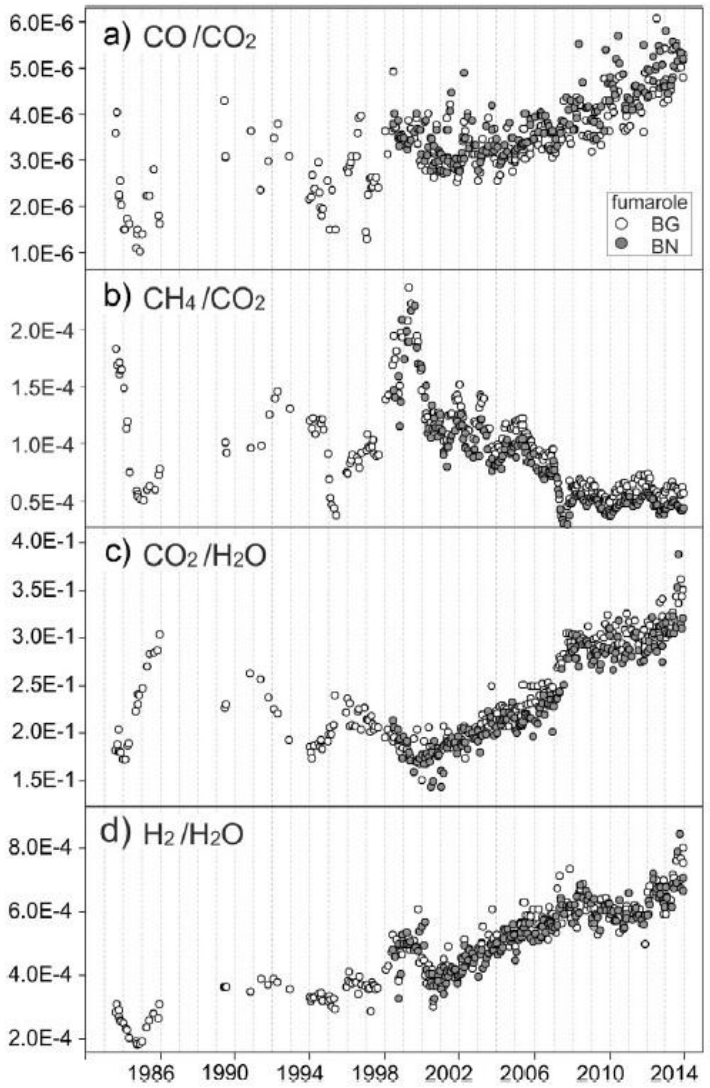

Chiodini et al., 2015, EPSL, 414

- During the phases of uplift, the CH_4 content of the fumaroles decreased, while the content of other gases of prevalent magmatic origin, such as CO_2 and H_2 tend to increase.
- The sharp increase in the proportion of the magmatic component over relatively short periods, was interpreted as resulting from magmatic fluid injections into the hydrothermal system.
- The delay between the uplift and geochemical signals would represent the transfer time of the magmatic fluids from the input zone to the fumarolic discharge areas.
- *CO* and CH_4 qualitatively indicate a temperature increase for the entire hydrothermal system, which is likely caused by the increment in the flux of the magmatic fluids that enter the hydrothermal system.
- The increment in the flux of the deep hot fluids would cause water vapor condensation within and at the border of the gas plume and heating of the rock by the latent heat release during condensation. The condensation of the steam may causes the continuous increase in non-condensable gases (CO_2) in fumaroles.
- When the magma depressurizes, it releases increasing amounts of steam that will heat the system, generating signs of long duration in the deformation patterns.

Phlegrean Fields

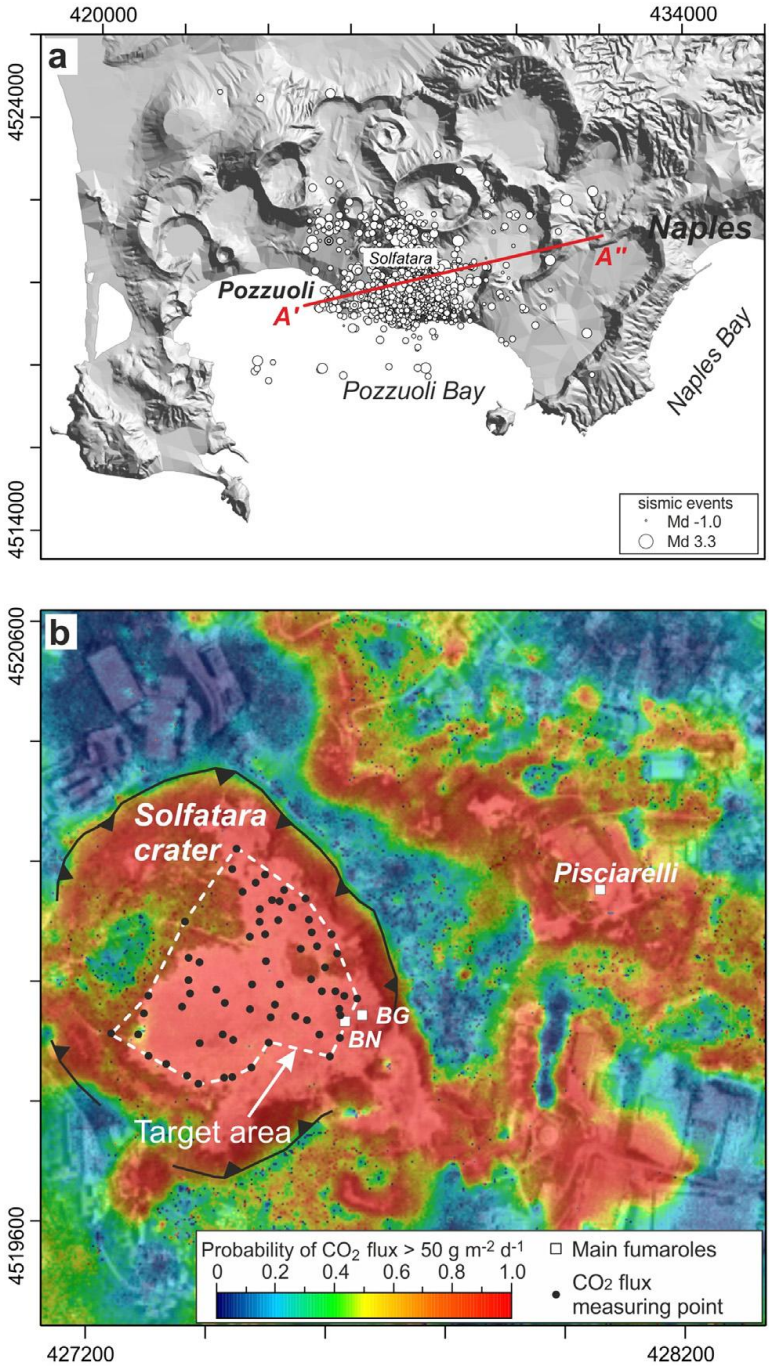

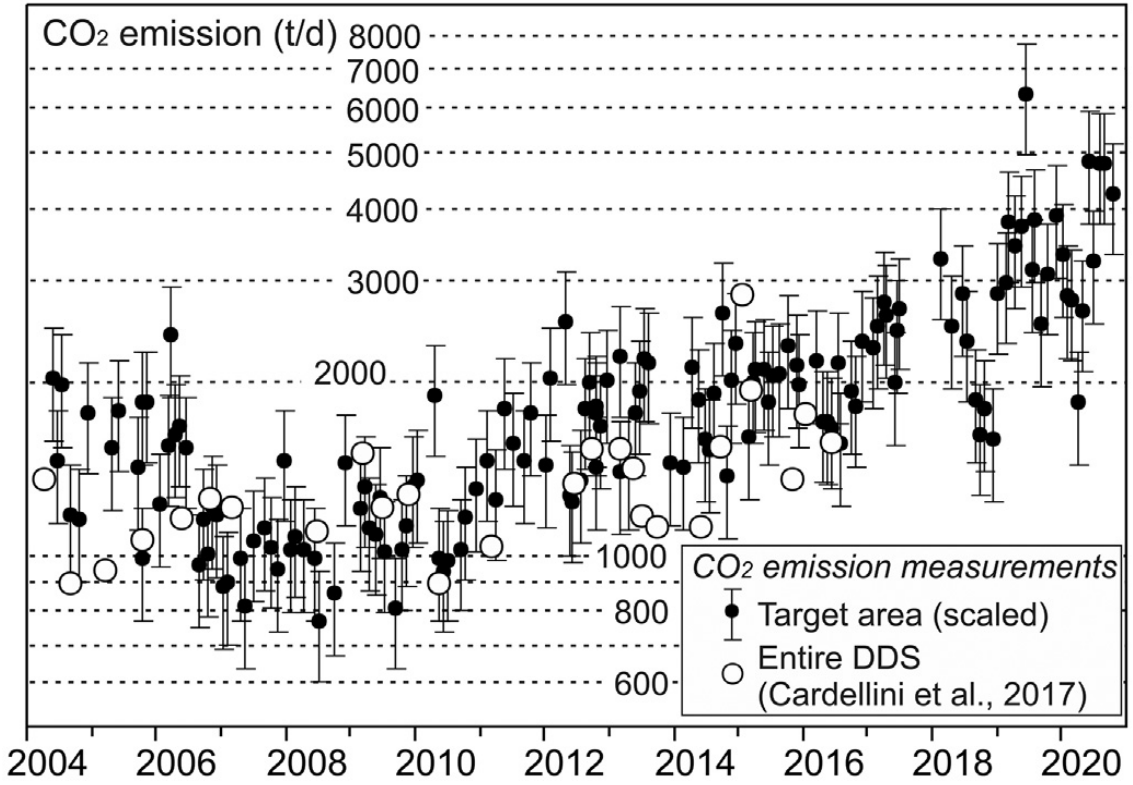

Chiodini et al., 2021, J. Volcanology and Geothermal Research, 414.

- The total CO_2 emissions from Solfatara DDS increased from ~1000 t d^{-1} in 2008–2010 up to 3000–4000 t d^{-1} in 2019–2020, while the current total CO_2 emission from Solfatara-Pisciarelli at ~5000 t d^{-1}. The pressurization of a steam-rich gas phase can induce its condensation.
- Deep condensate can potentially trigger earthquakes because the condensed liquid can lubricate pre-existing fractures and hydrothermal host rocks get hotter, increase in volume by thermal dilatation, and finally fracture.

Phlegrean Fields

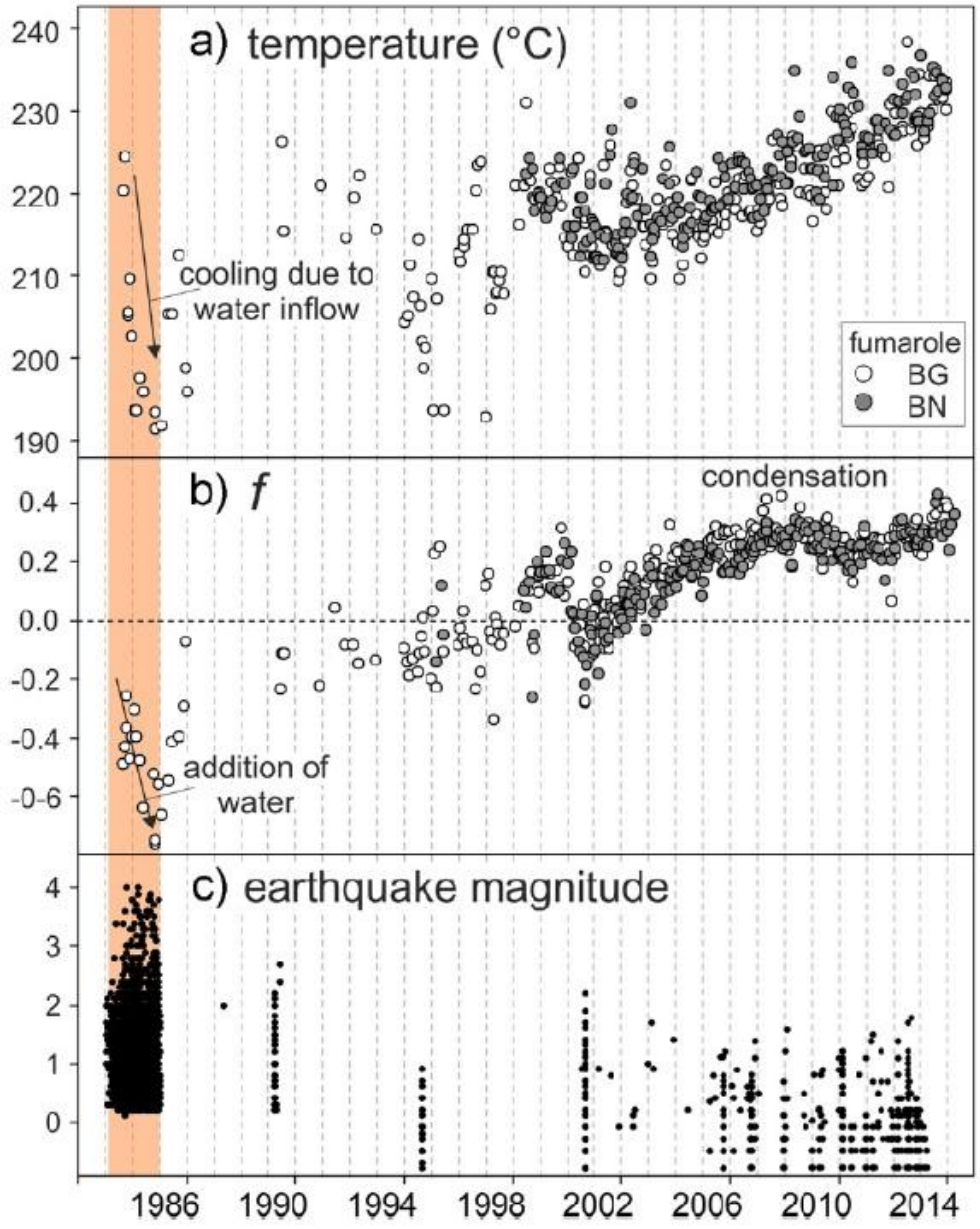

- From 1983 to 2014, the temperature estimations of the fumaroles range from 190°C to 240°C and show a continuous increasing trend during the 2005–2014 phase of ground acceleration.
- *T* and water fraction (*f*) have a marked negative anomaly during the 1983–1984 seismic, which might have been caused by a *T* decrease, as a result of the input of liquid water in the Solfatara plume (e.g., due to the increase the rock permeability by creating new fractures during the earthquakes).

From 2003-2014, the total amount of heat released by steam condensation was ~6.2 $\times 10^{12}$kJ. This would produce a 5°C heat increase in a mass of ~1.25 $\times 10^{12}$kg of rock, which corresponds to a volume of 0.625 km^3(with a density of 2000 kg/m^3).

For a volumetric expansion coefficient of 3×10^{-5}/°C, the volume increase would be of ~0.94 $\times 10^5$m^3.

Chiodini et al., 2015, EPSL, 414

Phlegrean Fields

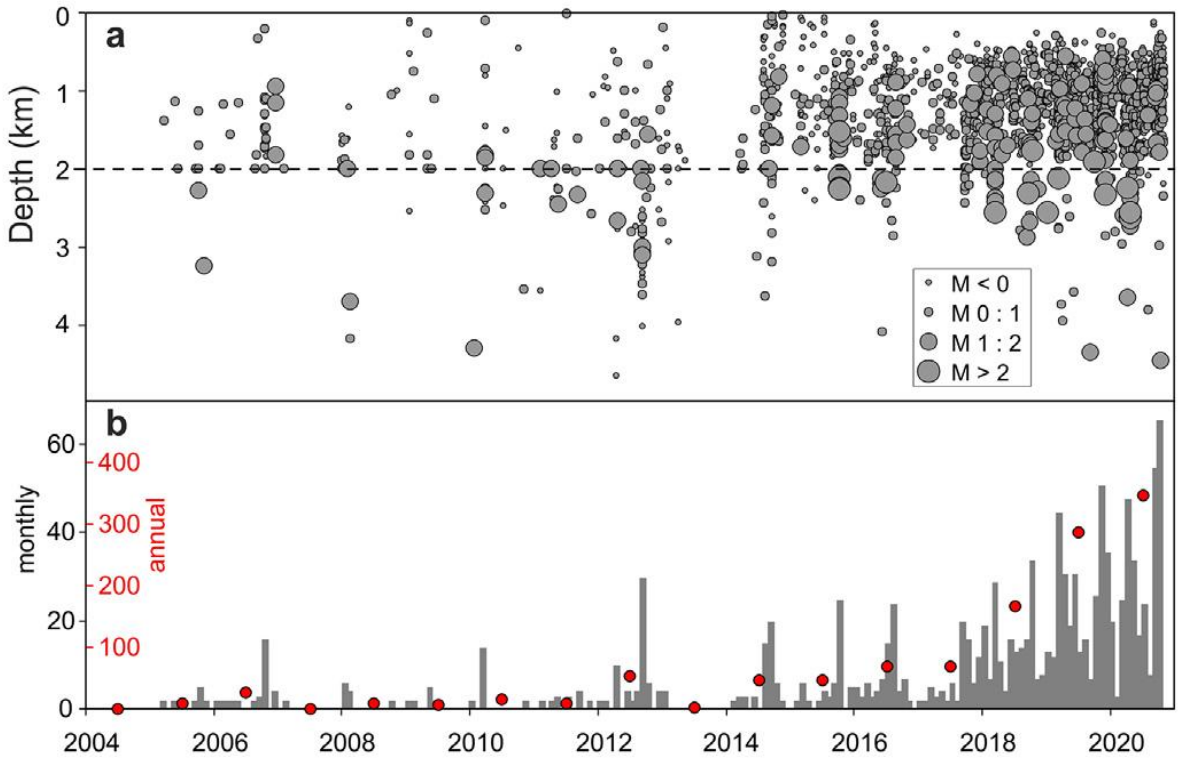

Chiodini et al., 2021, J. Volcanology and Geothermal Research, 414.

- The absence of deep events at CF (depth <3–4 km) likely reflects the high temperatures expected at depth, and a very shallow brittle-ductile transition. The heating at CF can be particularly efficient in reducing the rock tensile strength due to the presence of thermally unstable zeolites.
- Major breaches of the self-sealing zone caused by the increase of magmatic fluid pressure into the plastic zone, would allow the injection of the magmatic gases into the hydrothermal system, exerting a major control on the dynamic of CF.
- There is a maximum earthquake density between 1000 m and 2000 m, i.e. at depths compatible with the domain above the zone of magmatic fluids injections.
- Only the 25% of the earthquakes occur instead below the depth of 2000 m, possibly suggesting a progressive transition from brittle to plastic behavior of the rocks associated with very high temperatures.

Phlegrean Fields

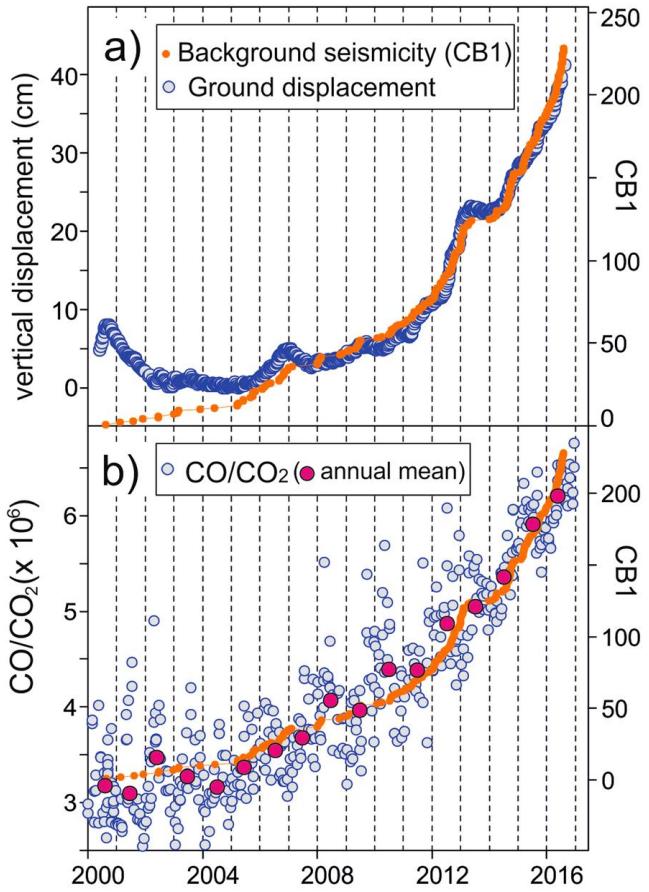

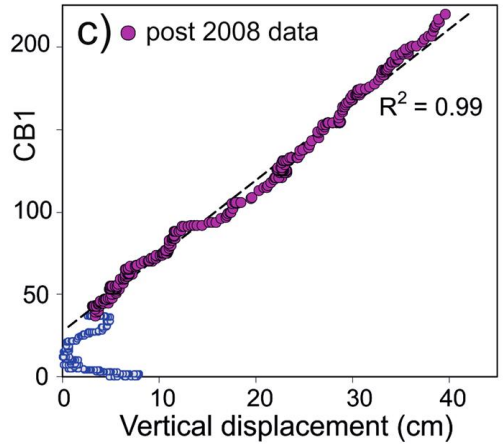

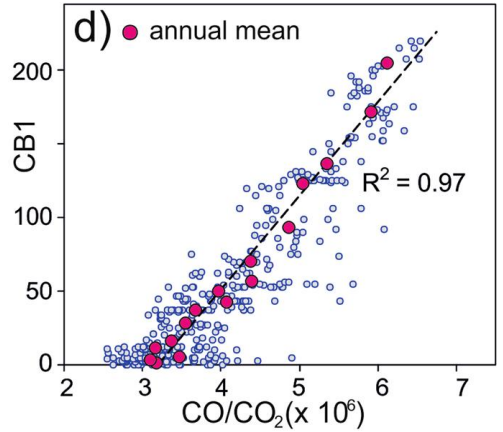

- The remaining seismic events after filtering all swarm events out of the earthquake catalogue represent the background seismicity.
- Their cumulative distribution, which simply corresponds to the sum of the days in which at least one earthquake has occurred, will be referred as CB1.

Chiodini et al., 2017, Scientific Reports, 7

- An acceleration in the ground displacement has started in 2006 and has been followed by a ~6-years-long period (until 2012–2013) when the signals seem to follow a power-law type curve.
- After one year characterized by no ground deformation and almost null seismicity, both uplift and seismicity drastically increase starting from 2014.
- This high correlation between background seismicity and compositional parameter of the fumaroles suggests that the increase of CB1 (and thus the corresponding uplift rates), proceeds concurrently with a temperature increase in the subsurface.
- These correlations indicate that the observed patterns are all likely controlled by the P and T increase of the hydrothermal system due to repeated, impulsive transfers of high amount of magmatic gases from depth.

Phlegrean Fields

The presence of a gas plume in the subsoil of Solfatara crater is evidencied by different factors:

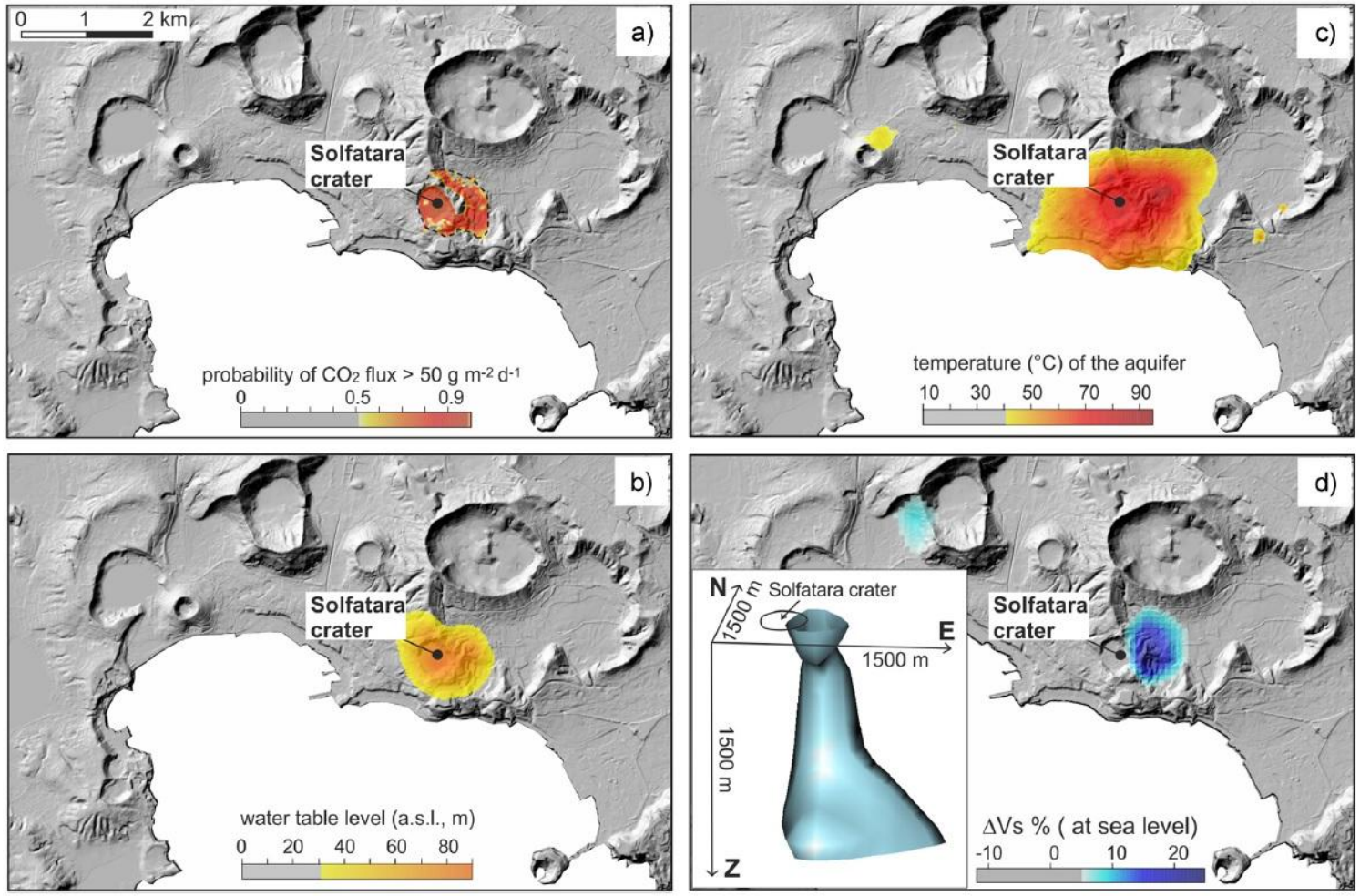

- The large amount of CO_2 release from diffuse degassing processes at Solfatara and its surroundings (~1500t/d), which is more compatible with the presence in the subsoil of a large zone where there is a gas phase, rather than with a boiling process of a liquid.
- At Solfatara, the aquifer is anomalously high for both the water table height and the water temperature. The height of the water level indicates that a pressurized gas plume sustains the aquifer here.
- The S-wave seismic velocity (*Vs*) models clearly delineate a vertical, high-*Vs* structure from the surface down to at least 1.5 km, which can be attributed to the presence of gas instead of liquid (*Vs* in dry samples of tuffs are systematically 10% to 50% higher than the same samples saturated with liquid).

Chiodini et al., 2015, EPSL, 414 Blue body: volume containing Vs anomalies larger than 18%

Phlegrean Fields

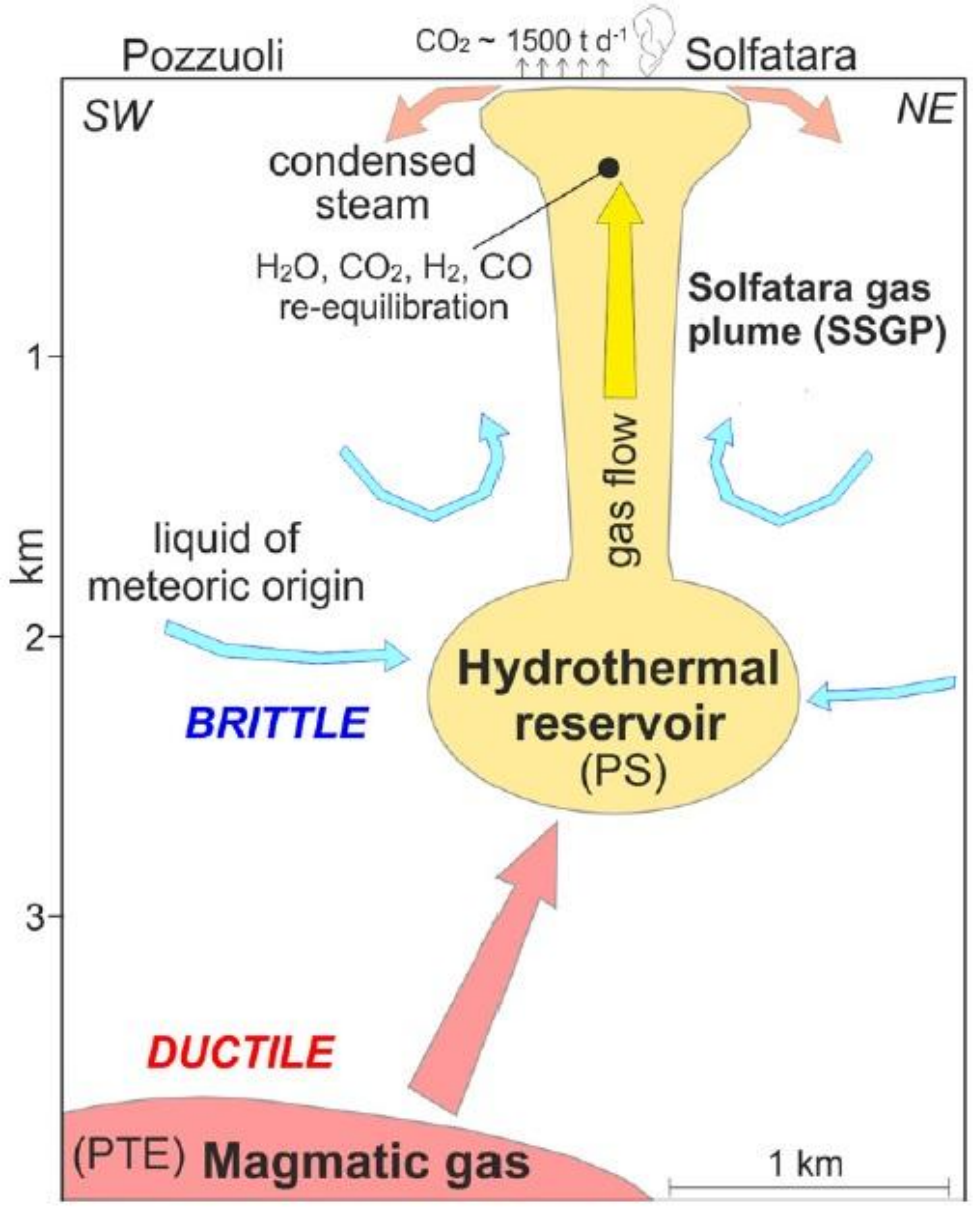

- Hot gases separate from the magma at depth, ascend toward the surface, mix with boiling meteoric water to form a gas plume that feeds fumaroles and diffuse soil degassing at Solfatara.
- The system consists of: (i) a deep zone of gas accumulation, located at ~4 km in depth (where also small batch of magma may exist), which supplies hot gas to the system; (ii) a shallower reservoir (~2 km in depth), where magmatic fluids mix and vaporize liquid of meteoric origin that forms the Solfatara gas plume. The observed deformation would be controlled by pressure changes in these two distinct sources.

Chiodini et al., 2015, EPSL, 414

Phlegrean Fields

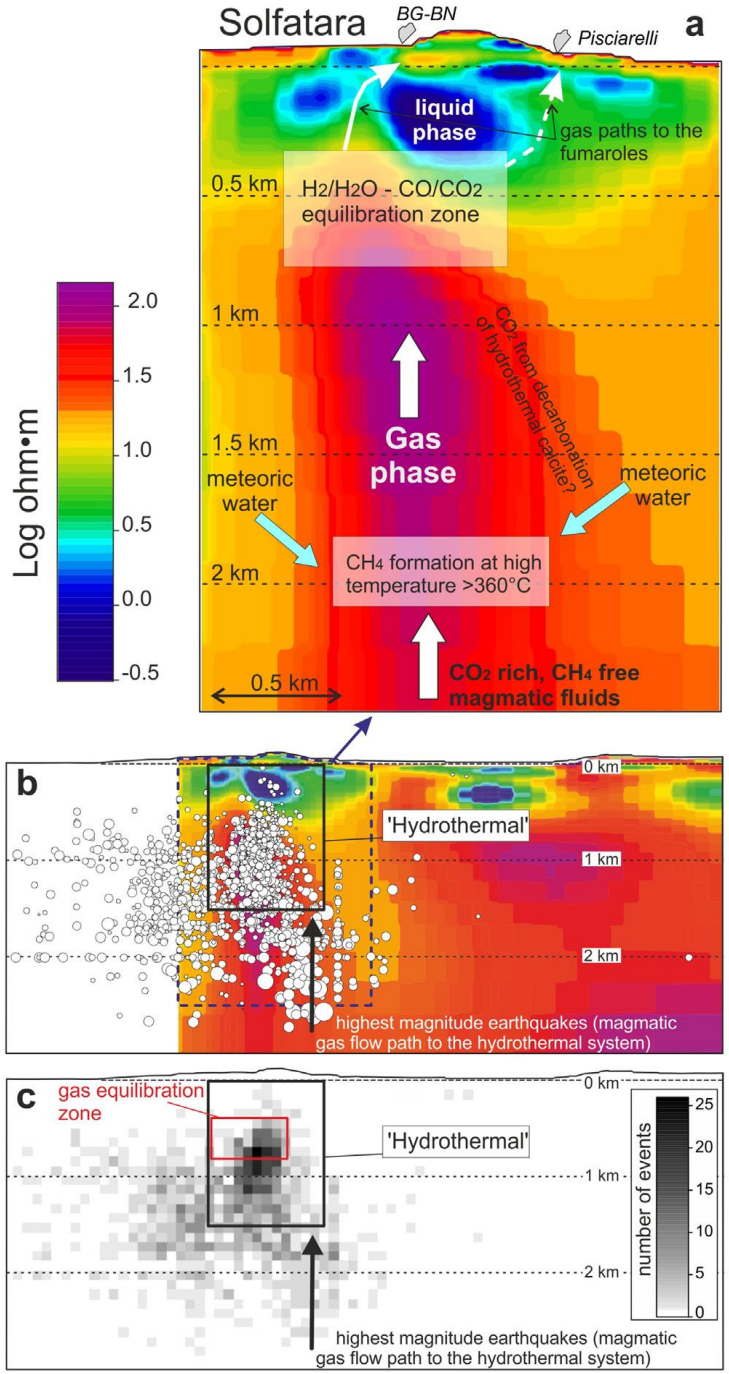

- A 2 km long vertically elongated resistivity structure in axis with Solfatara is interpreted as a permeable zone that favours gas ascent from the hottest and deepest portions of the system.
- Hot, methane free magmatic fluids enter the base (>2 km depth) of the system, mix with and vaporize meteoric liquids, and ultimately create the condition for CH_4 formation at temperatures >360 °C.
- From that zone, a gas plume rises up to 0.3–0.7 km, where the resistive structure is interrupted by conductive layer that reflect both hydrothermal altered zones and a liquid phase dominated environment.
- An escalating magmatic fluid inflow, with the release of H_2O-rich gases at the base of the hydrothermal system, causes its heating and pressurization, and in turn the increase of the CO_2 emission at the surface and seismicity.
- A dense earthquake cluster is observed at 0.5–1 km depth and is interpreted as the head of the gas front feeding the hydrothermal system. The generalised pressurization and heating of the CF gas dominated-hydrothermal system act as the main seismicity trigger.
- A second, deeper (>2km) seismicity cluster that corresponds to the source area irradiating the highest magnitude earthquakes, has been interpreted as the root of the gas plume, in which larger events are likely caused by pulsed magmatic fluid injections.

Chiodini et al., 2021, J. Volcanology and Geothermal Research, 414.

Phlegrean Fields

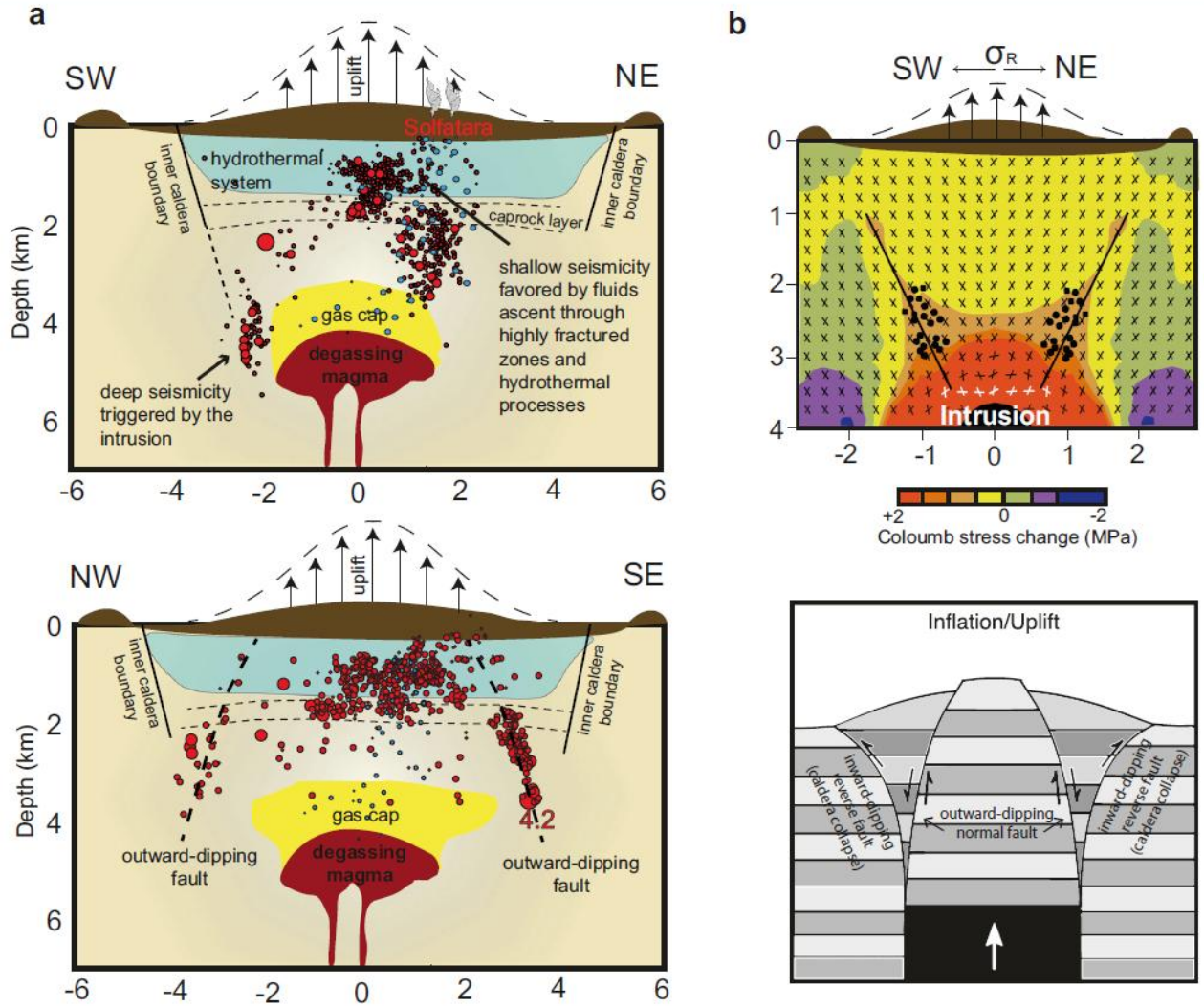

Giacomuzzi et al. 2025

- Shallow seismicity is mainly triggered by a channelized fluid ascent from depth, but deeper seismicity appears to be mainly controlled by the inflation of the magmatic reservoir located at about 4.5–5 km depth.
- In the offshore, seismicity mainly occurs near the inner caldera boundary, while the relatively shallower seismicity, related with hydrothermal activity triggered by deep magma degassing, in the northeastern inland appears to be controlled by minor fracture/fault zone.

Phlegrean Fields

- **According to the model of Chiodini et al., 2015, two main processes contribute to the ongoing CF bradyseism:**

1)Transient episodes of gas pressurization that are accompanied by fluid transfer from the deep magmatic gas zone to the shallower parts of the hydrothermal system, which trigger the short-term uplifting episodes.
2) A long-term process of heating of the system that causes (or contributes to) the 10-year-long pattern of accelerating ground deformation.

- **Lima et al., 2009 proposed a model for subsidence and uplift of the Phlegrean Fields based on the linkage between bradyseism and magma body cooling and concomitant crystallization and fluid phase exsolution from melt, with eventual expulsion of lithostatically pressured fluid into overlying country rock.**

Phlegrean Fields

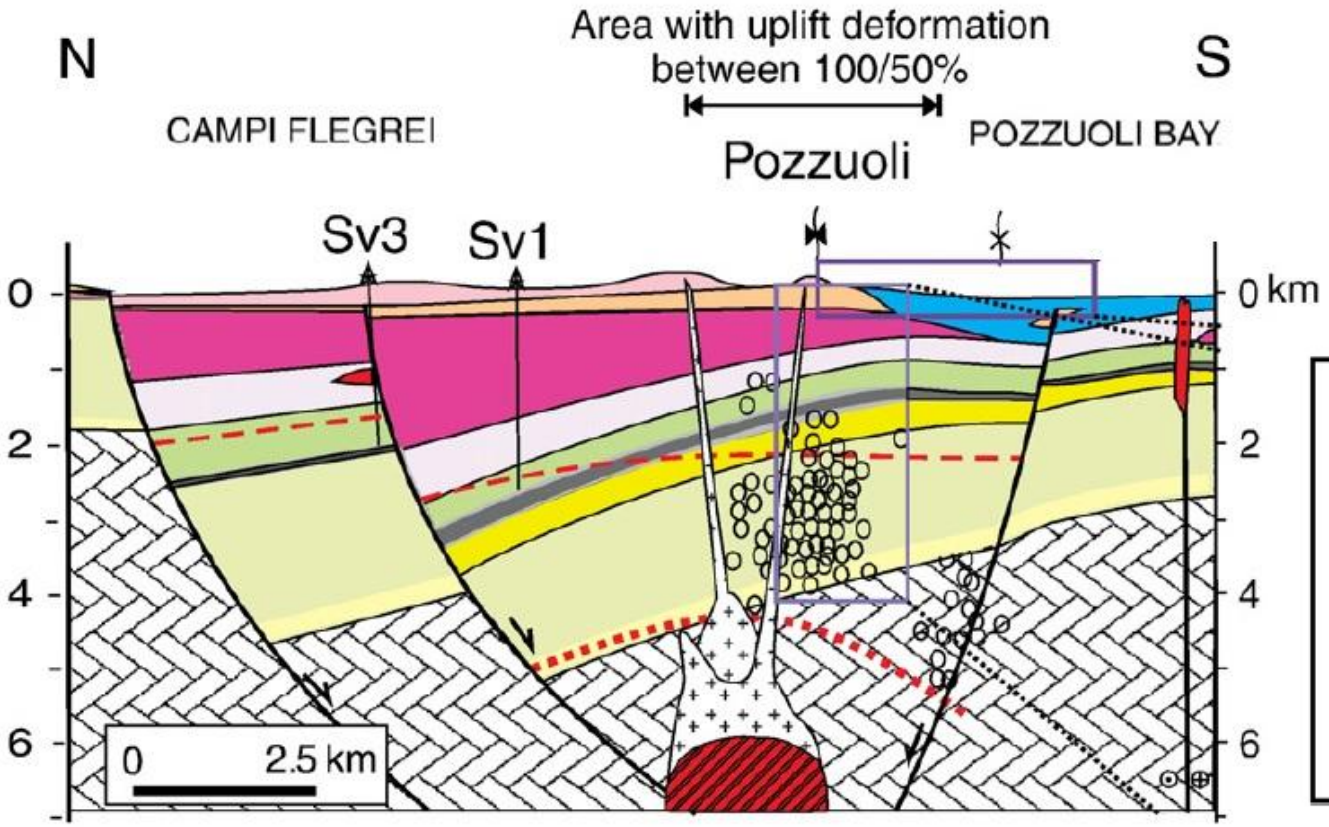

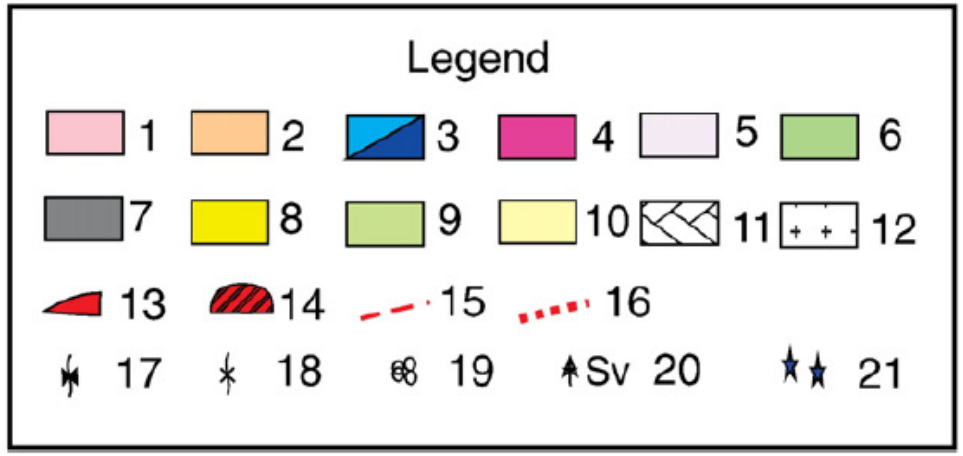

Lima et al., 2009, Earth-Science Reviews, 97

1. Holocene volcanics; 2. Neapolitan Yellow Tuff; 3. Main sediments post 39 ka; 4. Campania Ignimbrite and pre-CI tuffs; 5. Middle Pleistocene sandstones, siltstones and volcanics; 6. Middle Pleistocene marine sediments (sandstones and siltstones — unit C in text); 7. Fine grained Middle Pleistocene marine sediments (claystones and siltstones — Unit B in text); 8. Middle Pleistocene deep water debris flows; 9. Lower Pleistocene marine sediments; 10. Continental deposits and conglomerates; 11. Meso-Cenozoic substrate; 12. Crystallized magma; 13. Volcanic bodies; 14. Magma body; 15. Thermometamorphic boundary; 16. Impermeable zone surrounding the crystallizing magma body. 17. Pozzuoli Anticline; 18. Pozzuoli Bay Syncline; 19. 1983–84 earthquake hypocenters; 20. Deep geothermal wells; 21. Magmatic fluids.

Phlegrean Fields

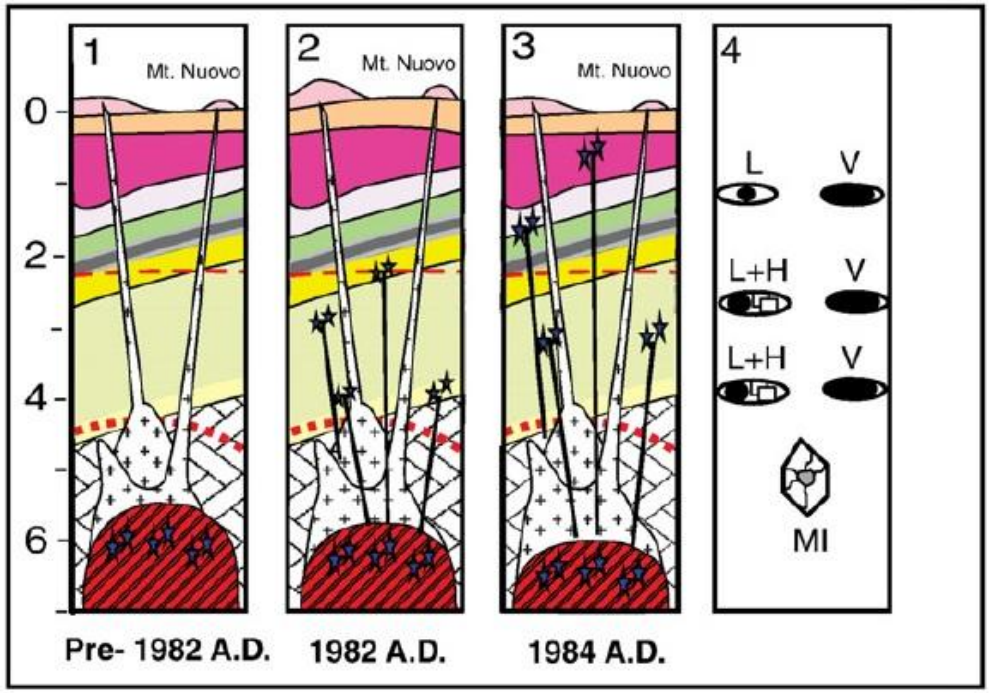

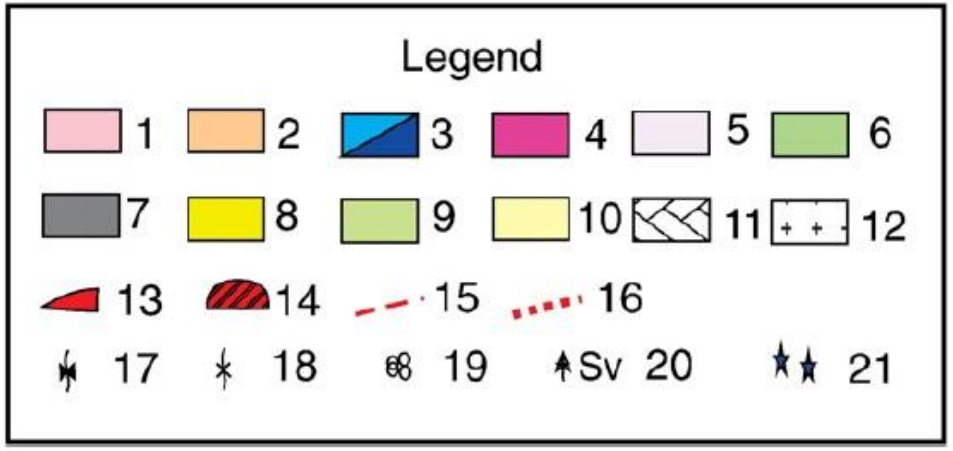

(1) Following the 1538 eruption, the magma body became a closed system, and magmatic volatiles accumulated below impermeable crystallized carapace.

(2) In 1982, the carapace confining the magmatic system fractured, allowing magmatic fluids to enter the overlying rocks beneath the low-permeability caprock (Unit B), causing vertical ground deformation.

(3) Ground deformation that began in 1982 ended and deflation began when fractures penetrated the low-permeability cap rock, allowing the deep fluids to migrate into the shallow hydrostatic aquifers and flow toward the surface.

Lima et al., 2009, Earth-Science Reviews, 97

L = Liquid-rich inclusion; V = Vapour-rich inclusion; L + H = Halite-bearing fluid inclusion; MI = Melt inclusion).

Phlegrean Fields

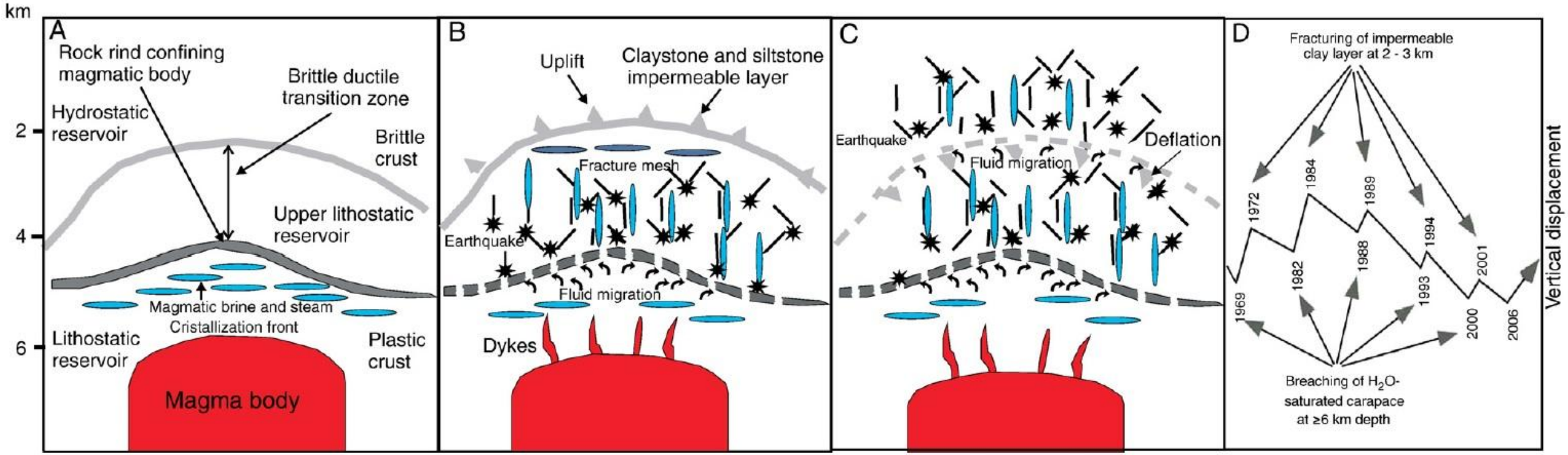

Lima et al., 2009, Earth-Science Reviews, 97

- During initial crystallization of the under-saturated melt, the volatile content of the melt increases as anhydrous phases precipitate (melt becomes saturated in volatiles and the pressure in the magma body increases). This fluid remains geopressured until fracture propagation enables the expulsion of magmatic fluids.
- High salinity brine and vapour may exsolve directly from the magma and due to its greater density and viscosity, the high salinity liquid usually “ponds” in the deeper portions of the system, while the lower salinity, low-viscosity vapour phase migrates to shallower levels of the system. Geopressured fluids can escape into the overlying rocks when rocks rind around the magma chamber is breached (inflation).
- When the overlying impermeable rocks fracture, the low salinity gas moves towards the surface and interacts and mixes with meteoric water (or seawater) present in fractures and pores at shallow depths, to produce a low salinity boiling assemblage (deflation).
- According to the model, the magma body is presently isolated from the overlying aquifers and the fraction of exsolved fluid is building within the magma chamber.

Phlegrean Fields

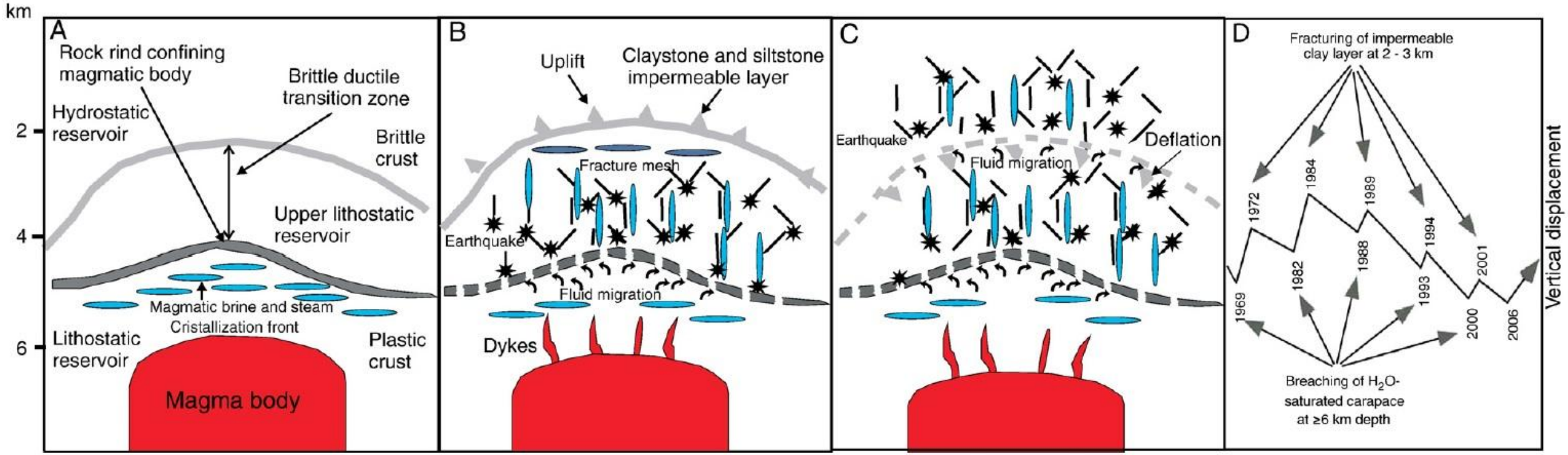

- Uplift occurs when magmatic fluids enter in the rocks beneath the lower permeability cap rock (~2.5–3.0 km).
- Uplift ends and deflation begins when fractures penetrate the lower permeability cap rock, allowing the deep magmatic fluids to migrate into the shallow aquifers and flow toward the surface.
- Bradyseism is driven by the transient connection between the deeper lithostatic reservoir and an overlying more permeable hydrostatic one. Magma solidification and associated magmatic fluid generation occur on a timescale of 10^3–10^4 yr. Transient fracture propagation events that connect the lower lithostatic reservoir with the upper hydrostatic one, accompanying irreversible fluid decompression, occurs on a timescale of 1-10 yr.
- A magmatic eruption may follow if the reduced confining pressure on the magma leads to a runaway process of bubble formation, ascent and growth (if an overpressure is generated by the magmatic–hydrothermal fluid on rocks above a low-permeability cap rock).
- As the magma body cools and crystallizes and the H_2O-saturated carapace migrates to greater depth, the energy and volume change associated with volatile exsolution decreases and the magnitude of future uplift events is likewise expected to decrease.

References

Main Readings:

Books:

- Eppelbaum, Kutasov, and Pilchin, 2014: Applied Geothermics, Chapter 4: Temperature anomalies associated with some natural phenomena, 161-224.
- Pasquale, Geothermics, Heat flow in the Lithosphere, Chapter 4: Temperature and Magmatic Processes, 79-99
- Jaupart and Mareshal, Heat Generation and Transport in the Earth, Chapter 11: Magmatic and Volcanic System
- Marsh, 2007, Magmatism, Magma, and Magma Chambers, Treatise of Geophysics, vol. 6, 275-333.
- Newhall, 2007, Volcanology 101 for Seismologists, Treatise of Geophysics, vol. 4, 351-388.
- Myron,2003, Igneous and metamorphic petrology 2° Ed., Chapter 6: Chemical Dynamics of Melts and Crystals.
- Myron,2003, Igneous and metamorphic petrology 2° Ed., Chapter 8: Physical and Thermal Dynamics of Bodies of Magma.

Articles:

- Chiodini et al., 2017, Clues on the origin of post-2000 earthquakes at Campi Flegrei caldera (Italy). Scientific Reports, 7, 4472.
- Chiodini et al., 2015, Evidence of thermal-driven processes triggering the 2005–2014 unrest at Campi Flegrei caldera, EPSL, 414, 58-67.
- Chiodini et al., 2021, Hydrothermal pressure-temperature control on CO2 emissions and seismicity at Campi Flegrei. Journal of Volcanology and Geothermal Research 414, 107245.
- Lima et al., 2009, Thermodynamic model for uplift and deflation episodes (bradyseism) associated with magmatic–hydrothermal activity at the Campi Flegrei (Italy), Earth-Science Reviews, 97, 44-58.

Further readings:

- Calò and Tramelli, 2025. Evidences of the structures controlling the unrest in Campi Flegrei, Italy; Joint interpretation of ambient noise and local earthquake tomography. Journal of Volcanology and Geothermal Research 457 (2025) 108236 .
- Giacomuzzi et al., 2024. Tracking transient changes in the plumbing system at Campi Flegrei Caldera. Earth Planet. Sci. Lett. 637 (2024) 118744.
- Giacomuzzi et al., 2025. Causal processes of shallow and deep seismicity at Campi Flegrei caldera. Communications Earth & Environment | (2025) 6:70.
- Giordano et al., 2008, Viscosity of magmatic liquids: A model Earth and Planetary Science Letters, 271,123–134.